NACA

RESEARCH MEMORANDUM

for the

U. S. Air Force

STABILITY AND CONTROL CHARACTERISTICS AT LOW SPEED OF A 1/10-SCALE MODEL OF MX-1554A DESIGN

By Vernard E. Lockwood and Martin Solomon

Langley Aeronautical Laboratory
Langley Field, Va.

NATIONAL ADVISORY COMMITTEE
FOR AERONAUTICS
WASHINGTON

NACA RM SL53A05

NATIONAL ADVISORY COMMITTEE FOR AERONAUTICS

RESEARCH MEMORANDUM

for the

U. S. Air Force

STABILITY AND CONTROL CHARACTERISTICS AT LOW SPEED OF A 1/10-SCALE MODEL OF MX-1554A DESIGN

By Vernard E. Lockwood and Martin Solomon

SUMMARY

An investigation was made of the low-speed stability and control characteristics of a 1/10-scale model of the proposed MX-1554A design. This design employs a triangular wing and triangular stabilizing surfaces.

The present paper contains the results of a stability and control investigation of a model configuration thought to be representative of the final airplane configuration. The paper also contains the results of a series of tests to determine:

1. The effects of wing incidence on stability characteristics.

2. The effects of slotted flap on stability and control characteristics.

3. The effects of wing and tail height on longitudinal stability and control.

4. The effects of external tanks and speed brakes on the aerodynamic characteristics.

5. The effects of ground board on the aerodynamic characteristics.

6. The effects of spoilers, tip ailerons, flaps, and differential tail deflection on the lateral control characteristics.

7. The effects of an unswept wing on longitudinal and lateral characteristics.

[redacted]

INTRODUCTION

An investigation of the stability and control characteristics of a 1/10-scale model of a preliminary design of MX-1554A has been conducted in the Langley 300 MPH 7- by 10-foot tunnel. This design employs a delta wing and tail configuration. The original purpose of this investigation was to determine a horizontal-tail location which would provide satisfactory longitudinal stability and to determine the lateral and directional stability characteristics. Certain deficiencies were indicated which resulted in a more detailed investigation with considerable emphasis being placed on longitudinal and lateral control.

The present paper contains the results of a stability and control investigation of a model configuration thought to be representative of the final configuration with the exception of the aileron detail. In addition, the paper contains the results of tests to determine the effects on the aerodynamic characteristics of change in wing incidence, variation of wing and tail height, wing plan form, slotted flaps, addition of speed brakes and external tanks, deflection of spoilers, tip ailerons, differentially operated flaps and tail surfaces, and the effect of the presence of a ground board on the pertinent characteristics.

SYMBOLS

All data are referred to the stability axes as indicated in figure 1. A point of 32.0 percent of the wing mean aerodynamic chord was used as center of moments for the delta configuration. This point corresponds to 33.3 percent of the mean aerodynamic chord for the unswept-wing configuration. The symbols used in this paper are defined as follows:

C_L	lift coefficient, Lift/qS
C_X	longitudinal-force coefficient, X/qS
C_Y	lateral-force coefficient, Y/qS
C_l	rolling-moment coefficient, L/qSb
C_m	pitching-moment coefficient, M/qS$\bar{c}$
C_n	yawing-moment coefficient, N/qSb
X	longitudinal force along X-axis, lb
Y	lateral force along Y-axis, lb

[redacted]

Z	force along Z-axis (lift equals -Z), lb
L	rolling moment about X-axis, ft-lb
M	pitching moment about Y-axis, ft-lb
N	yawing moment about Z-axis, ft-lb
q	free-stream dynamic pressure, $\rho V^2/2$, lb/sq ft
S	wing area, sq ft
$\bar{c}$	wing mean aerodynamic chord, ft
b	wing span, ft
V	free-stream velocity, ft/sec
ρ	mass density of air, slugs/cu ft
α	angle of attack of fuselage reference line, deg
i	angle of incidence of wing or stabilizer with respect to fuselage reference line, deg
δ	control-surface deflection in a plane perpendicular to hinge line, deg (percent projection when used as a spoiler based on wing mean aerodynamic chord)
H	height of center of gravity above ground board at $\alpha = 0^\circ$, in.
h	height of the wing or tail above the fuselage reference line, (positive when above), in.
β	angle of sideslip, deg

$C_{l_\beta} = \frac{\partial C_l}{\partial \beta}$

$C_{n_\beta} = \frac{\partial C_n}{\partial \beta}$ } lateral-stability parameters

$C_{Y_\beta} = \frac{\partial C_Y}{\partial \beta}$

[redacted]

Subscripts:

a	aileron
e	elevator
f	flap
r	rudder
t	tail (horizontal)
w	wing
L	left
R	right
s	spoiler

APPARATUS AND METHODS

The model used in the present investigation was a 1/10-scale model of the preliminary design of MX-1554A. The wing and stabilizing surfaces have notched delta plan forms with a small amount of sweepback of the trailing edges. The physical characteristics of this model are presented in figure 2. The original model configuration (fig. 3) contained no control surfaces but these were added later in the program (fig. 4). The model was equipped with angle blocks to provide for the desired wing-incidence change with the center of rotation that is designated as the wing rotation point in figure 2. Besides the original wing position (A), the delta wing was also tested at two other heights on the fuselage designated as B and C in figure 5. An unswept-wing model of approximately the same wing area was also tested, the characteristics of which are given in figure 2(b). The unswept wing was tested at position A of the delta configuration and tail 1 was used with the unswept wing.

Several horizontal-tail configurations were investigated, the mean aerodynamic chords and locations of which are shown in figure 5. All of these configurations had the same leading-edge and trailing-edge sweep. The pertinent information regarding the various configurations designated from 1 to 6 is given in the following table (the vertical location is given with respect to the fuselage reference line):

[redacted]

Tail	Vertical location, in.	Span, in.	Airfoil section
1	-3.80	21.19	NACA 65A003
2	-3.30	21.19	NACA 65A003
3	-1.65	21.19	$\frac{1}{8}$ - inch plate with round leading edges and square trailing edges
4	1.31	21.19	Do.
5	1.50	25.50	NACA 65A003
6	4.00	21.19	NACA 65A003

Tail numbers 3, 4, and 5 were pivoted about a point corresponding to 47 percent of the mean aerodynamic chord of the exposed panel. This location of the pivot caused unporting of the surfaces which resulted in large gaps between the fuselage and the section of the tail at the tail-fuselage juncture at negative incidences with tail 2 and positive incidences of tails 4 and 5.

Most of the investigation was made with the vertical tail in the position indicated by the solid line in figure 2. For a few tests, however, the tail was at the position indicated by the dashed line.

A double slotted flap was used in the investigation to increase the lift at low angles of attack. The details of the flap and vane configuration which gave the greatest increment in lift at low angles of attack are shown in figure 6.

The details of the spoilers and tip ailerons which were used as lateral-control devices are shown in figure 7. The spoilers were wedge-shaped, were made of solid wood, and extended over the same span as that of the flap. For one test, however, the spoiler span was extended to about 71 percent of the semispan by the addition of a $\frac{1}{16}$ - inch plate to the surface of the wood spoiler as shown in figure 7.

A fence and a chord-extension were tested as air-flow control devices for one model configuration that exhibited longitudinal instability. The geometry of these configurations is given in figure 8.

The model had no internal ducting leading from the air scoop. To delay separation which would ordinarily occur from the sharp edges of the scoop, modeling clay was used to refair the throat and edges as shown in figure 4.

[redacted]

The model was also tested with wing tanks, landing gear, and speed brakes which were furnished by the manufacturer. These items are shown in figures 2 and 4.

A ground board was constructed for use with the model to simulate the airplane in the presence of the ground. The board was made of two pieces of 1-inch plywood 12 feet long and when put together completely spanned the tunnel as shown in figure 4. The relative position of the model and board which was adjustable in height is shown in figure 2(b).

Unless otherwise stated in the legends of the figures, the following description applies to the model configuration:

$i_w = 0^\circ$; $\delta_{a_L} = 0^\circ$; $i_t = 0^\circ$; $\delta_f = 0^\circ$; $\delta_e = 0^\circ$

Rearmost vertical-tail location

External tanks off

Speed brakes off

Landing gear off and doors closed

TESTS

The tests were conducted in the Langley 300 MPH 7- by 10-foot tunnel at the approximate conditions given in the following table:

Model configuration	Dynamic pressure, lb/sq ft	Mach number	Reynolds number
Original (no controls)	101.5	0.266	2,590,000
With controls; $\delta_f = 0^\circ$	49.0	.183	1,840,000
With controls; $\delta_f = 57^\circ$	25.0	.131	1,400,000
With ground board; $\delta_f = 57^\circ$	27.0	.136	1,390,000

The Reynolds number is based on a wing mean aerodynamic chord of 17.93 inches.

[redacted]

CORRECTIONS

The angle of attack and drag have been corrected for jet-boundary effects computed on the basis of unswept wings by the method of reference 1. The correction to pitching moment due to tunnel induced upwash at the tail was found to be negligible.

Tare corrections from the single support strut were not applied to the data. It is thought that these corrections would be small increments in pitching moment and drag only.

Corrections have been applied to the data resulting from vertical buoyancy on the support strut, tunnel air-flow misalinement, and longitudinal-pressure gradient in the tunnel.

PRESENTATION OF RESULTS

The results of the investigation of the MX-1554A are presented in the following manner:

(a) The results of tests of the model as originally received from the contractor are presented in figures 9 to 18. The effect of wing incidence and tail position on the longitudinal stability characteristics are presented in figures 9 and 10 and the effect of sealing the gap at the wing-fuselage juncture is presented in figure 11. The results of tests to determine the effect of wing incidence and model configuration, including model break-down tests, on the lateral stability characteristics of the original model configuration are presented in figures 12 to 18.

(b) In an effort to obtain a more satisfactory configuration, numerous modifications were made to the model, the results of which are presented in figures 19 to 40. The effect of wing incidence, fences, and chord extensions, with flaps deflected, on the longitudinal characteristics are presented in figures 19, 20, and 21, respectively. The longitudinal characteristics with an unswept wing are shown in figure 22. The results of tests to determine the effect of tail height, tail area, and wing position with and without flaps deflected on the longitudinal stability characteristics are presented in figures 23 to 29. The longitudinal control effectiveness of the elevator is shown in figure 30. The results of tests to determine the effect of wing incidence and vertical-tail location on the lateral stability characteristics are given in figure 31. The lateral stability characteristics with the unswept wing are shown in figure 32. The lateral control characteristics utilizing the original tip ailerons are shown in figures 33 and 34. The lateral control effectiveness of several spoiler arrangements is given

in figures 35 and 36. The effectiveness obtained by deflecting the flaps differentially as lateral-control devices is shown in figures 37 and 38. The results of tests utilizing both the large and small horizontal tails. operated differentially to provide lateral control are presented in figures 39 and 40.

(c) From the results of tests presented in paragraph (b), the contractor revised the model and a more complete investigation was made, the results of which are presented in figures 41 to 48. The effect of several model components on the longitudinal stability characteristics are shown in figures 41 and 42. The longitudinal control characteristics as affected by tanks and brakes are presented in figure 43 for the flap-neutral configuration and in figure 44 for the flap-deflected condition; the data of figure 45 show the effect of proximity to the ground for the case with flaps deflected. The lateral stability characteristics as affected by flap deflection, tanks, and brakes are presented in figures 46 and 47. The effectiveness of the rudder is shown in figure 48.

Trim lift characteristics obtained from figures 41 to 45 are presented in figure 49. An estimation of the effect of a 6-percent mean-aerodynamic-chord rearward shift in center-of-gravity location on the trim characteristics is given in figure 50.

The effective downwash angles for several model configurations are presented in figure 51. The effect of proximity of the ground on the downwash characteristic is shown in figure 52. Some of the downwash curves may be subject to considerable error, particularly in the cases with the flap deflected, where large extrapolations of tail effectiveness were necessary between the tail-off and tail-on tests.

Langley Aeronautical Laboratory,
National Advisory Committee for Aeronautics,
Langley Field, Va.

Vernard E. Lockwood
Vernard E. Lockwood
Aeronautical Research Scientist

Martin Solomon
Martin Solomon
Aeronautical Research Scientist

Approved: Charles H. Zimmerman
for Thomas A. Harris
Chief of Stability Research Division

ecc [redacted]

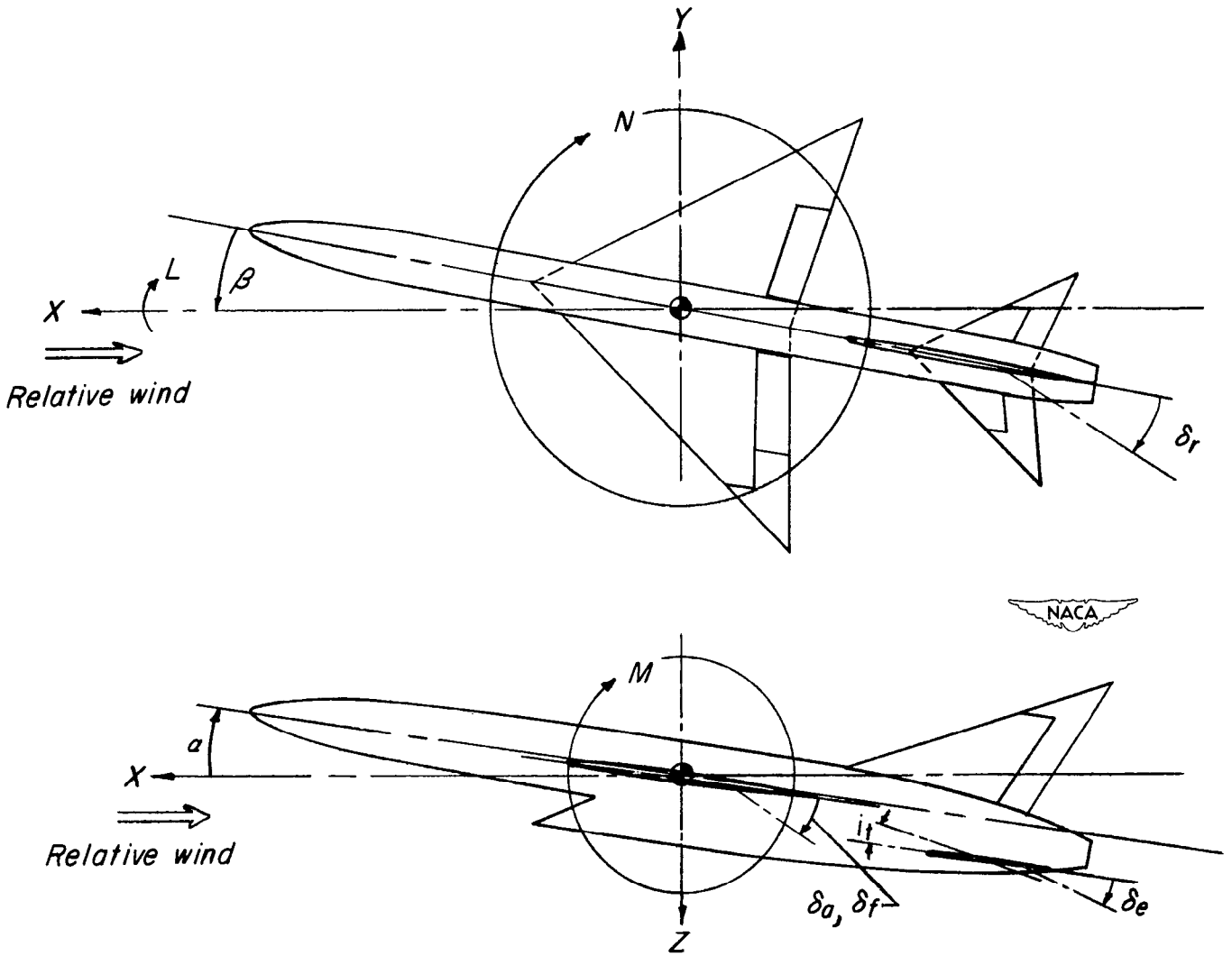

Figure 1.- System of axes and control-surface deflections. Positive directions of forces, moments, and angles are indicated by arrows.

Physical Characteristics

Wing:	
Aspect ratio	3.2
Span	42.976 in.
Area	4.01 sq ft
Root chord	26.900 in.
Mean aerodynamic chord	17.933 in.
Airfoil section (parallel to air stream)	NACA 65A003
Sweepback	
Leading edge	55°
Trailing edge	10°
Incidence (variable)	0°,4°,8°,14°
Horizontal tail:	
Aspect ratio	3.4
Area (total)	.908 sq ft
Airfoil section	NACA 65A003
Vertical tail:	
Aspect ratio (exposed)	1.6
Area (exposed)	.874 sq ft
Airfoil section	NACA 65A003

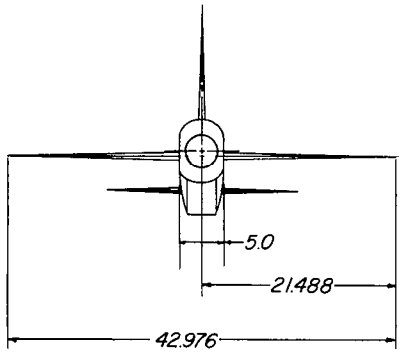

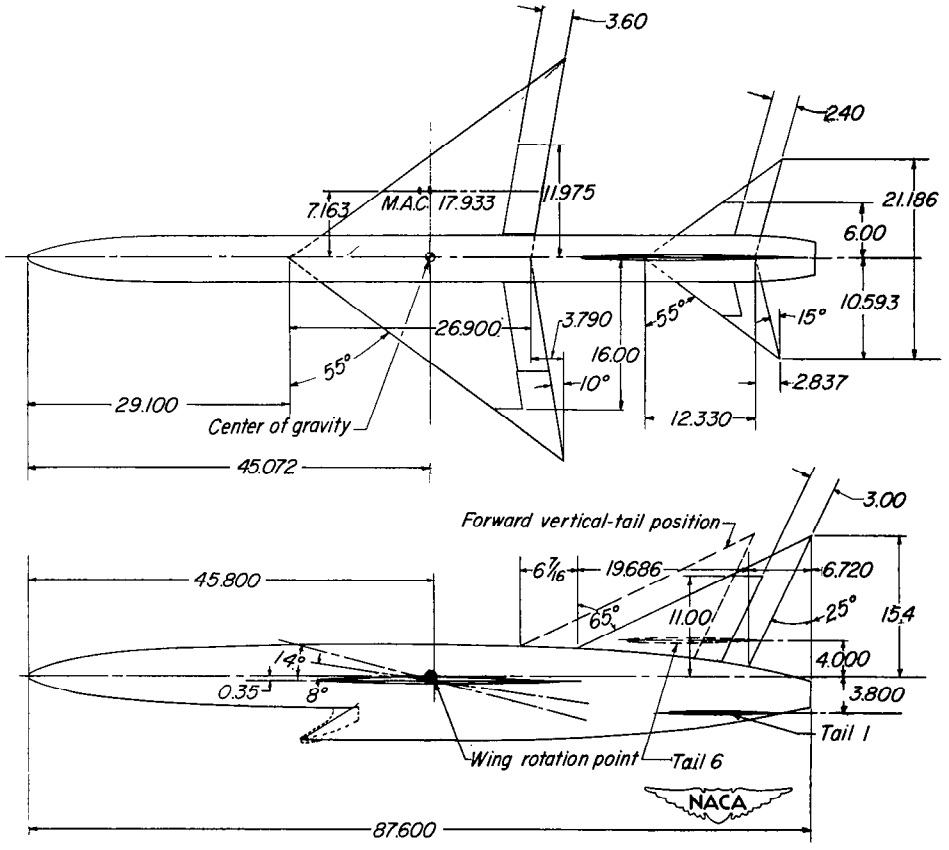

(a) Delta-wing configuration (clean).

Figure 2.- Three-view drawings of the model configurations tested. All dimensions are in inches unless otherwise noted.

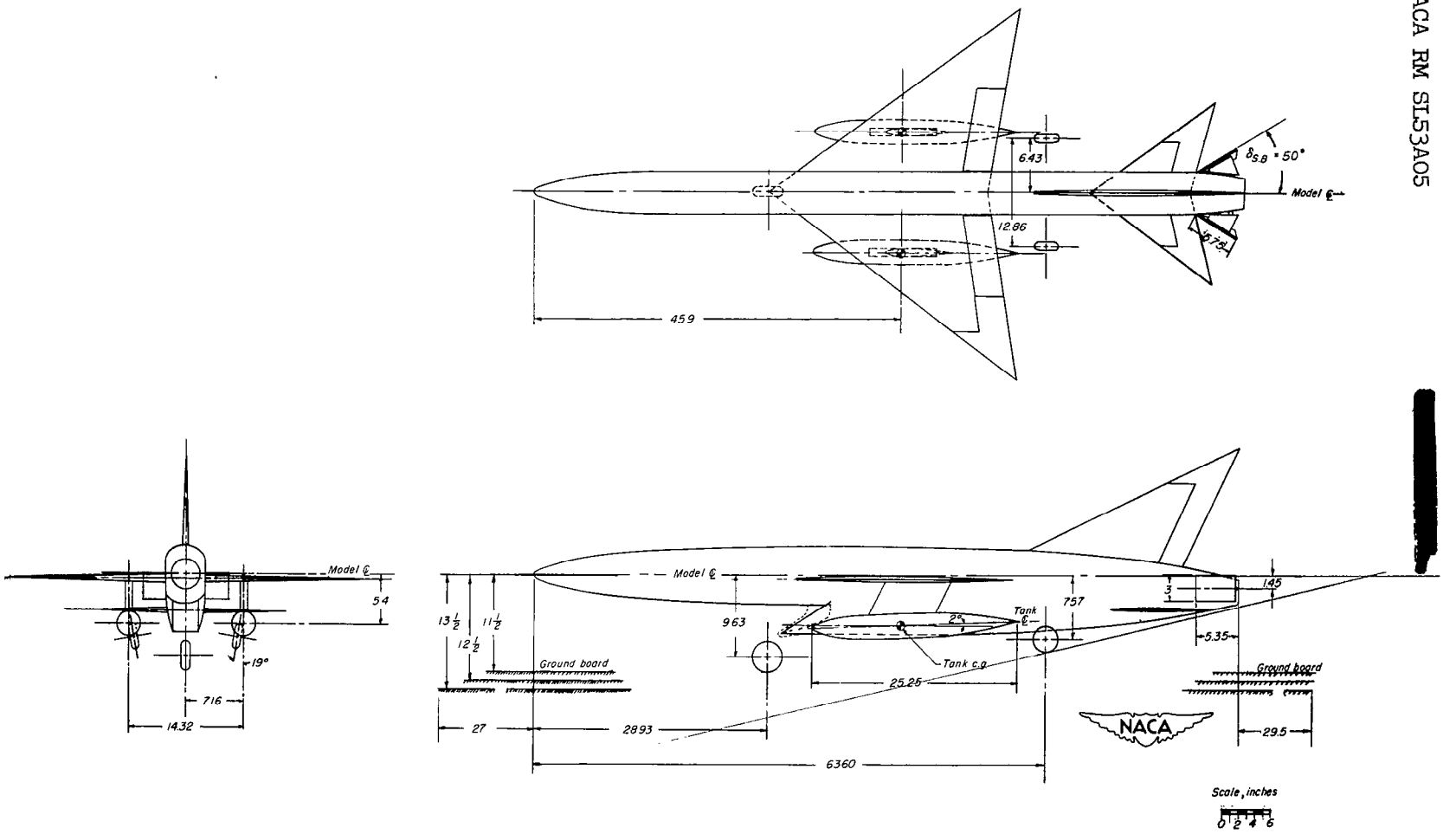

(b) Delta-wing configuration (stores, speed brakes, and landing gear).

Figure 2.- Continued.

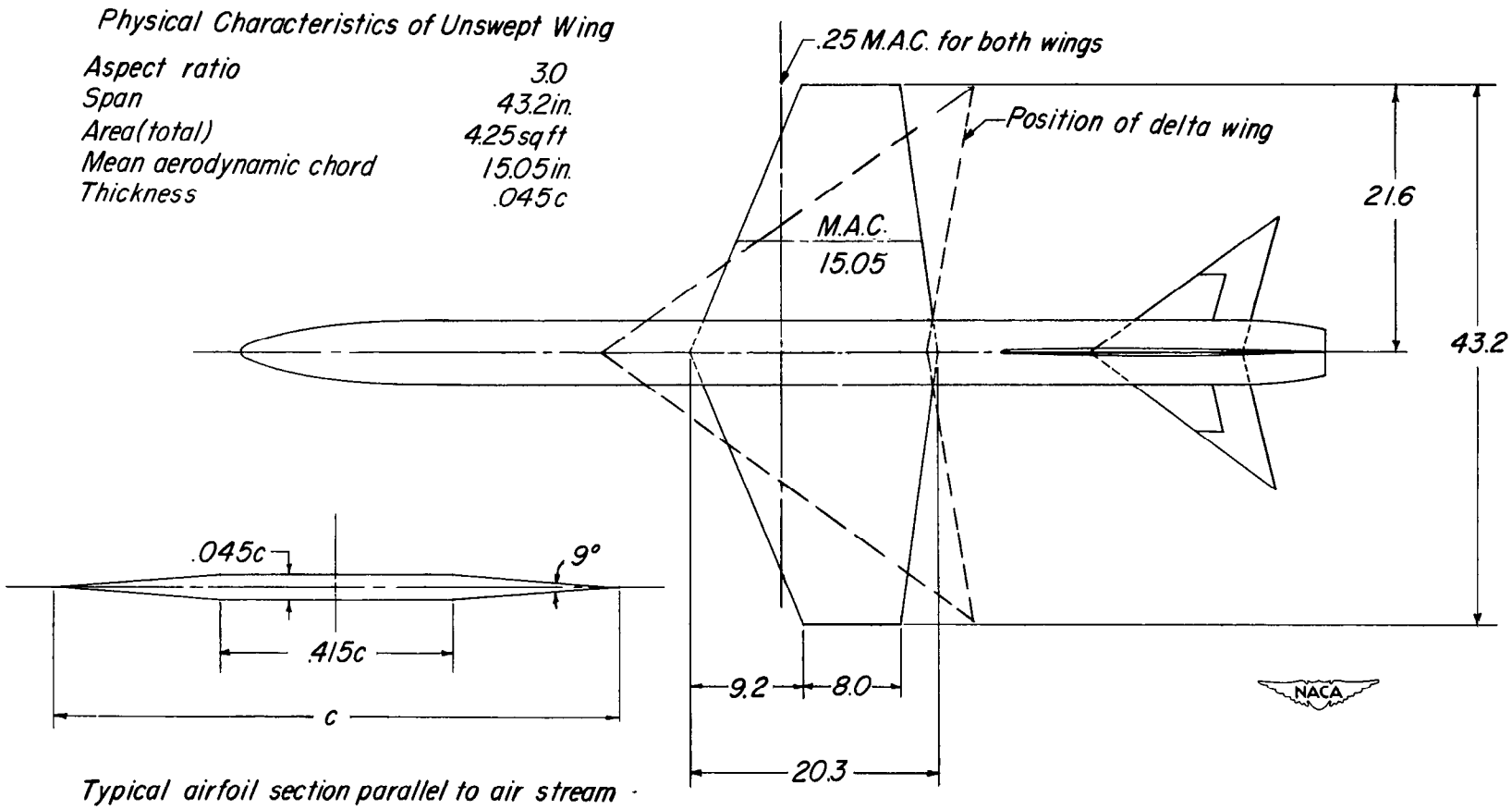

(c) Unswept-wing configuration (clean).

Figure 2.- Concluded.

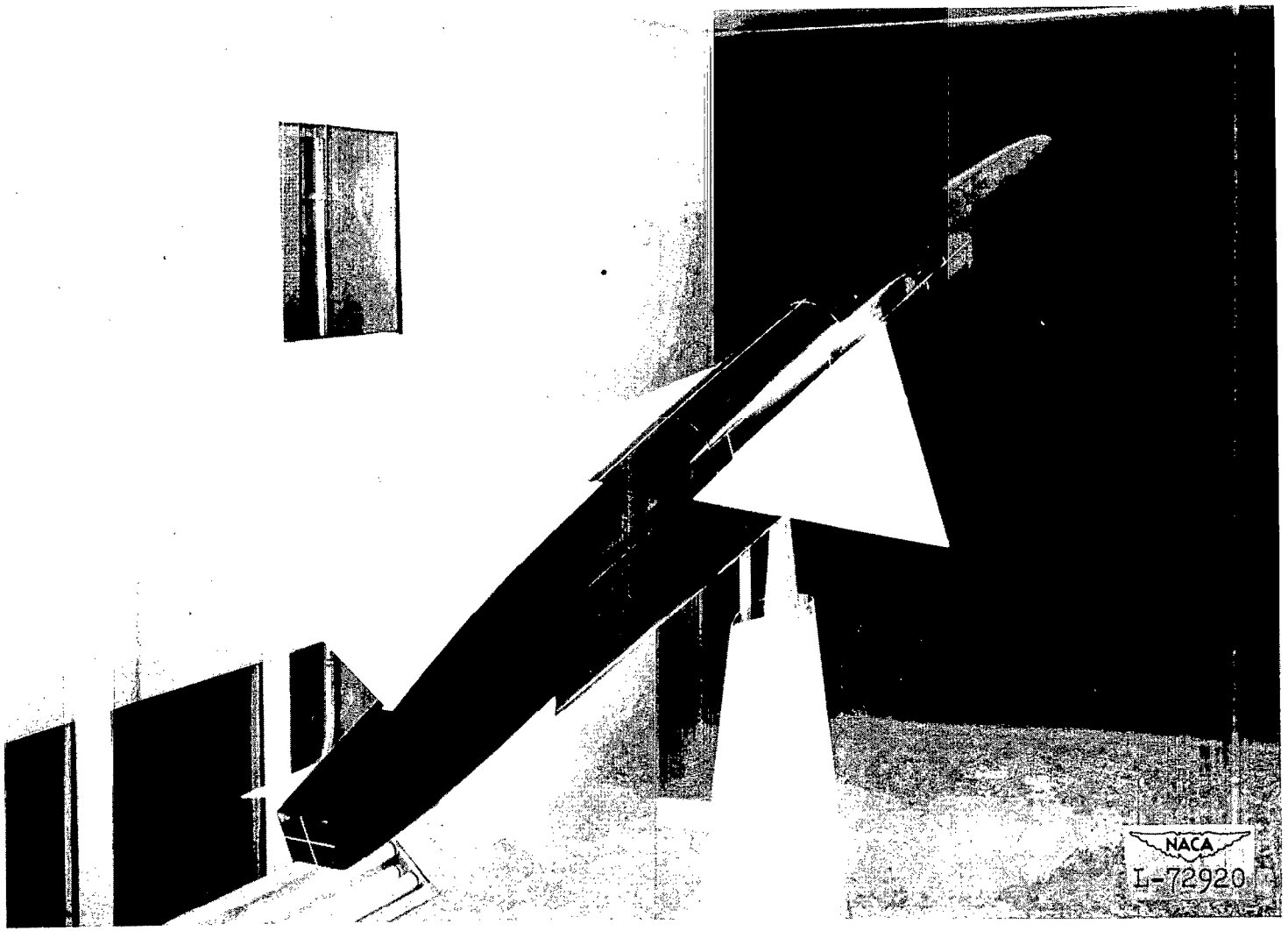

Figure 3.- View of original model mounted in tunnel. Wing position A; $i_w = 0^\circ$; tail 1.

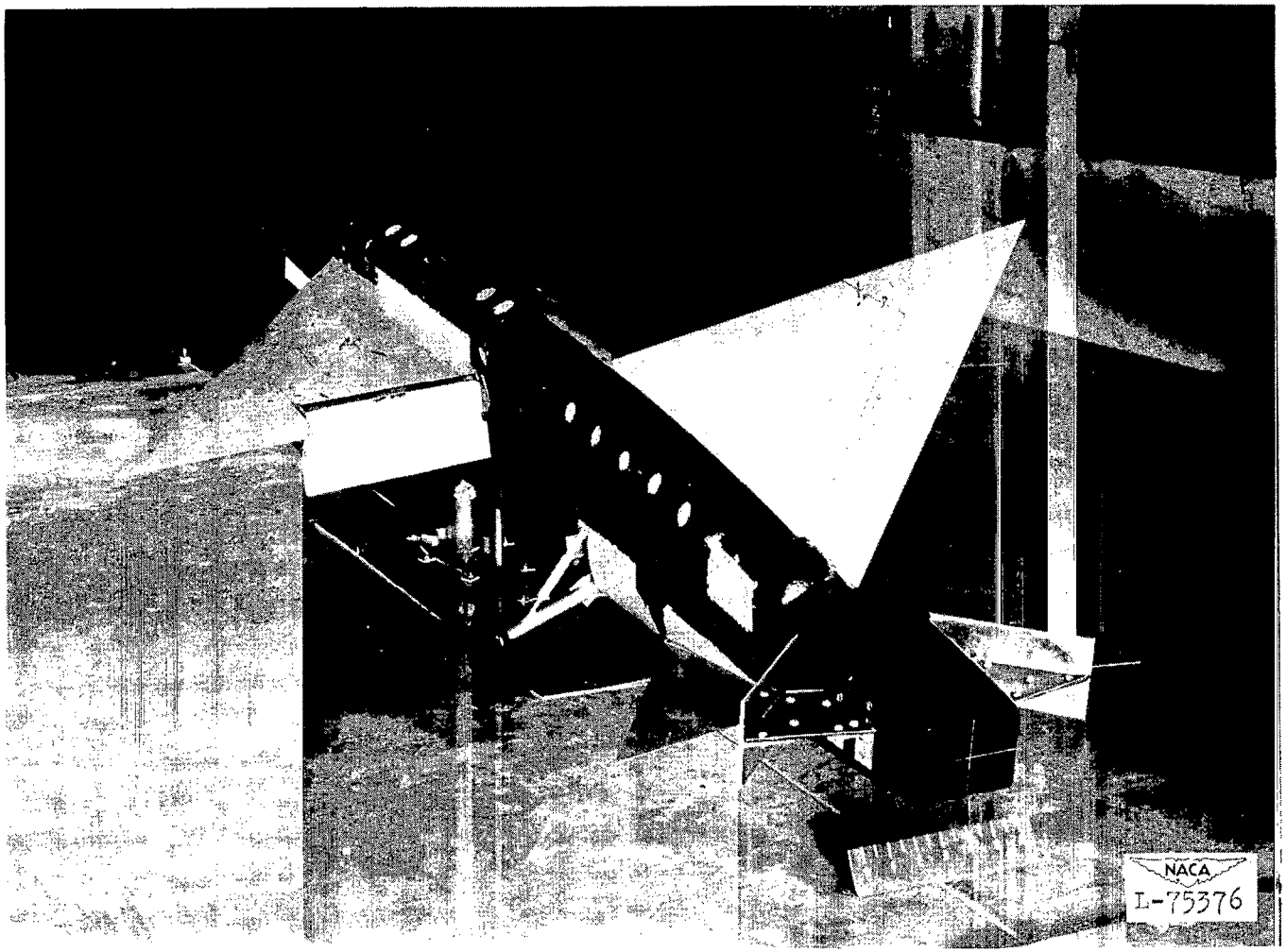

Figure 4.- Views of the model in the landing configuration in the presence of the ground board. Wing position B; $i_w = 0^\circ$; tail 2; tanks on; brakes deflected 50°; $\delta_f = 57^\circ$.

Figure 4.- Concluded.

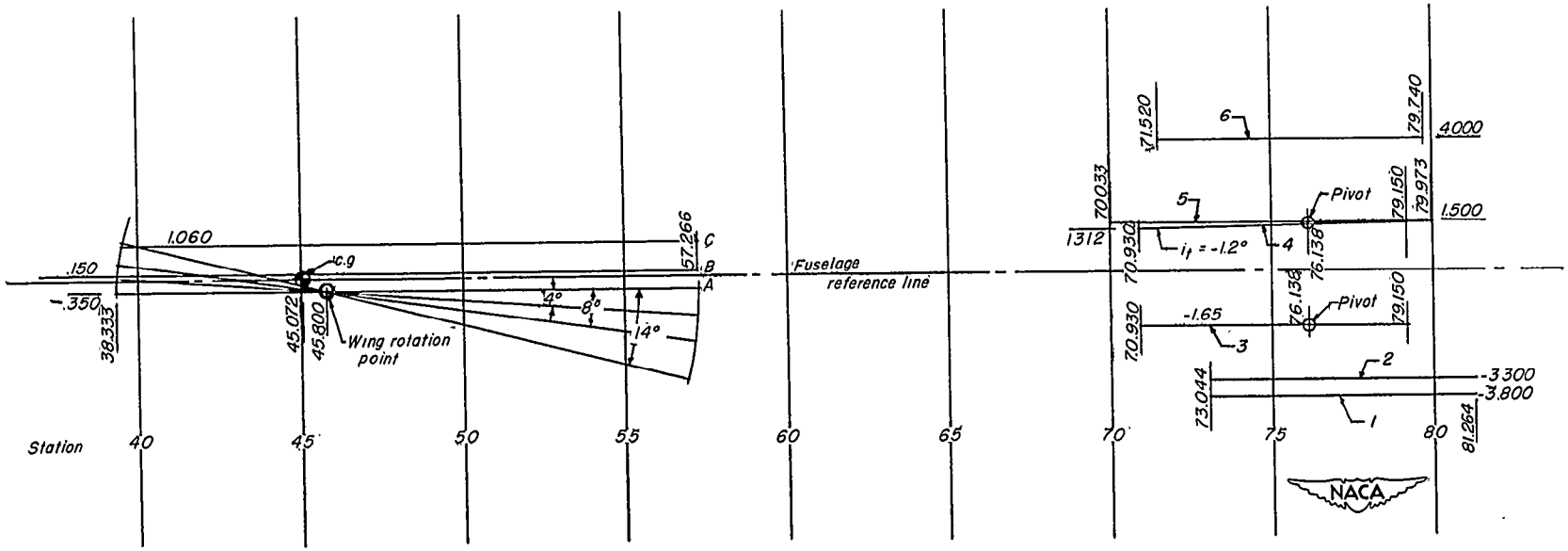

Note: Unswept wing was tested at position A; tail 1 was used with this unswept wing.

Figure 5.- Schematic drawing showing locations of the various wing and tail positions.

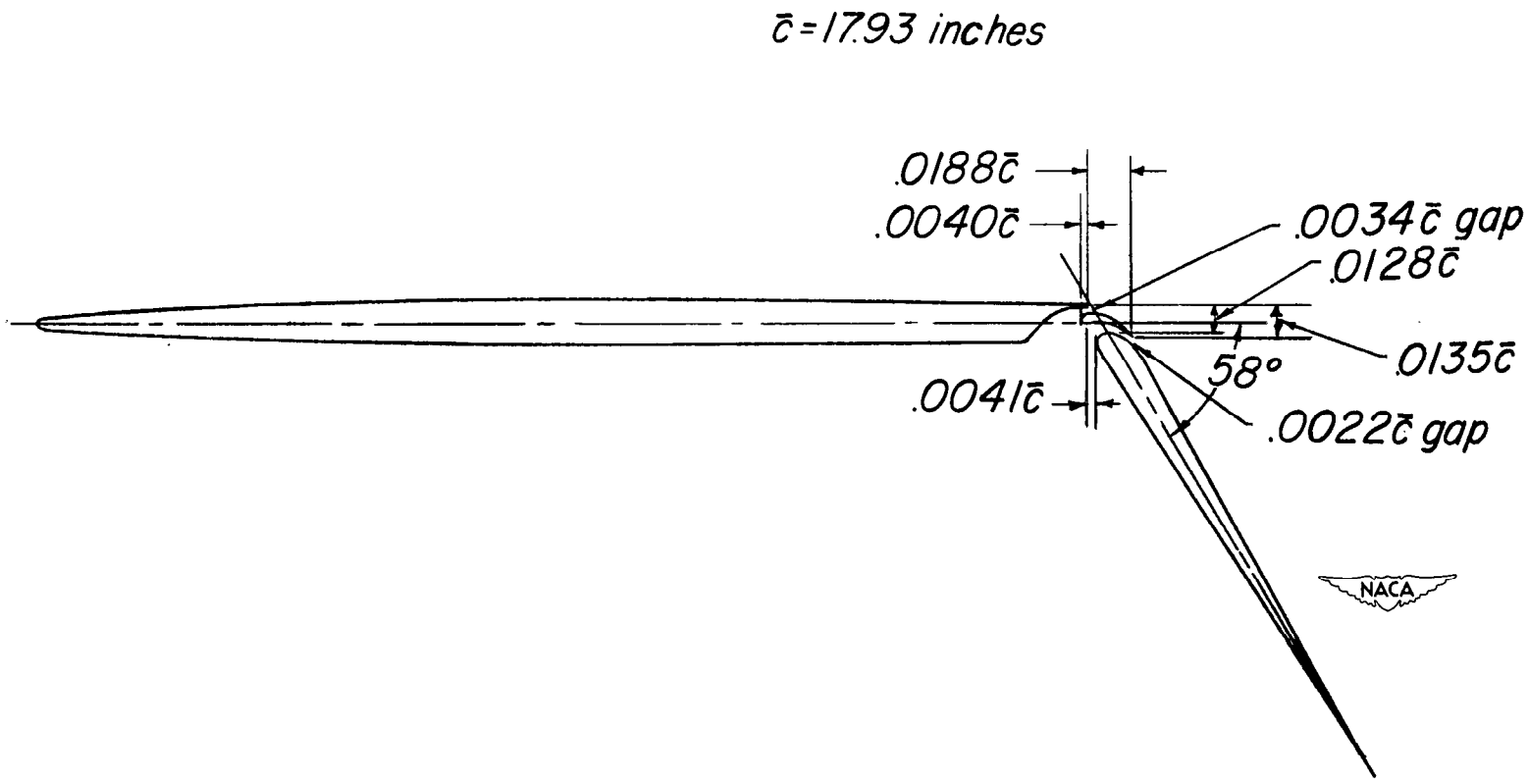

Figure 6.- The optimum flap configuration tested.

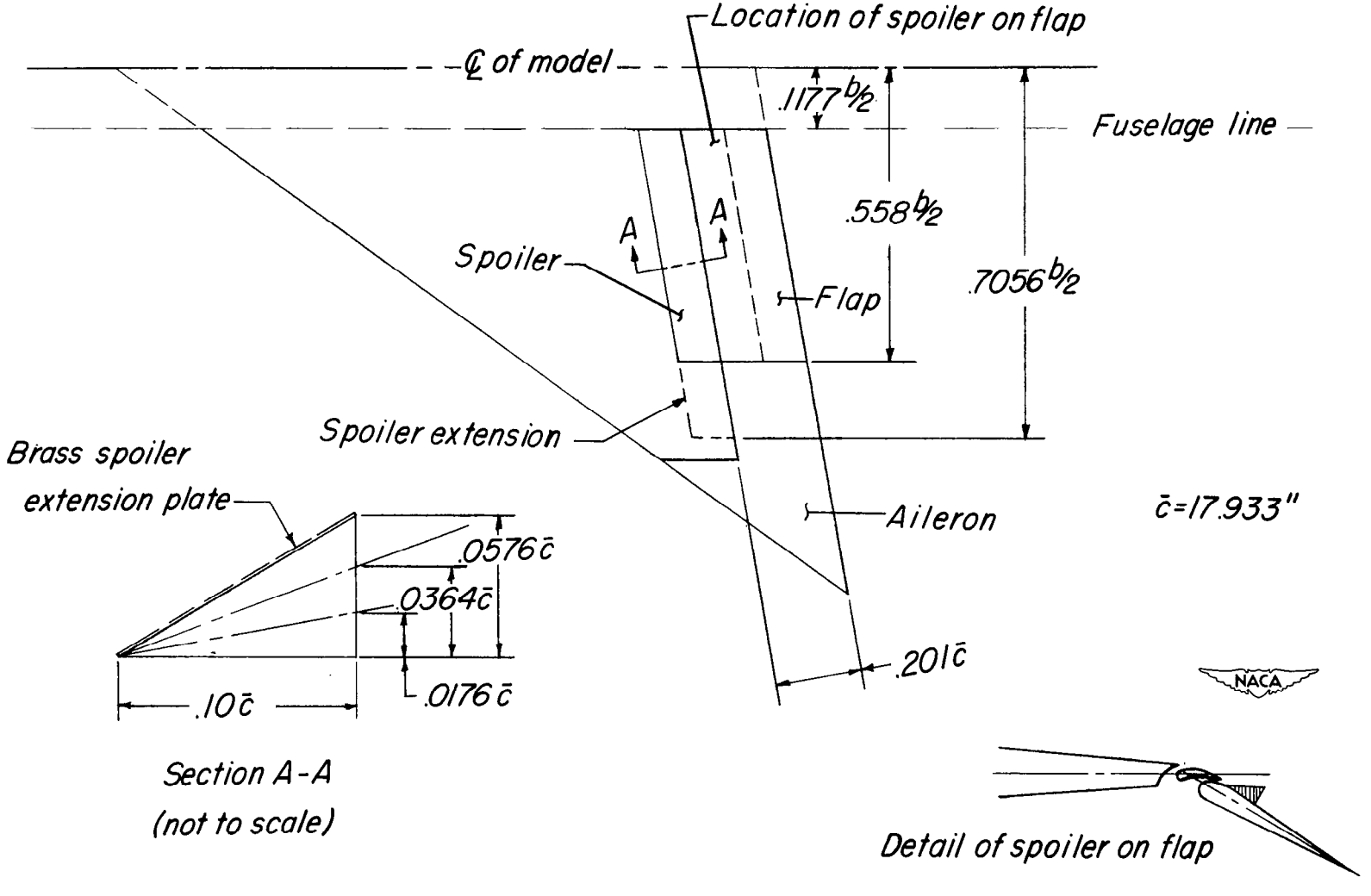

Figure 7.- The details of the spoiler configurations tested.

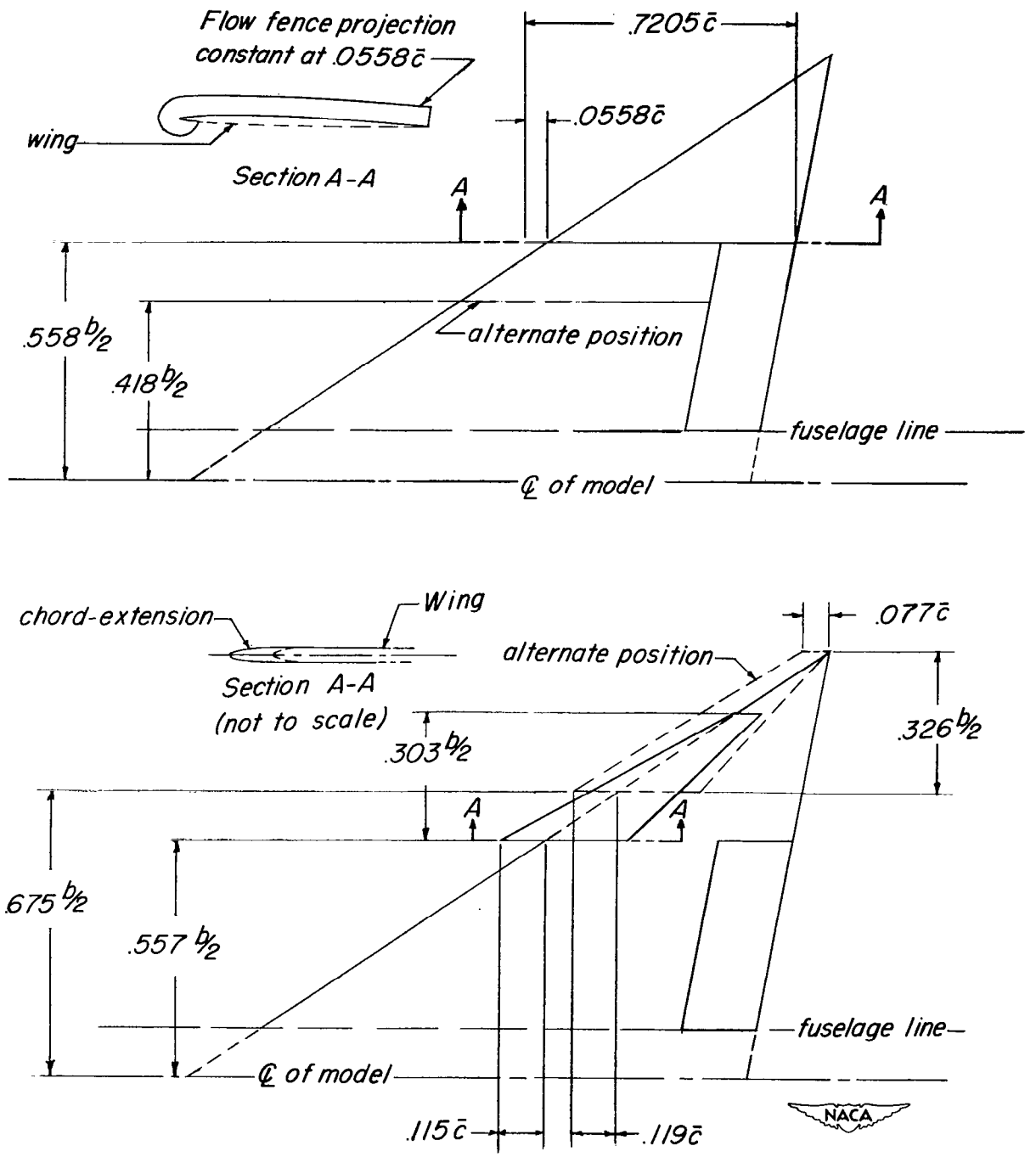

Figure 8.- The auxiliary flow control devices tested.

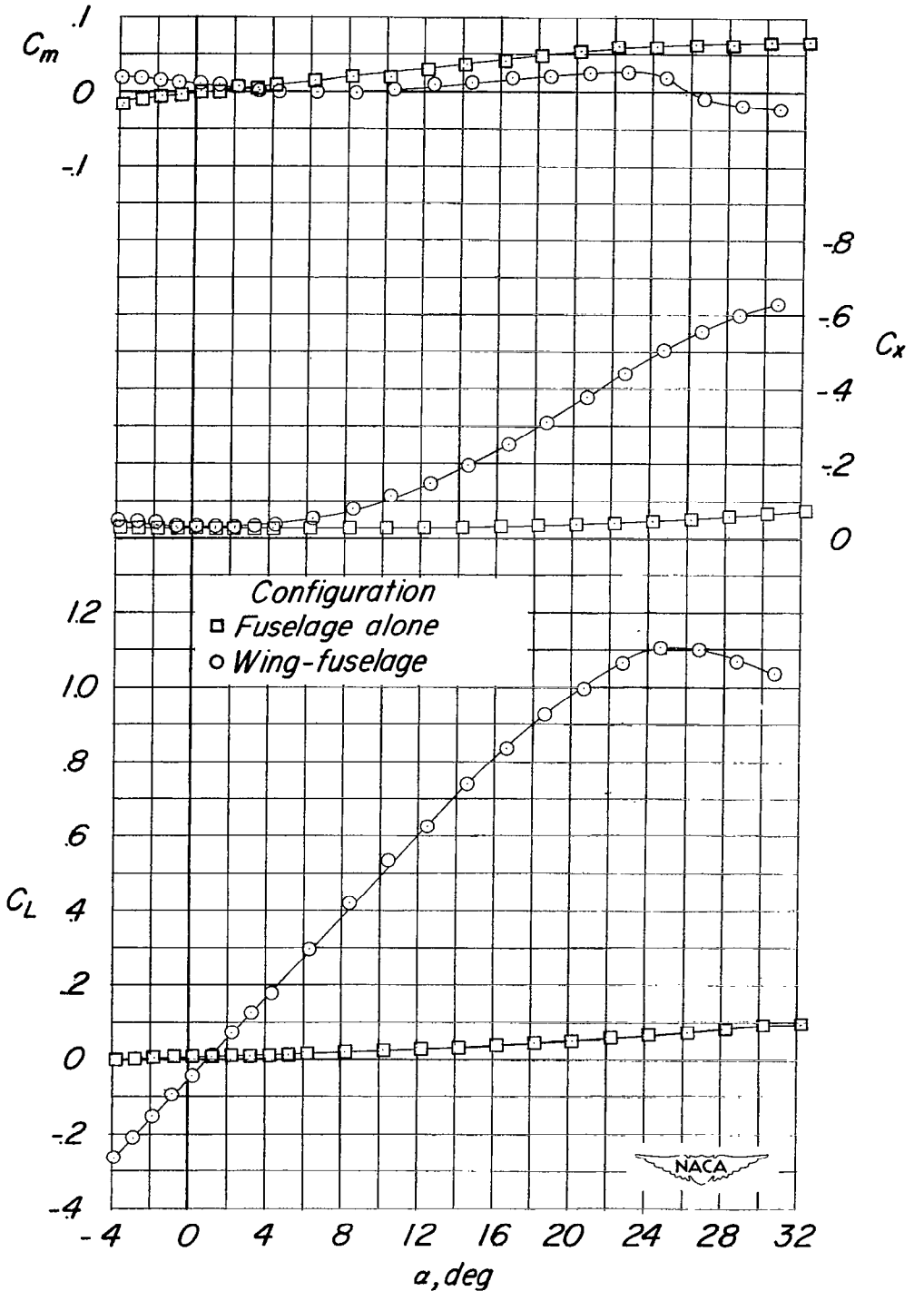

Figure 9.- The aerodynamic characteristics in pitch of the fuselage and wing-fuselage configurations. Wing position A; $i_w = 0°$; q = 101.5 lb/sq ft.

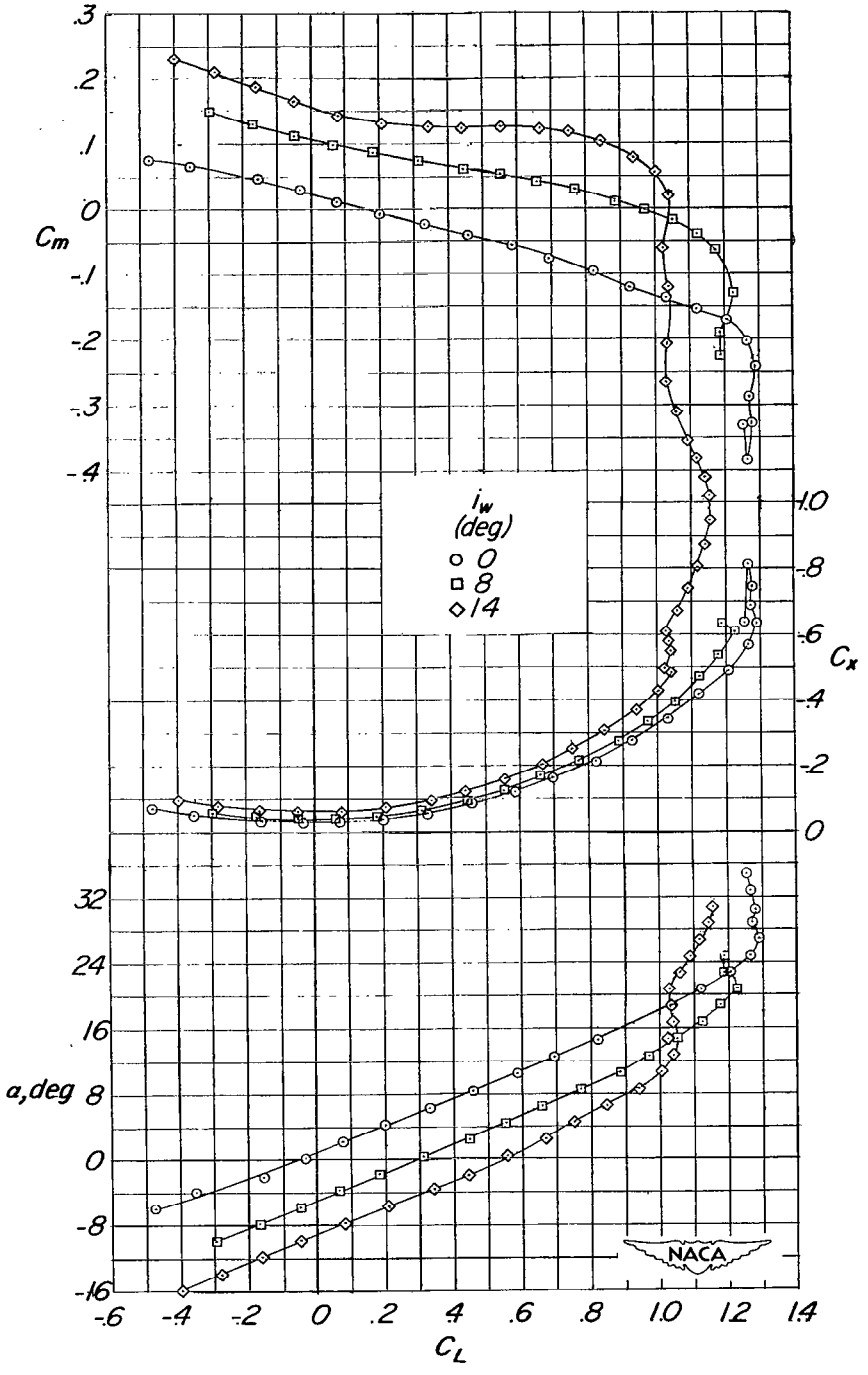

(a) Tail 1.

Figure 10.- The effect of wing incidence on the aerodynamic characteristics in pitch. Wing position A; q = 101.5 lb/sq ft.

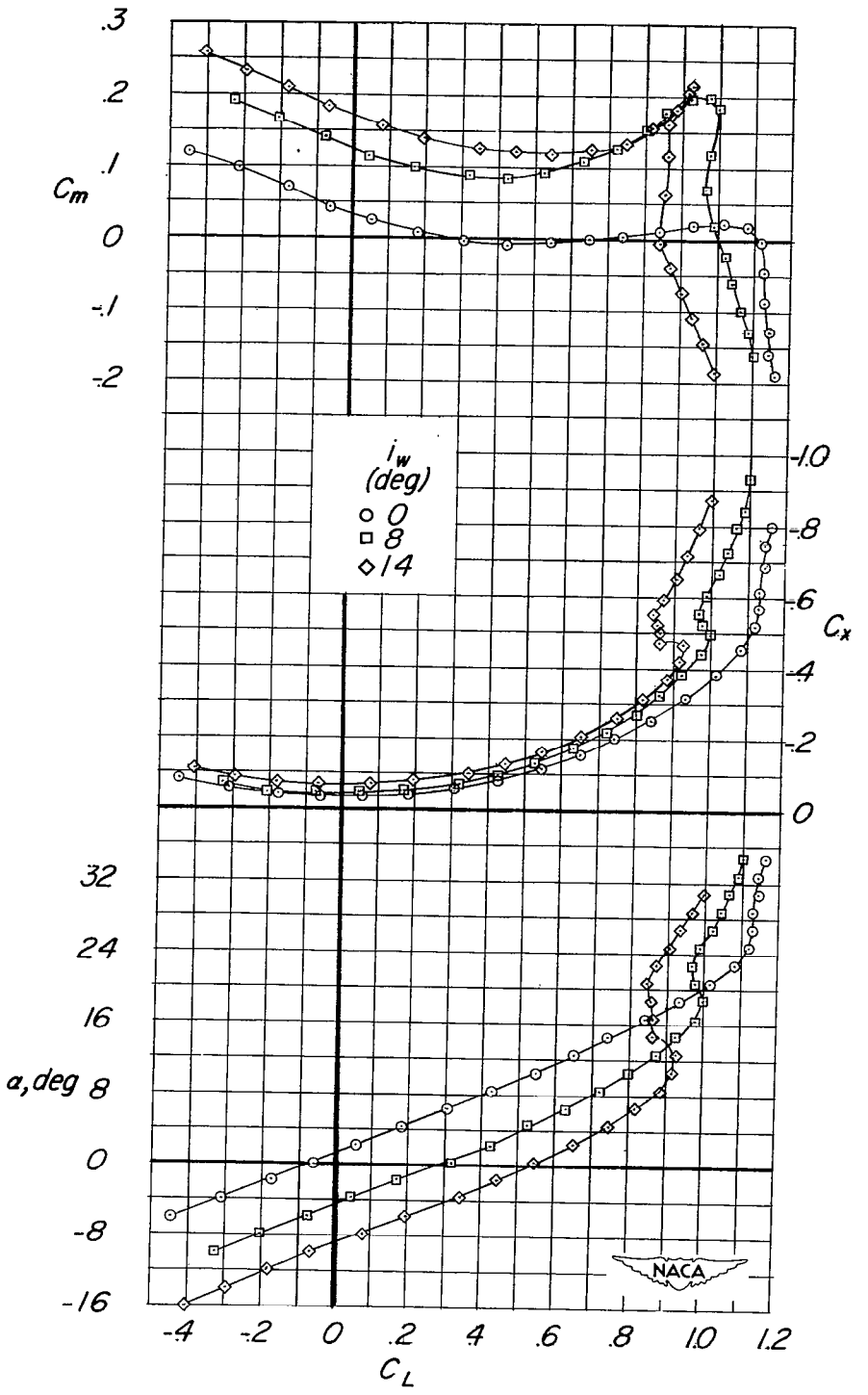

(b) Tail 6.

Figure 10.- Continued.

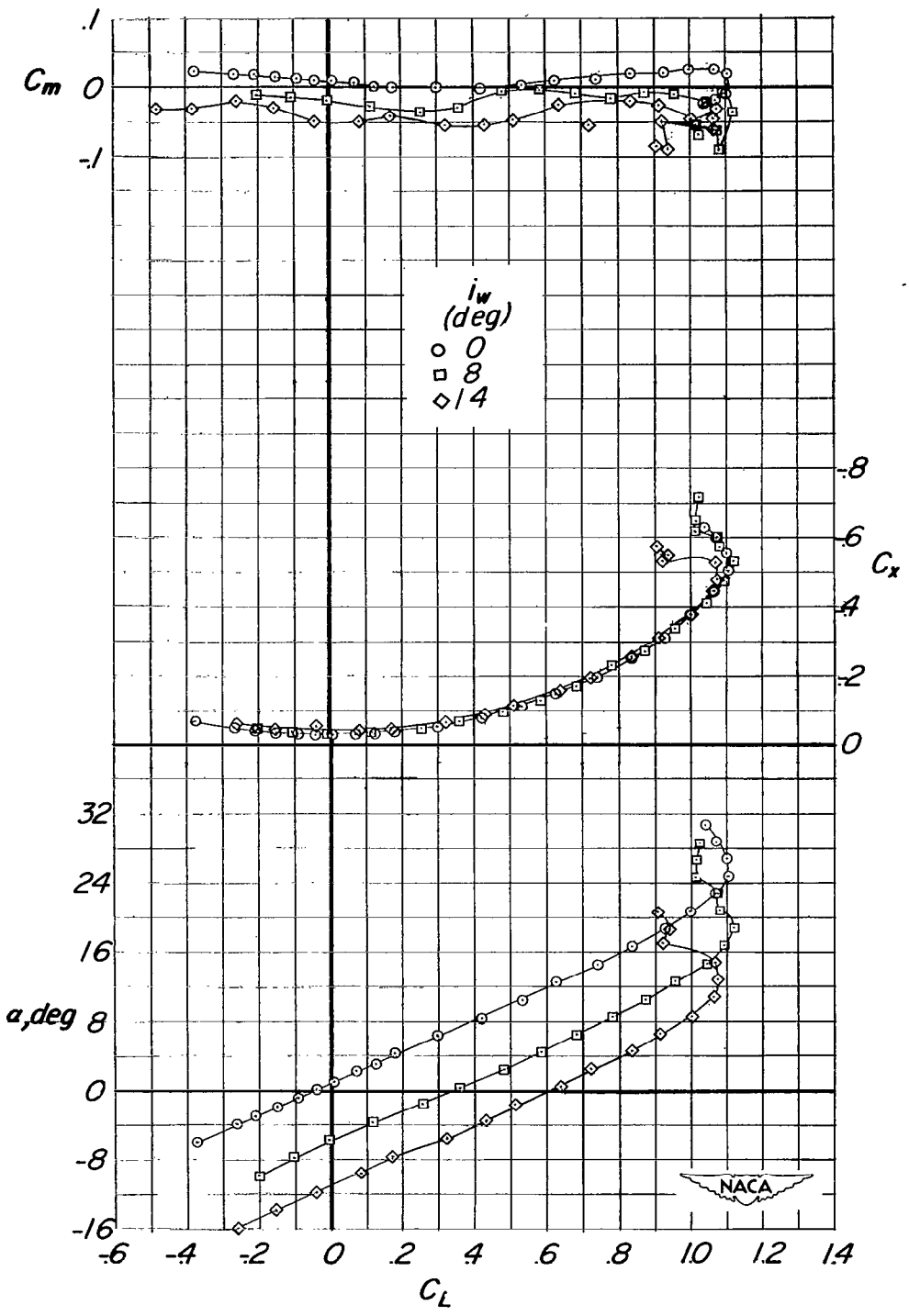

(c) Tail off.

Figure 10.- Concluded.

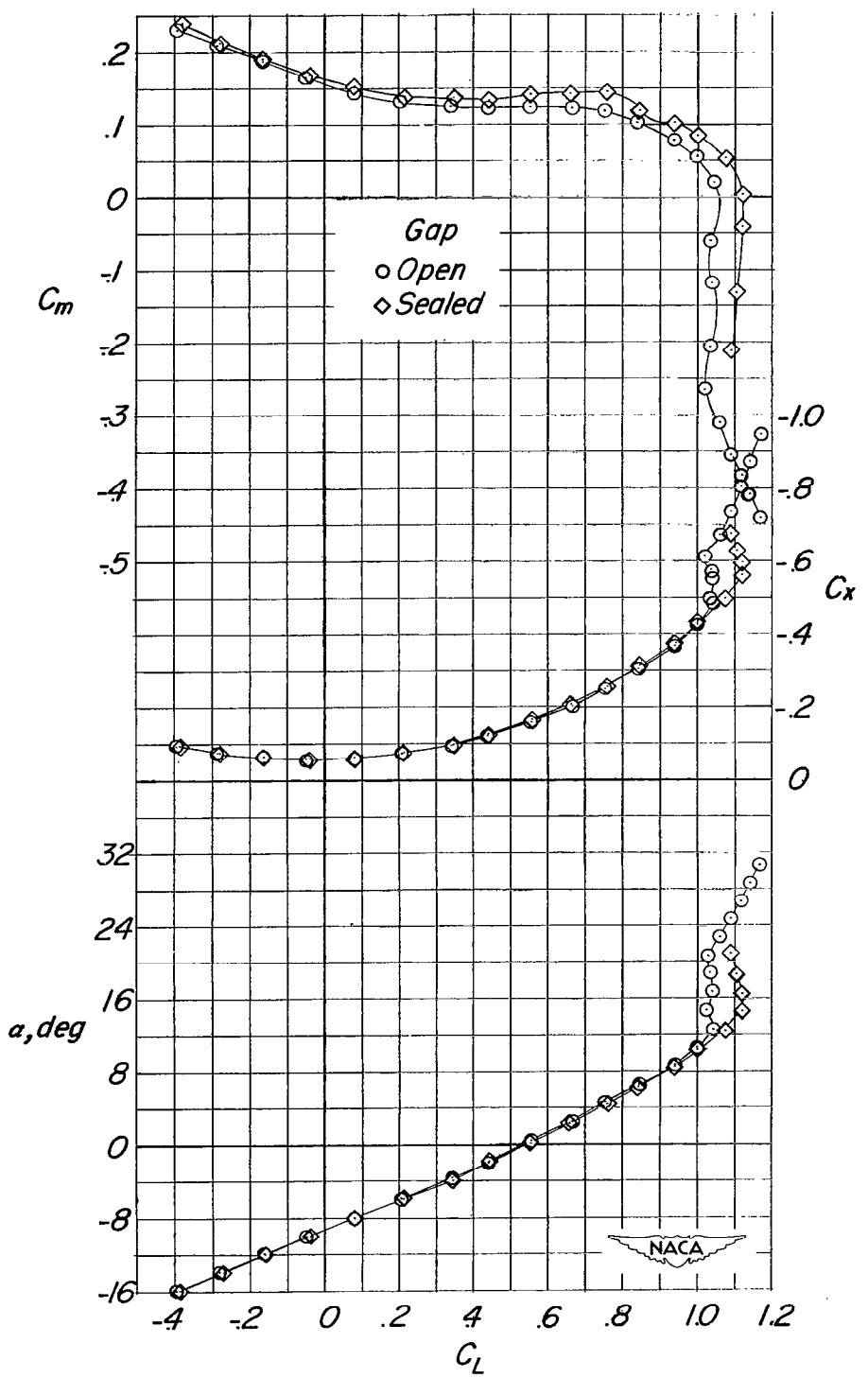

Figure 11.- The effect of gap at the wing-fuselage juncture on the aerodynamic characteristics in pitch. Wing position A; $i_w = 14^\circ$; tail 1; q = 101.5 lb/sq ft.

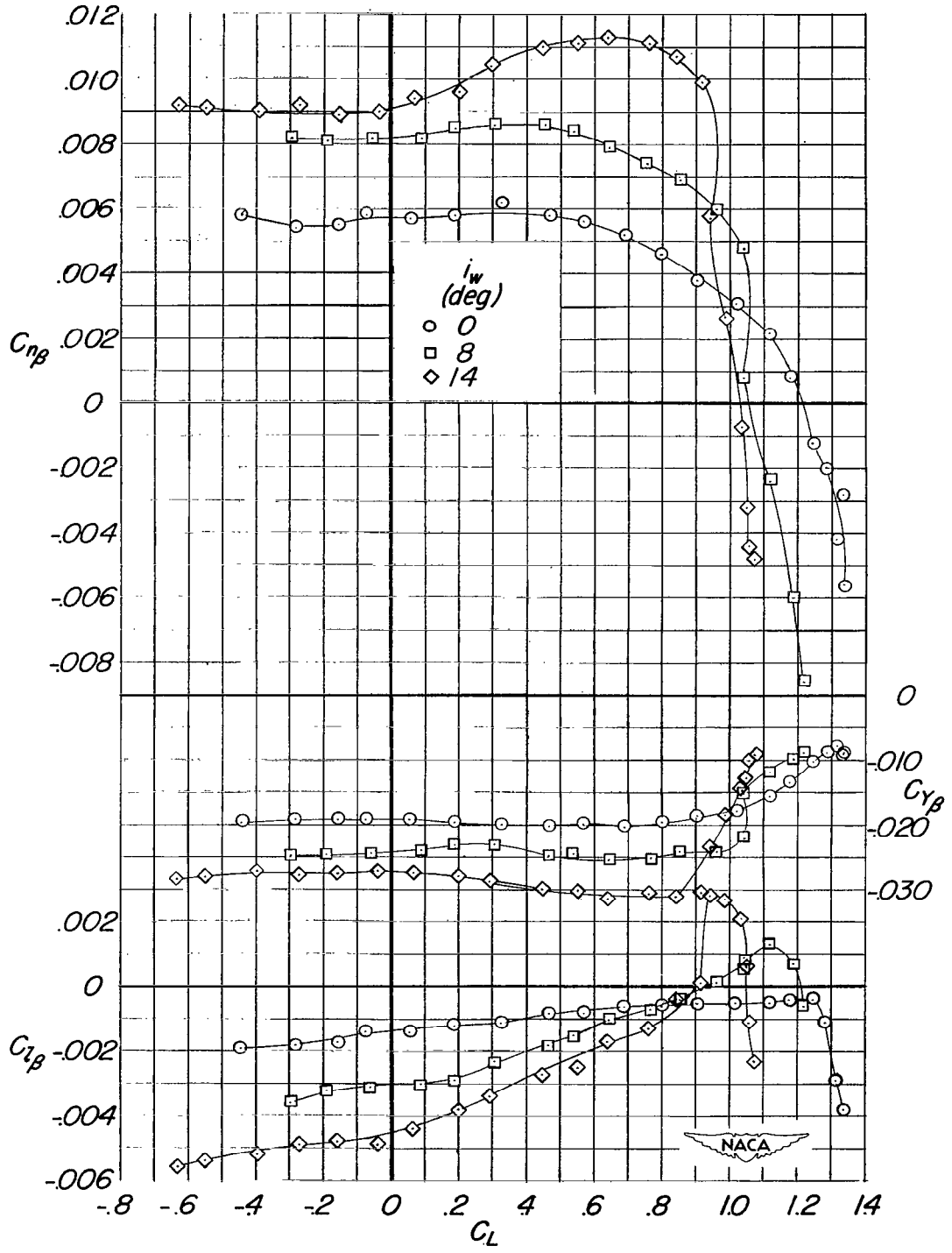

Figure 12.- Effect of wing incidence on the variation of the lateral-stability parameters with lift coefficient. Wing position A; tail 1; $i_t = 0^\circ$.

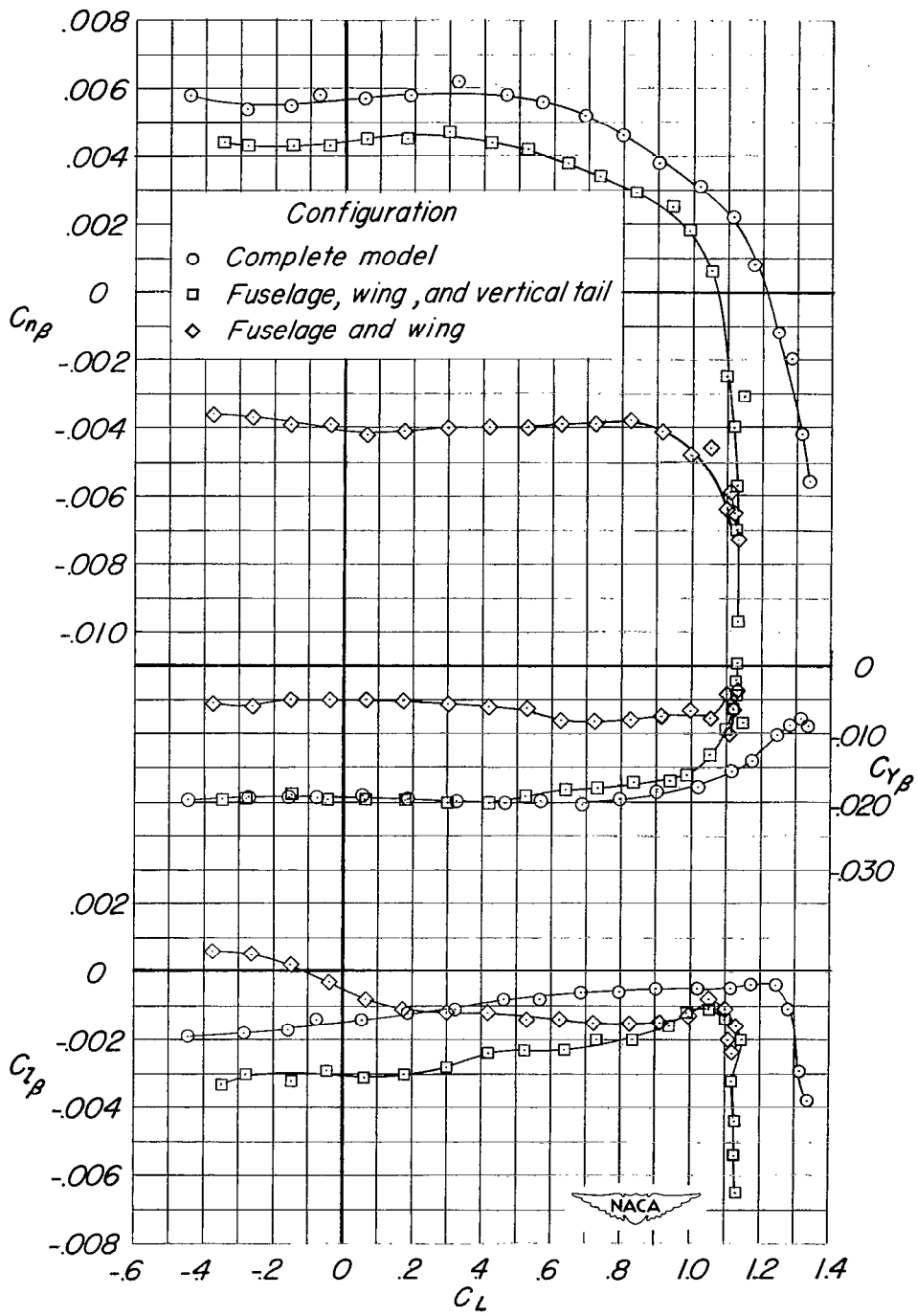

(a) $i_w = 0^\circ$.

Figure 13.- Effect of model configuration on the variation of the lateral-stability parameters with lift coefficient. Wing position A; tail 1; $i_t = 0^\circ$.

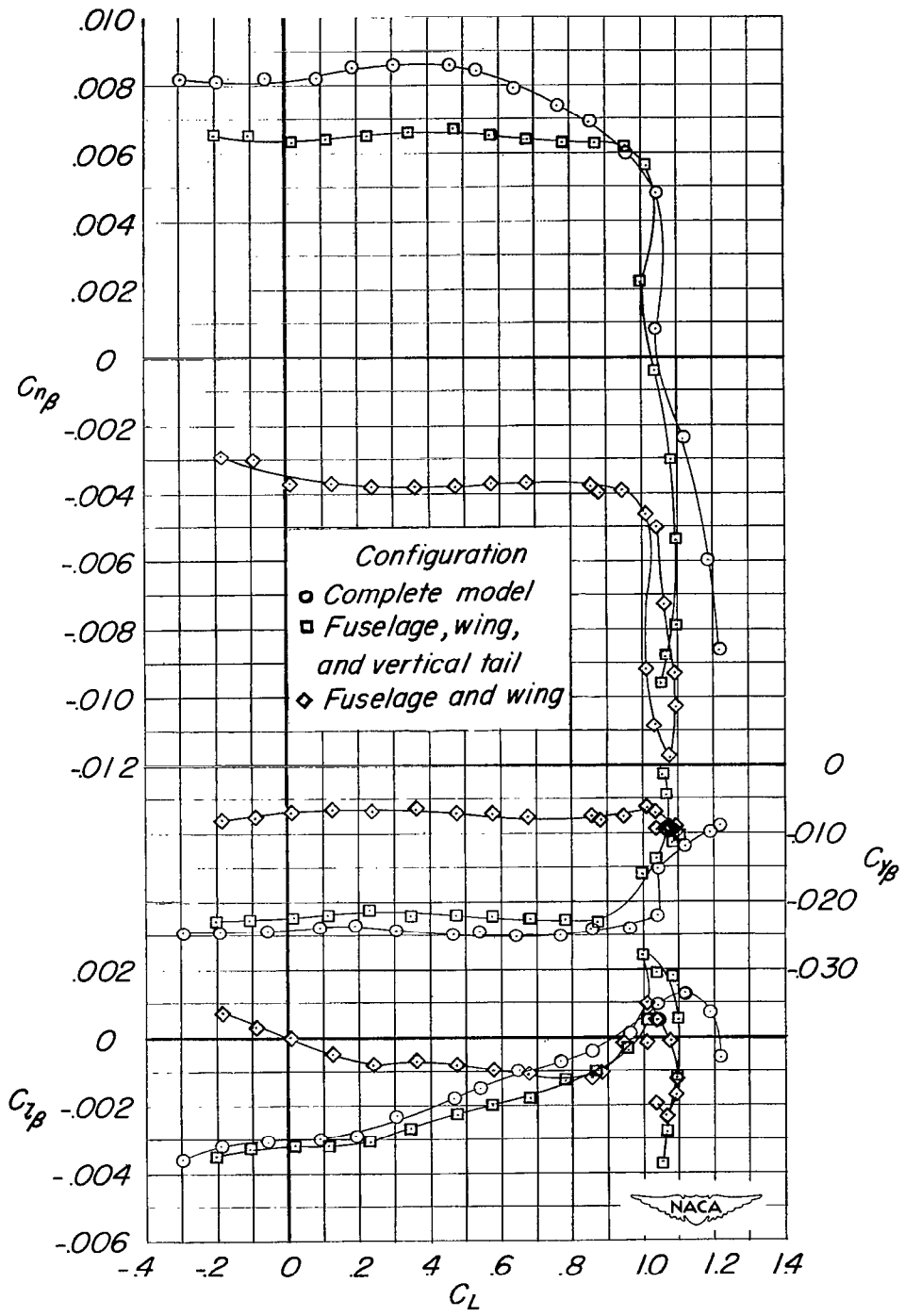

(b) $i_w = 8^\circ$.

Figure 13.- Continued.

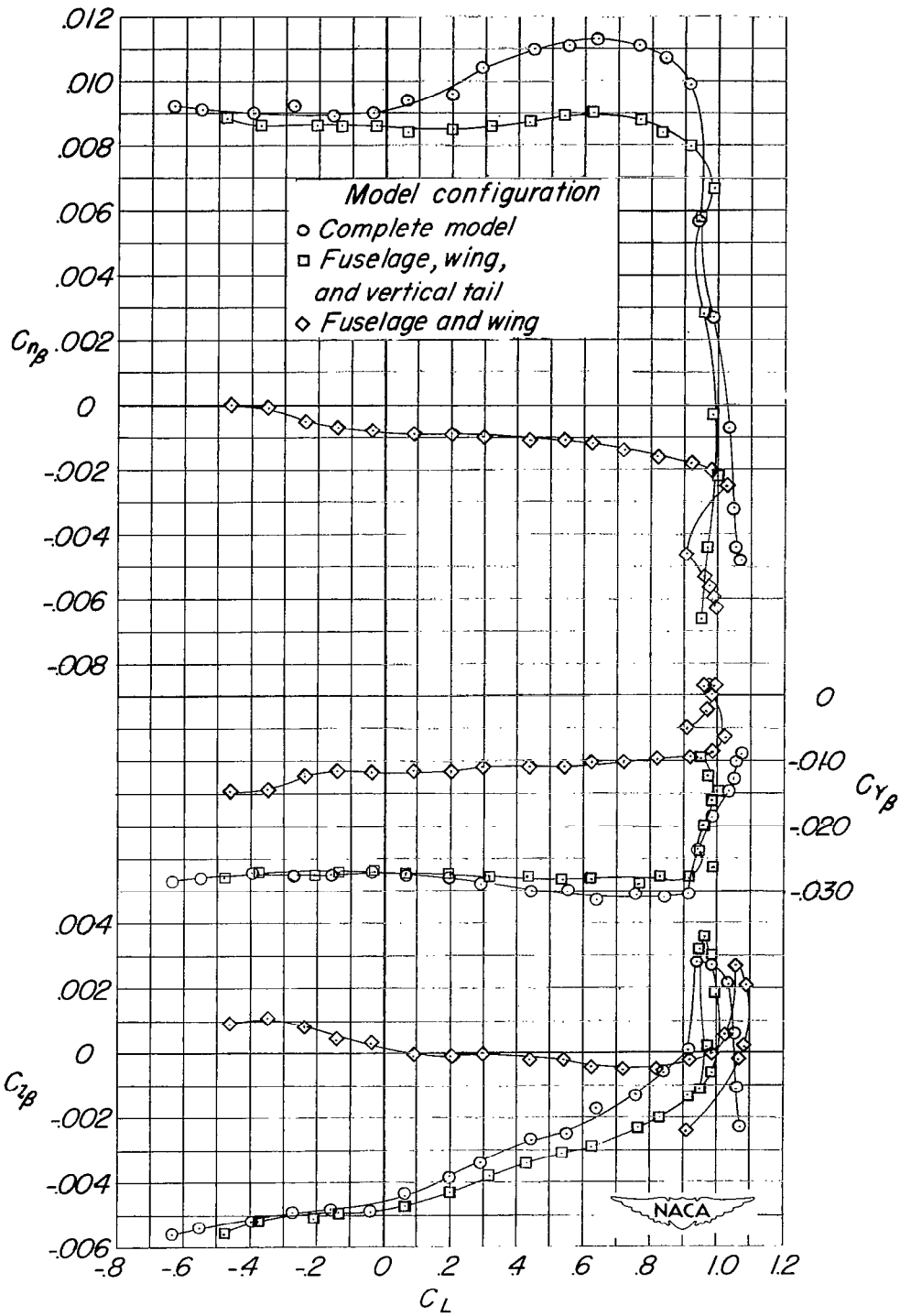

(c) $i_w = 14^\circ$.

Figure 13.- Concluded.

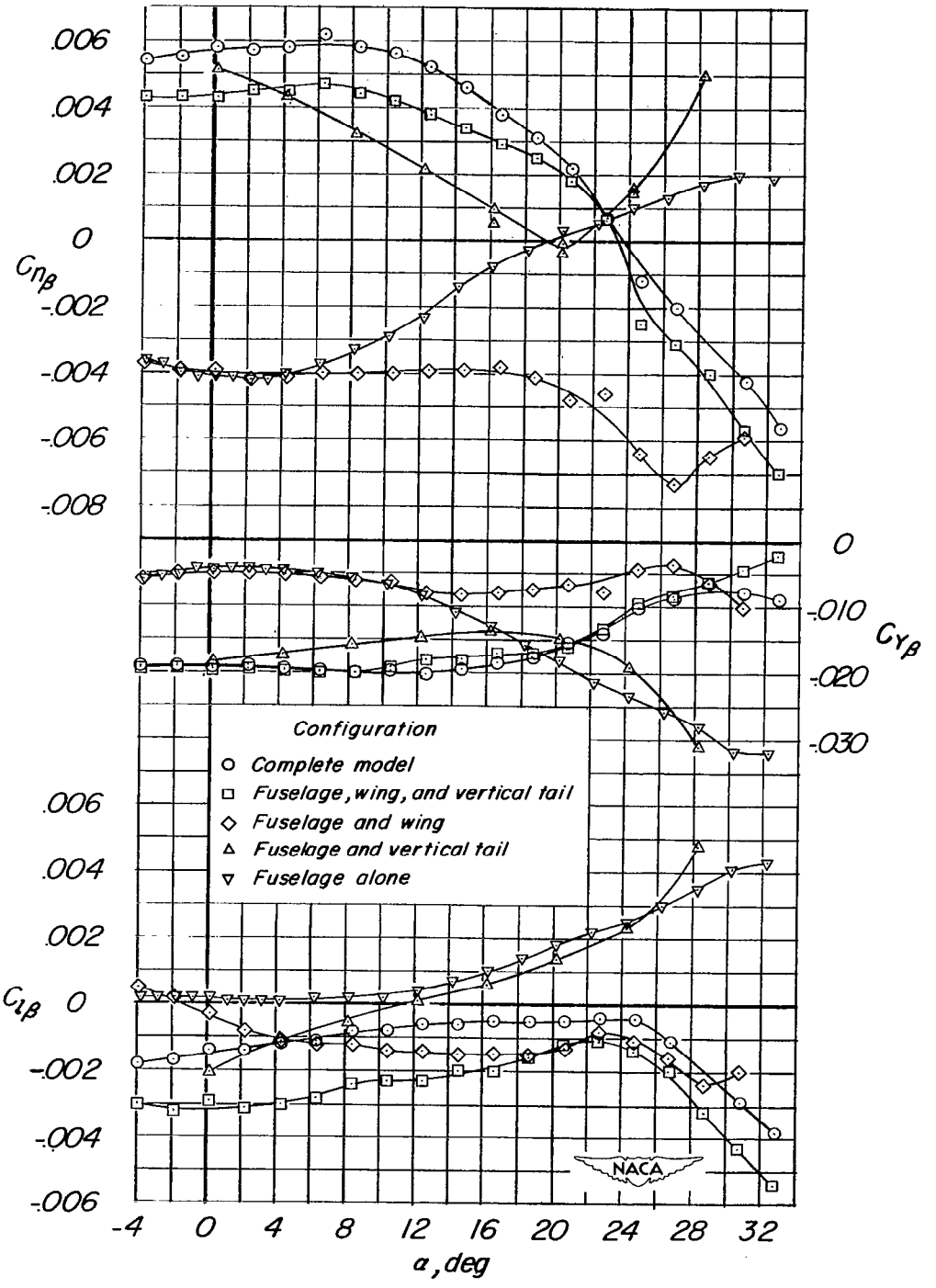

Figure 14.- Effect of model configuration on the variation of the lateral-stability parameters with angle of attack. Wing position A; tail 1; $i_t = 0^\circ$; $i_w = 0^\circ$.

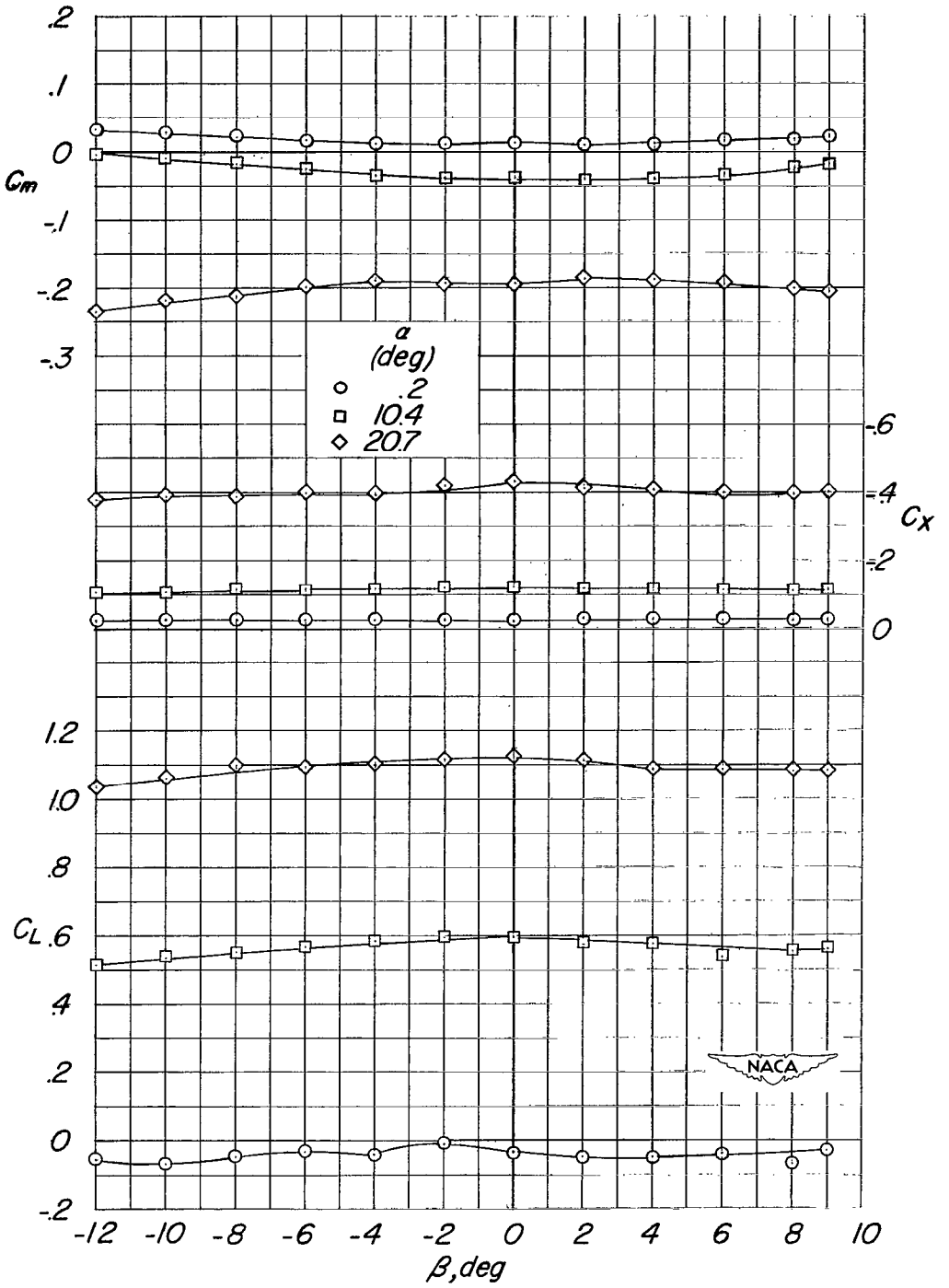

(a) $i_w = 0^\circ$.

Figure 15.- The effect of angle of attack on the aerodynamic characteristics in sideslip. Wing position A; tail 1; $i_t = 0^\circ$; q = 101.5 lb/sq ft.

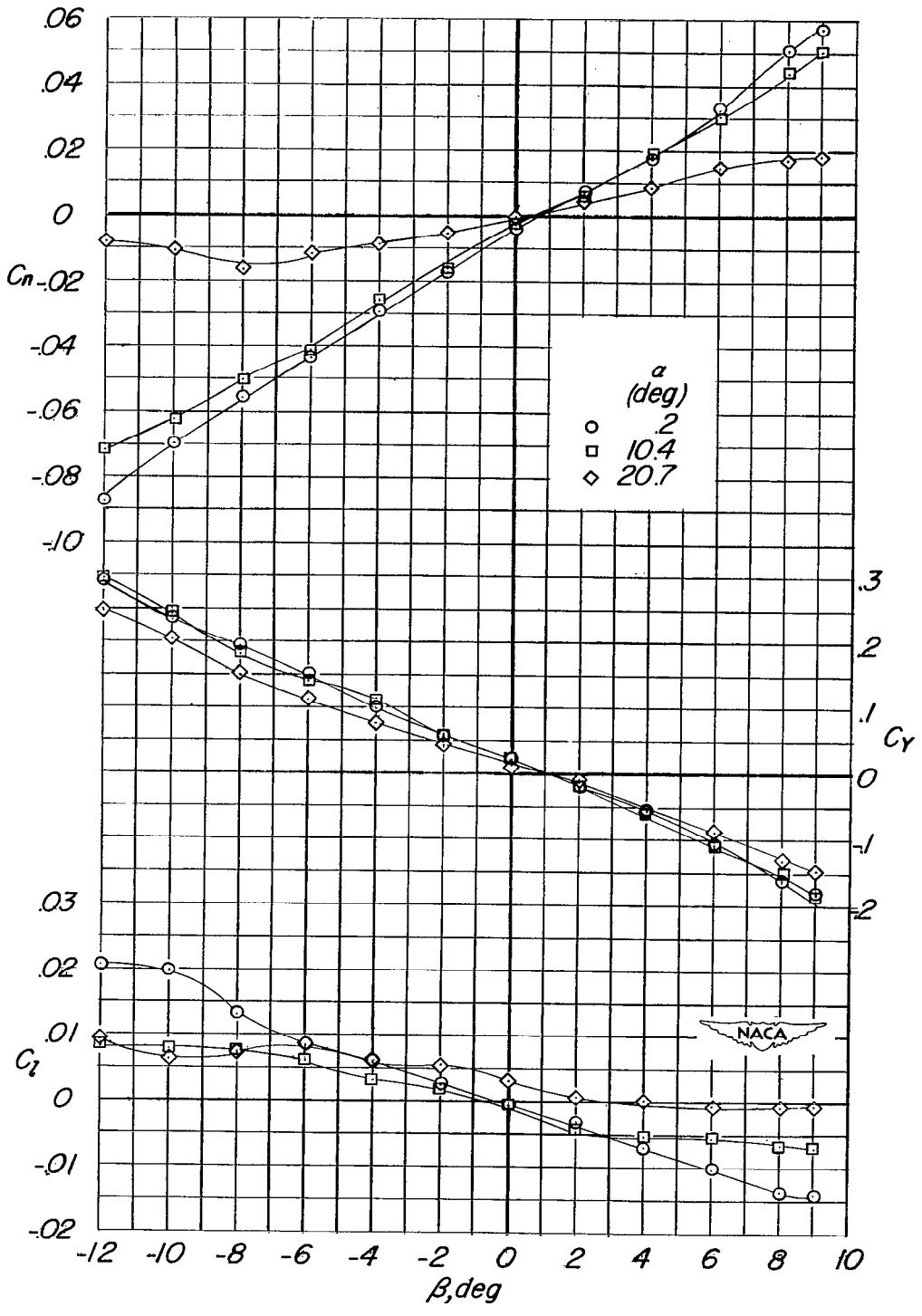

(a) Concluded.

Figure 15.- Continued.

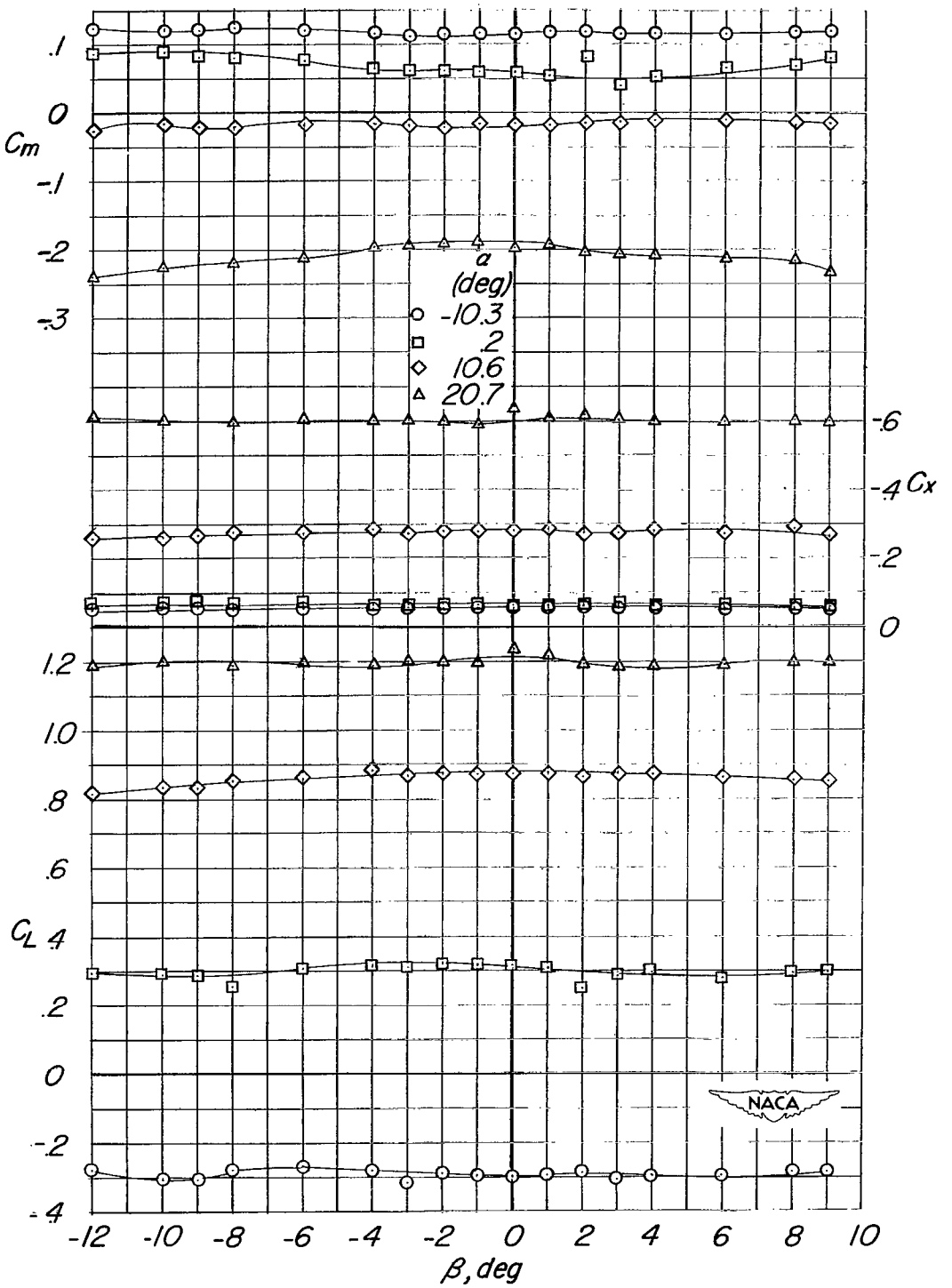

(b) $i_w = 8°$.

Figure 15.- Continued.

[redacted]

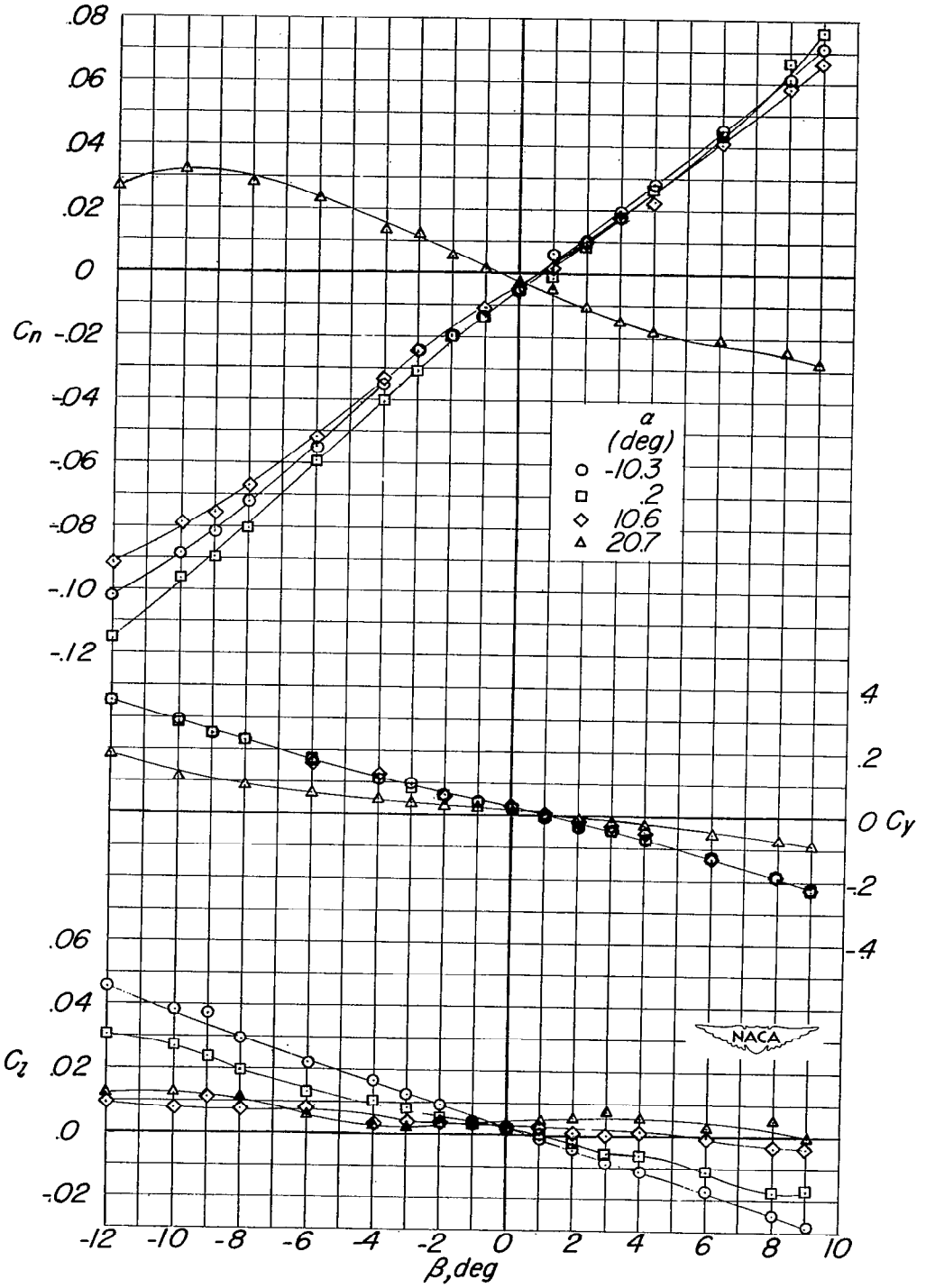

(b) Concluded.

Figure 15.- Continued.

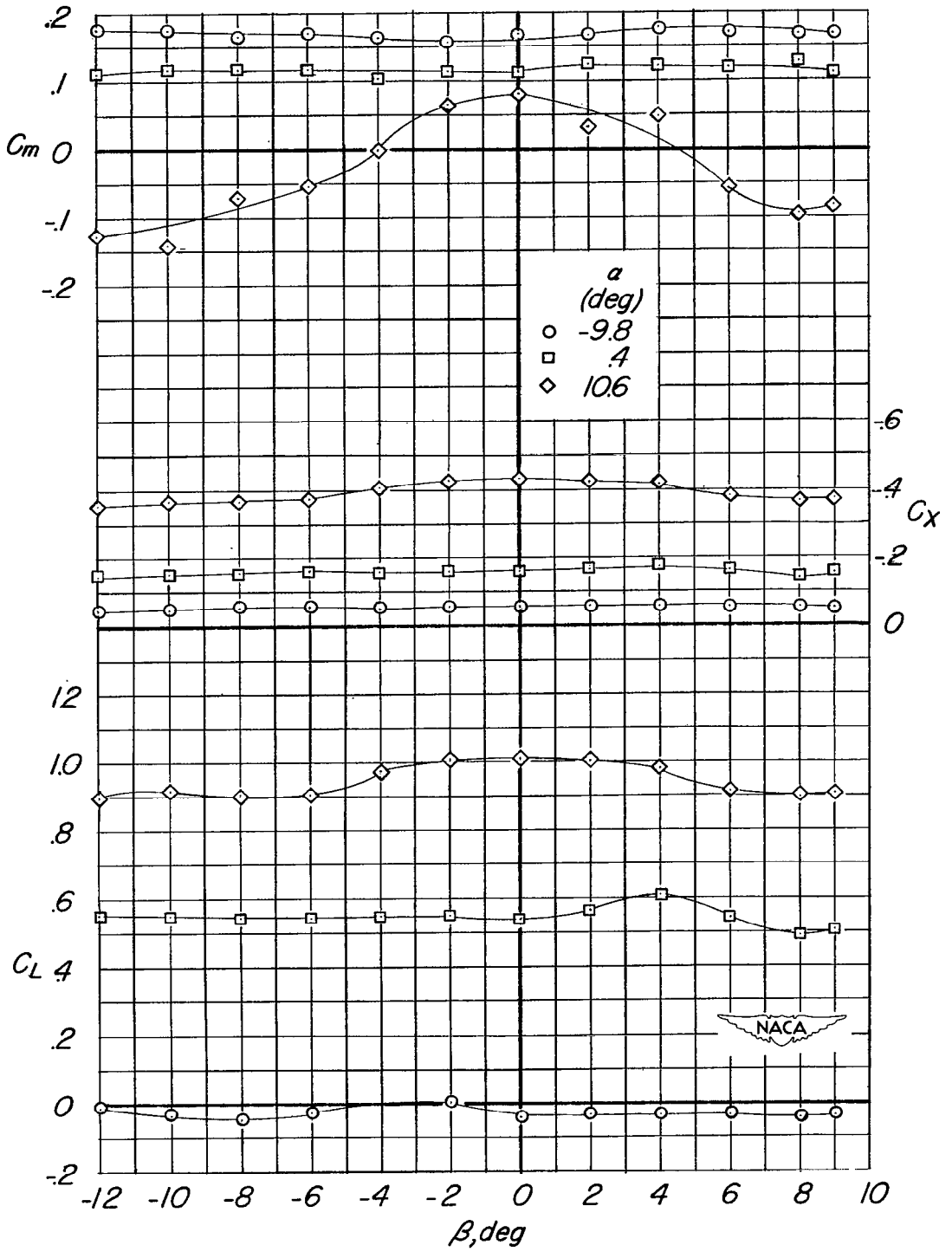

(c) $i_w = 14^\circ$.

Figure 15.- Continued.

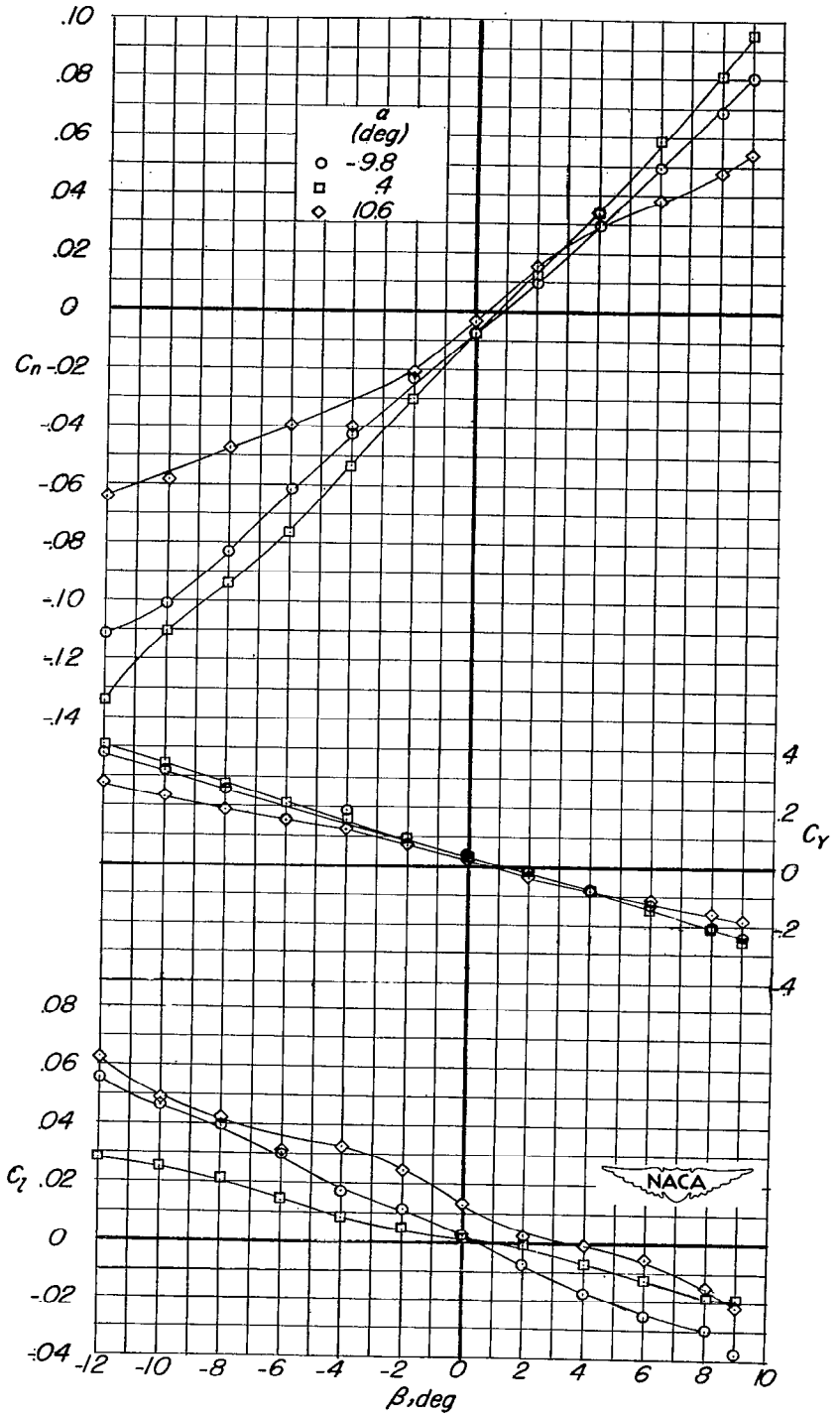

(c) Concluded.

Figure 15.- Concluded.

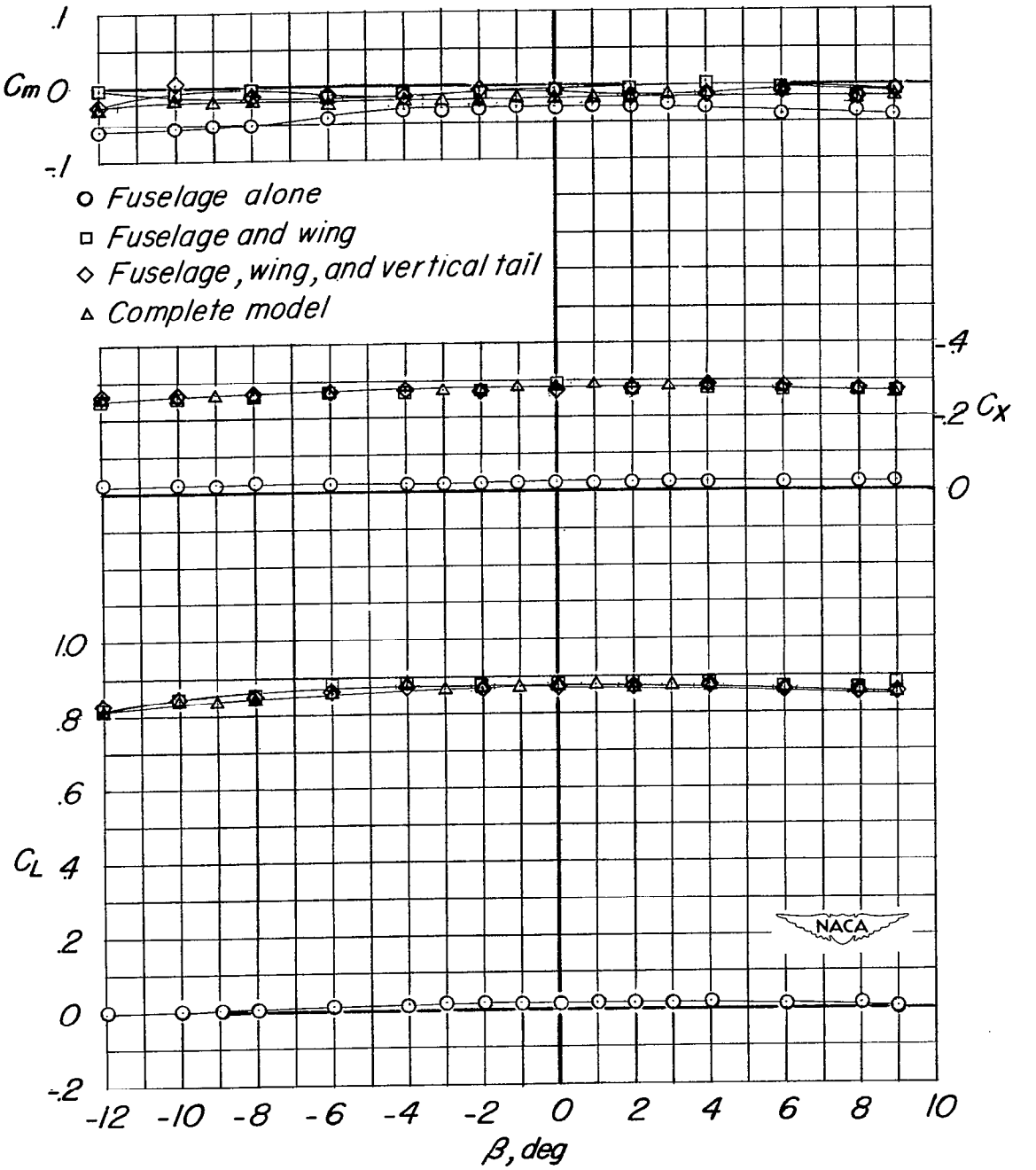

Figure 16.- Effect of model configuration on the aerodynamic characteristics in sideslip. Wing position A; tail 1; $i_w = 8^\circ$; q = 101.5 lb/sq ft.

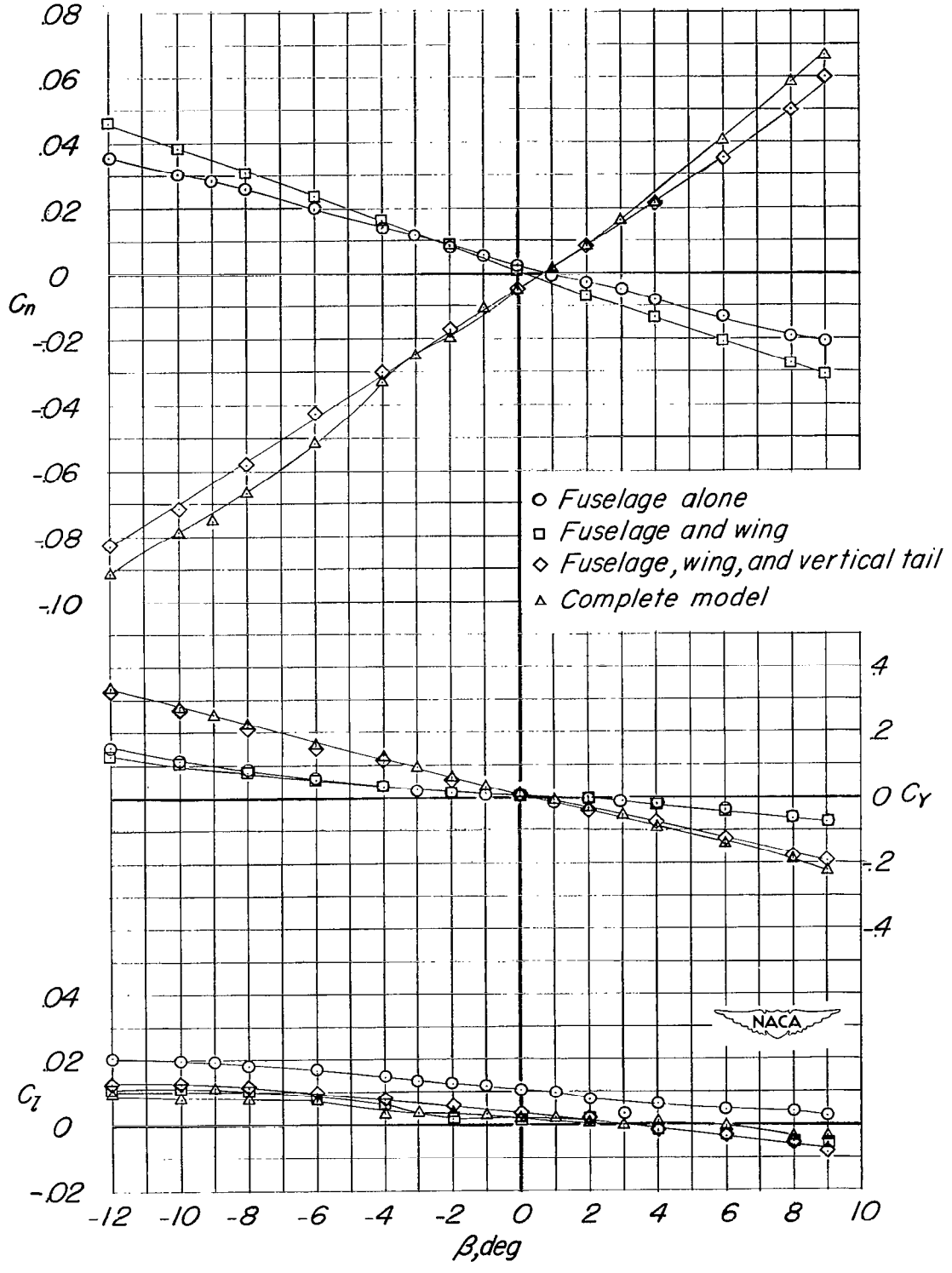

Figure 16.- Concluded.

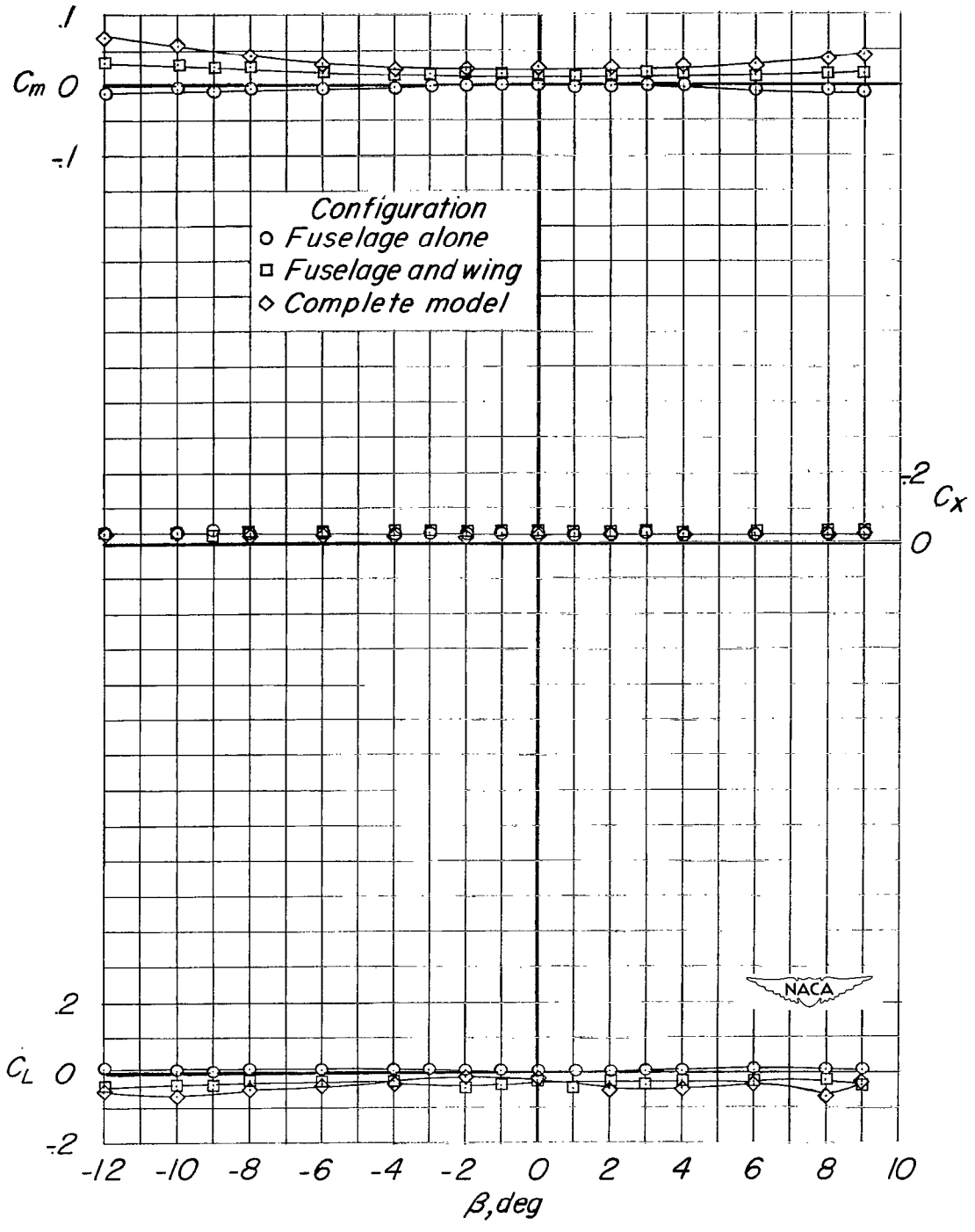

(a) $\alpha = 0.2^{\circ}$.

Figure 17.- Effect of model configuration on the aerodynamic characteristics in sideslip. Wing position A; $i_w = 0^{\circ}$; tail 1; q = 101.5 lb/sq ft.

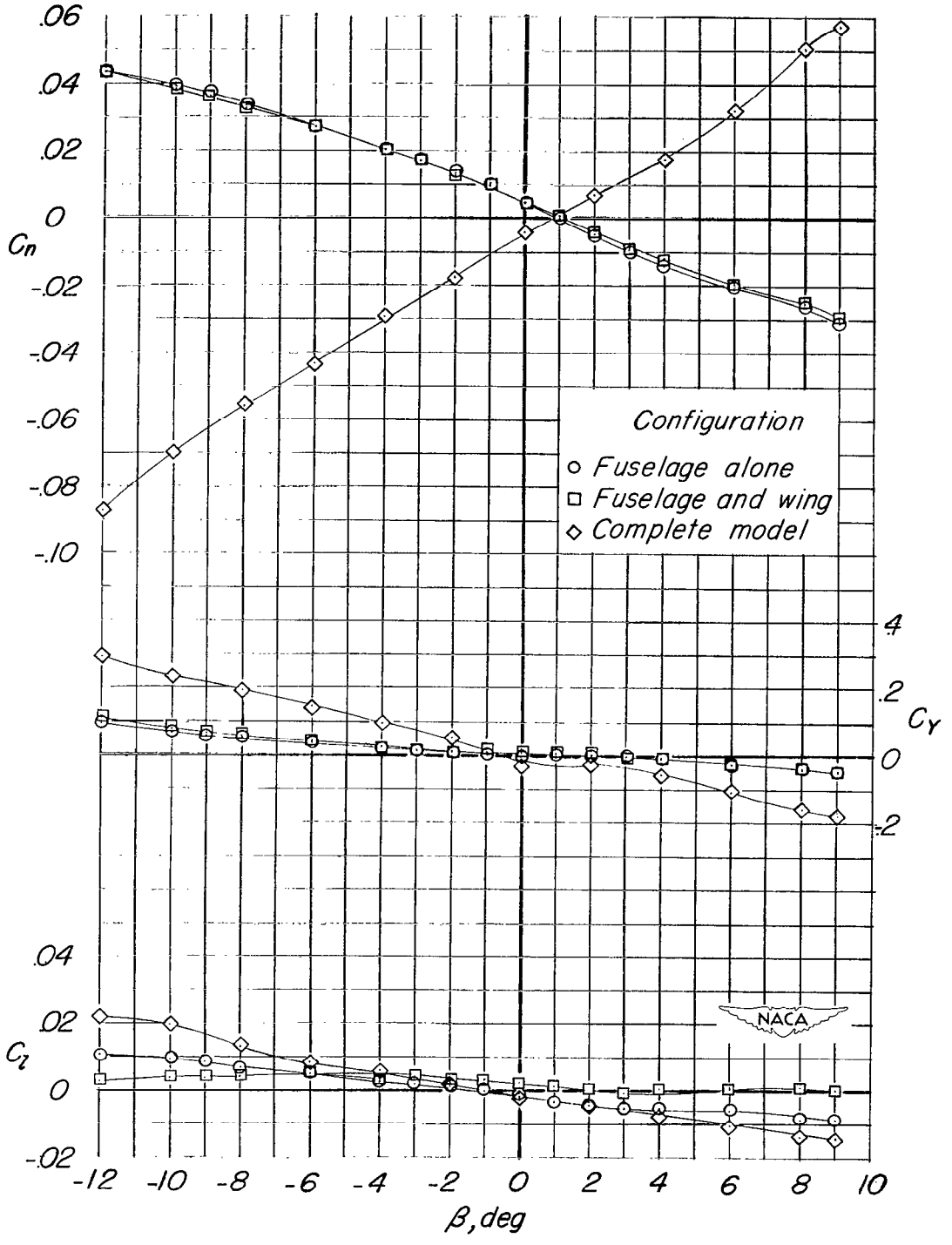

(a) Concluded.

Figure 17.- Continued.

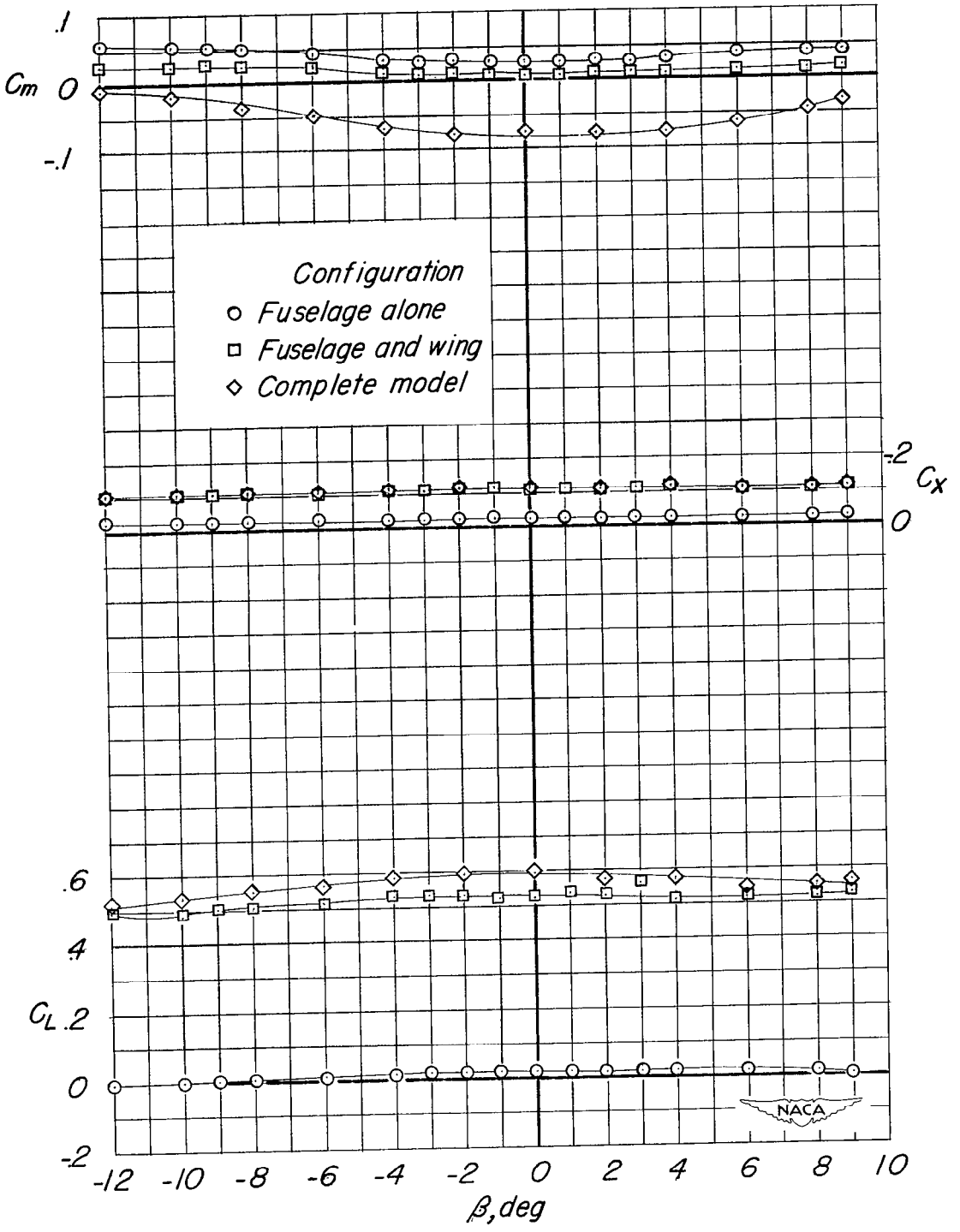

(b) $\alpha = 10.4^{\circ}$.

Figure 17.- Continued.

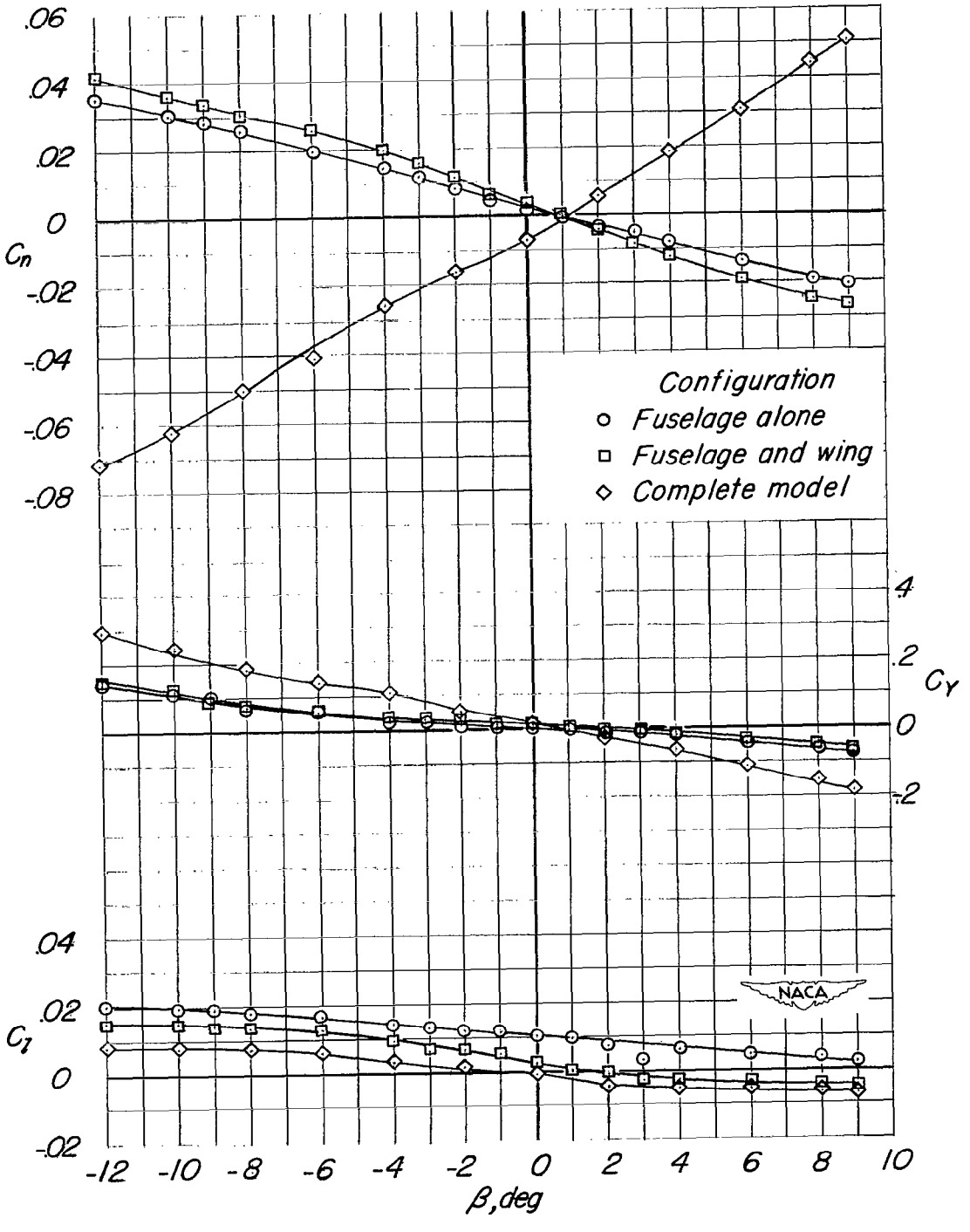

(b) Concluded.

Figure 17.- Continued.

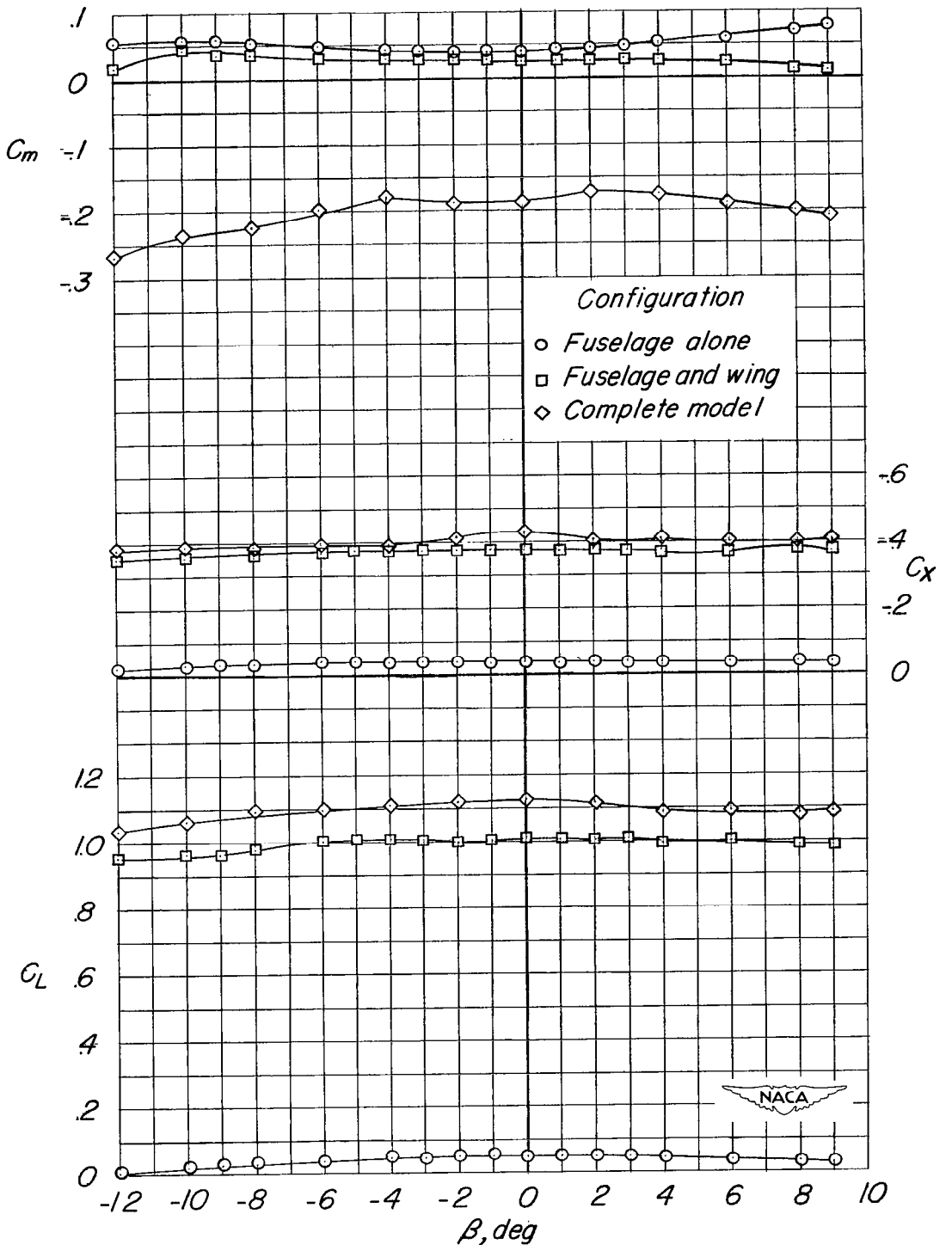

(c) $\alpha = 20.6^{\circ}$.

Figure 17.- Continued.

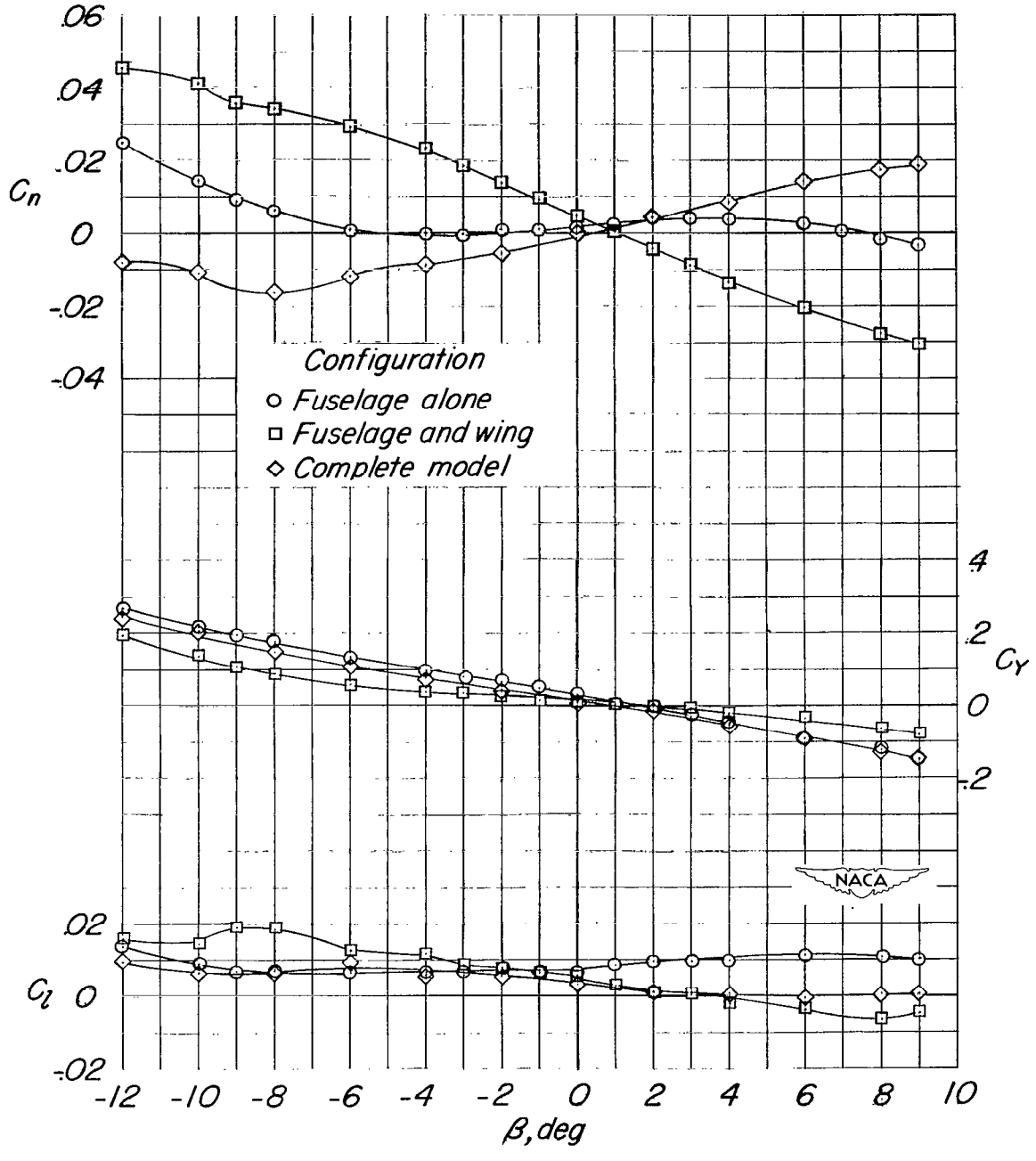

(c) Concluded.

Figure 17.- Concluded.

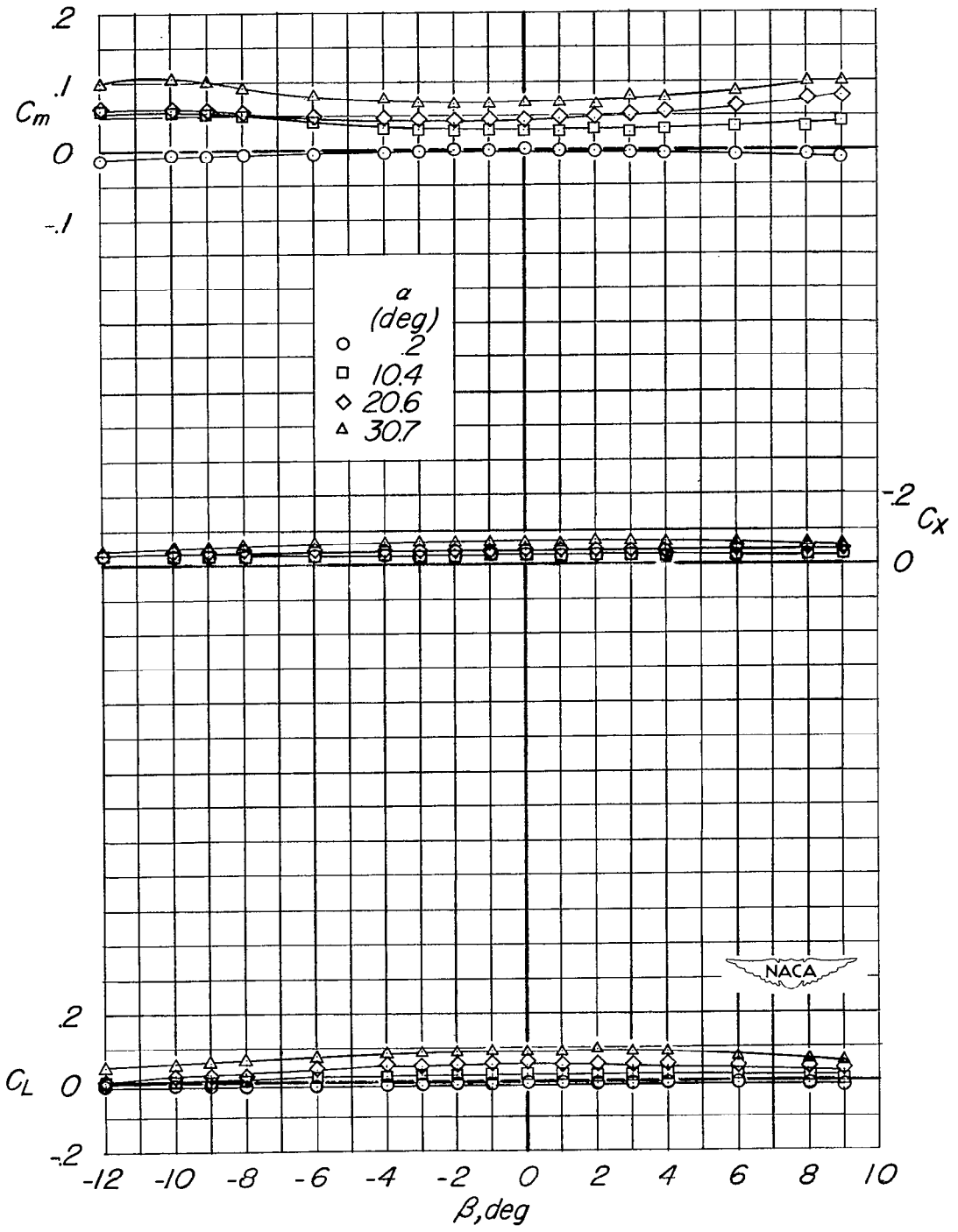

(a) Fuselage alone.

Figure 18.- The effect of angle of attack on the aerodynamic characteristics in sideslip. q = 101.5 lb/sq ft.

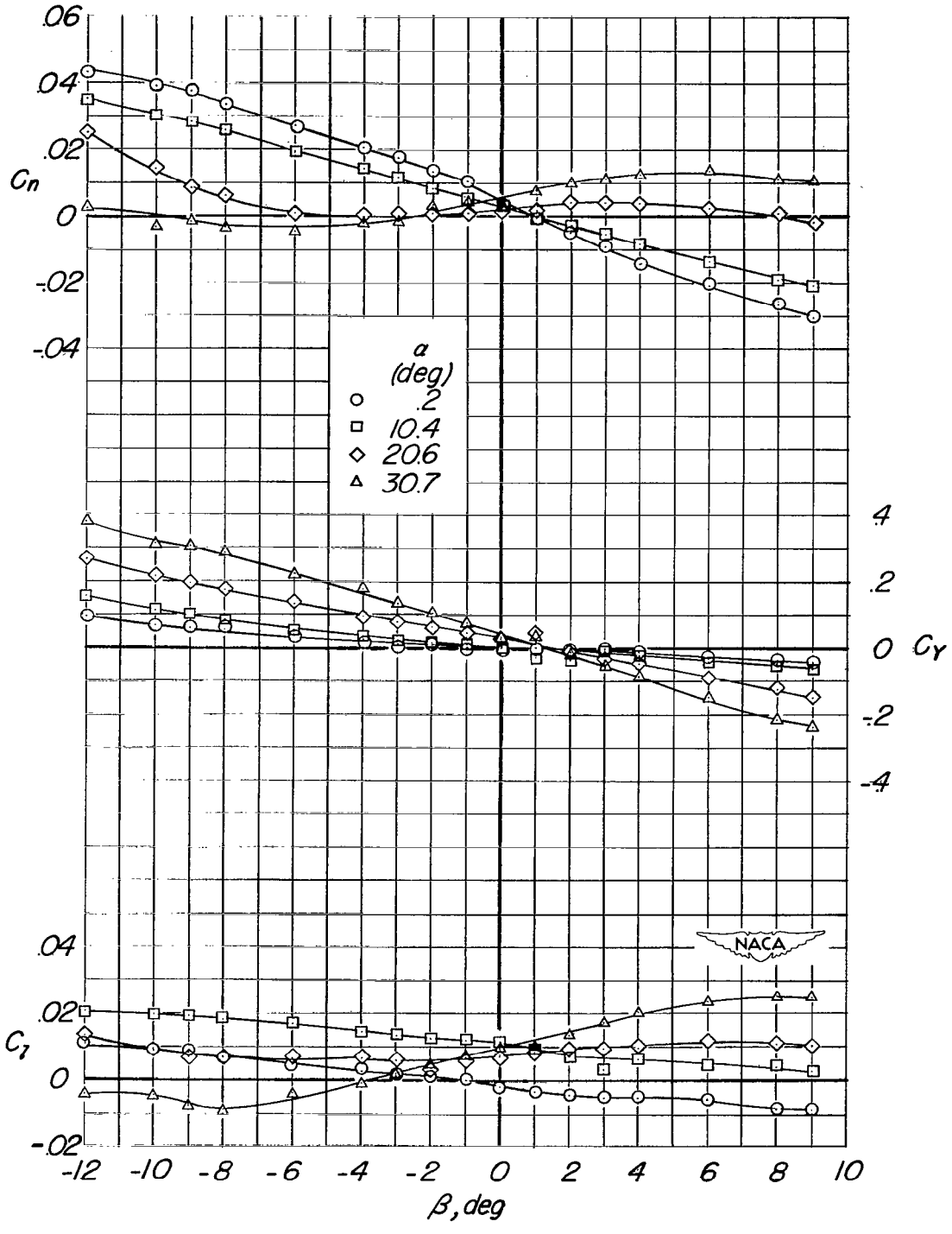

(a) Concluded.

Figure 18.- Continued.

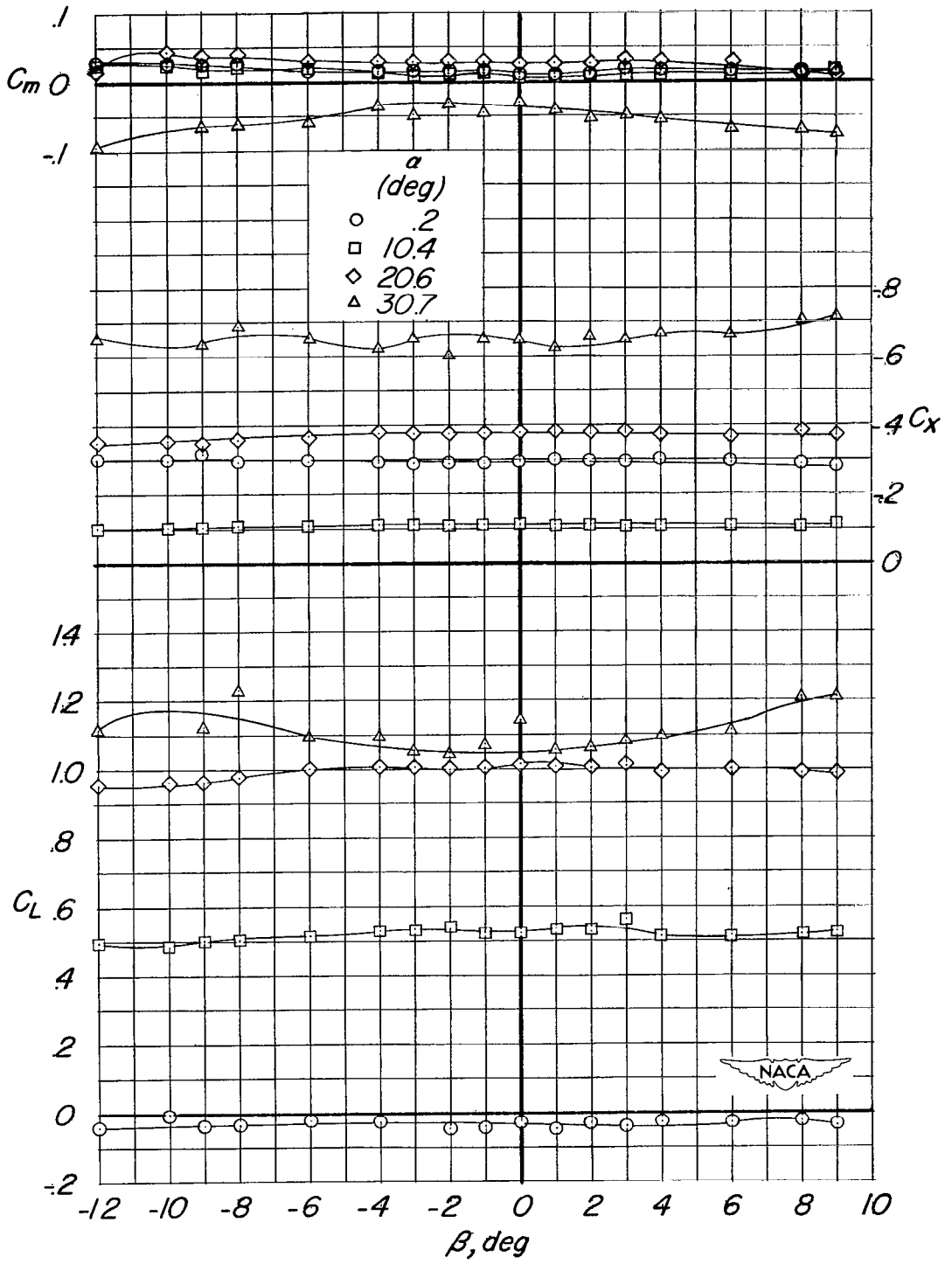

(b) Fuselage and wing (position A).

Figure 18.- Continued.

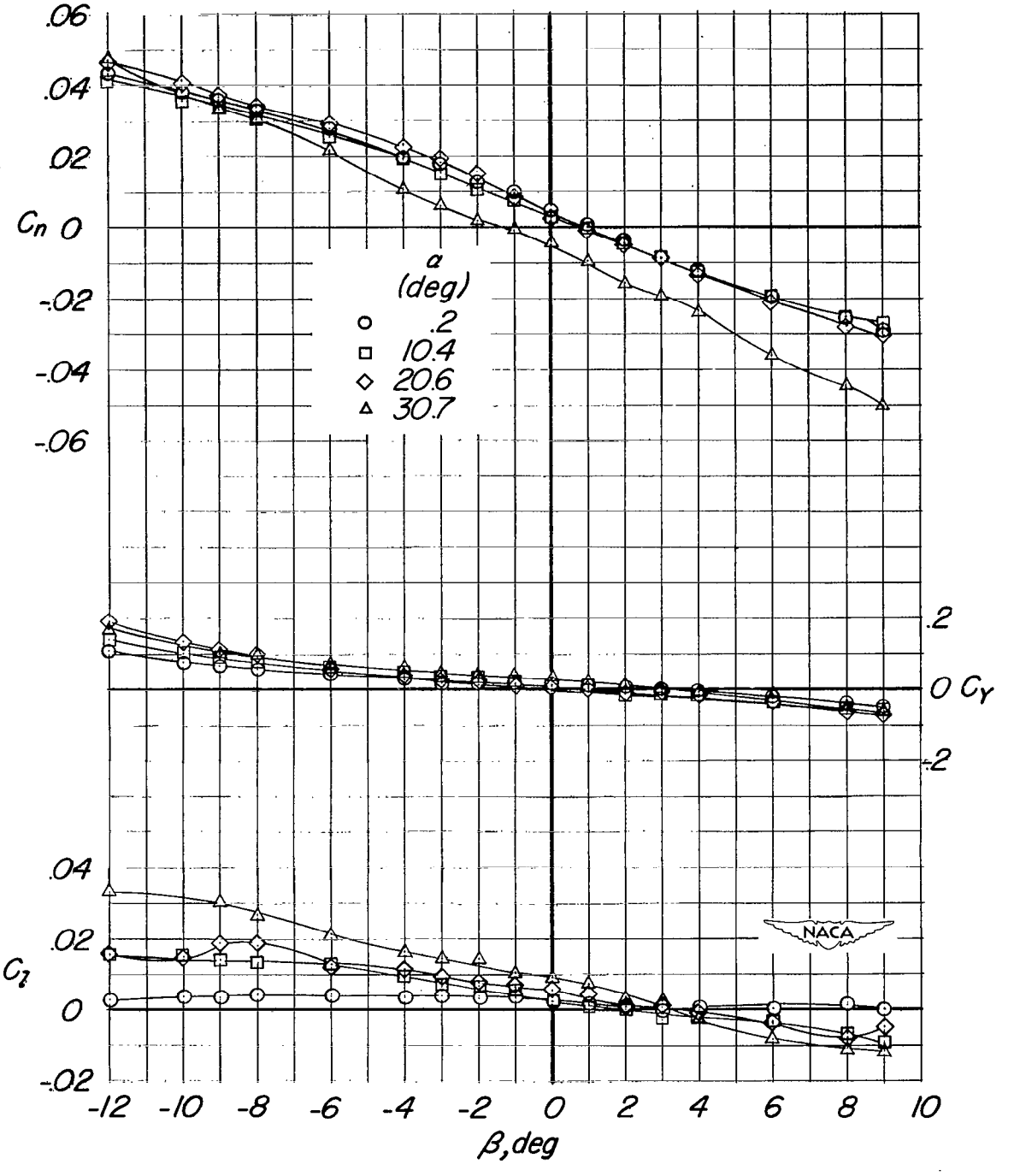

(b) Concluded.

Figure 18.- Concluded.

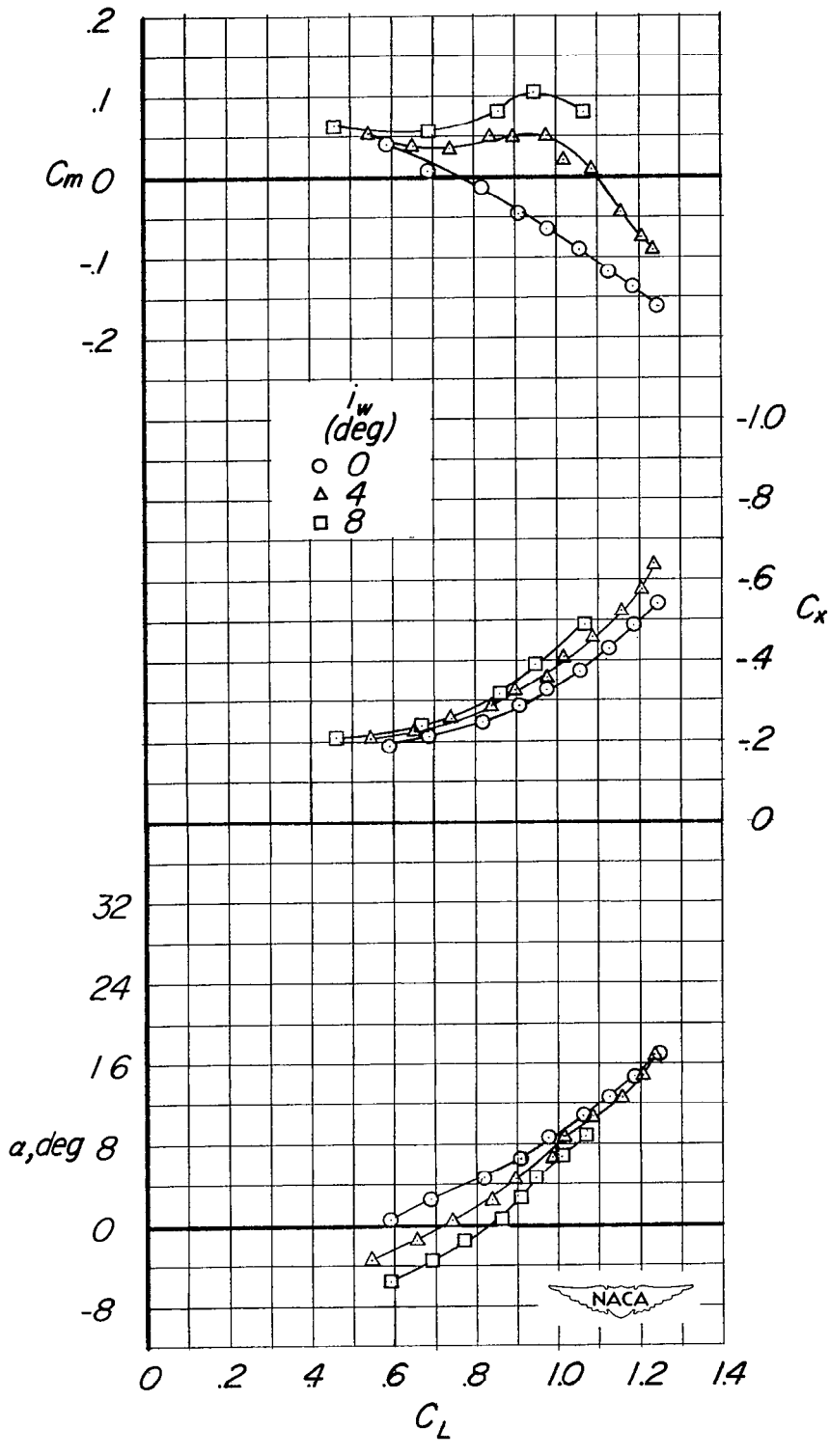

Figure 19.- The effect of wing incidence on the aerodynamic characteristics in pitch. Gear off; $\delta_f = 58^\circ$; wing position A; tail 1.

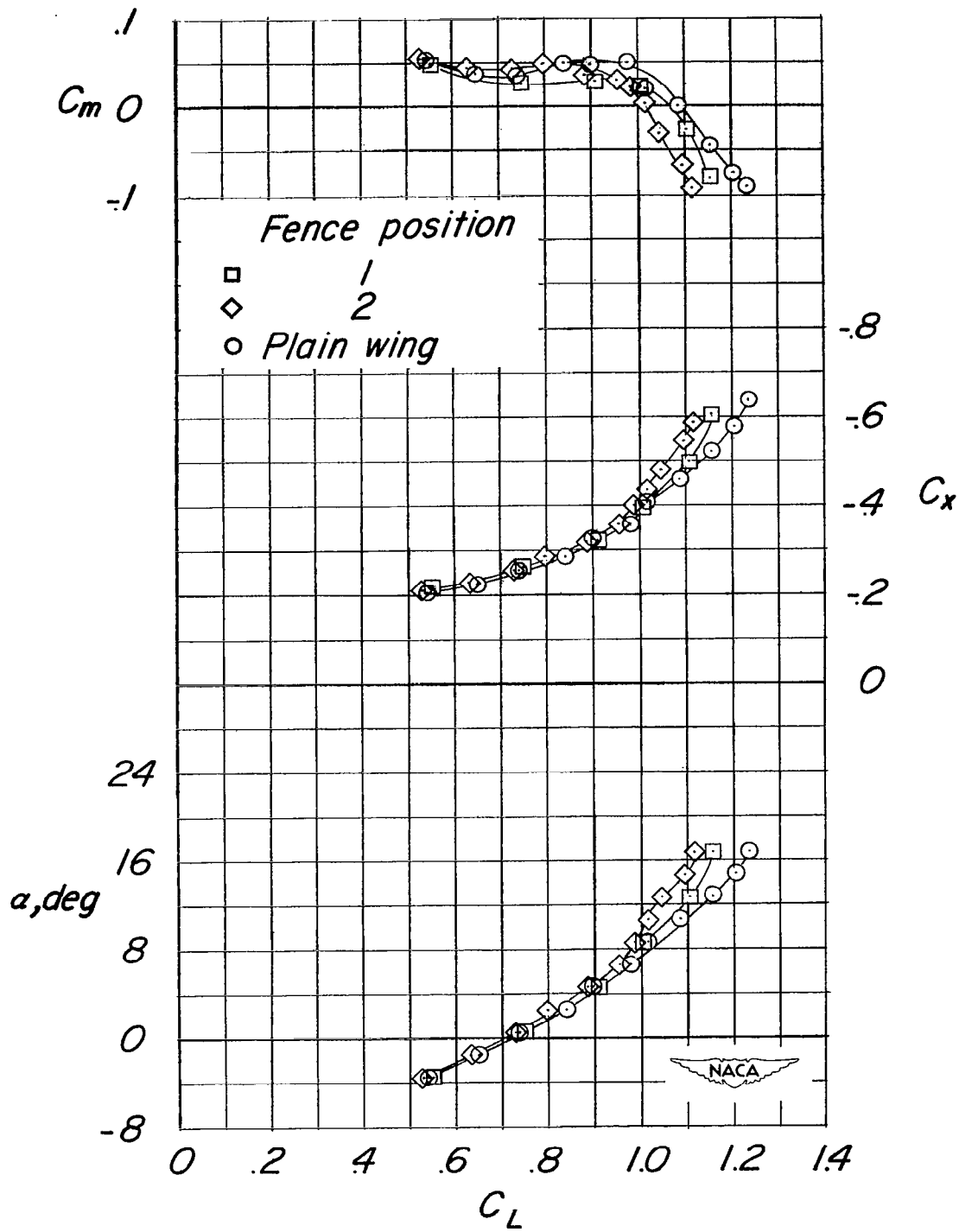

Figure 20.- The effect of flow fences on the aerodynamic characteristics in pitch. Wing position A; $i_w = 4^\circ$; gear off; $\delta_f = 58^\circ$; tail 1.

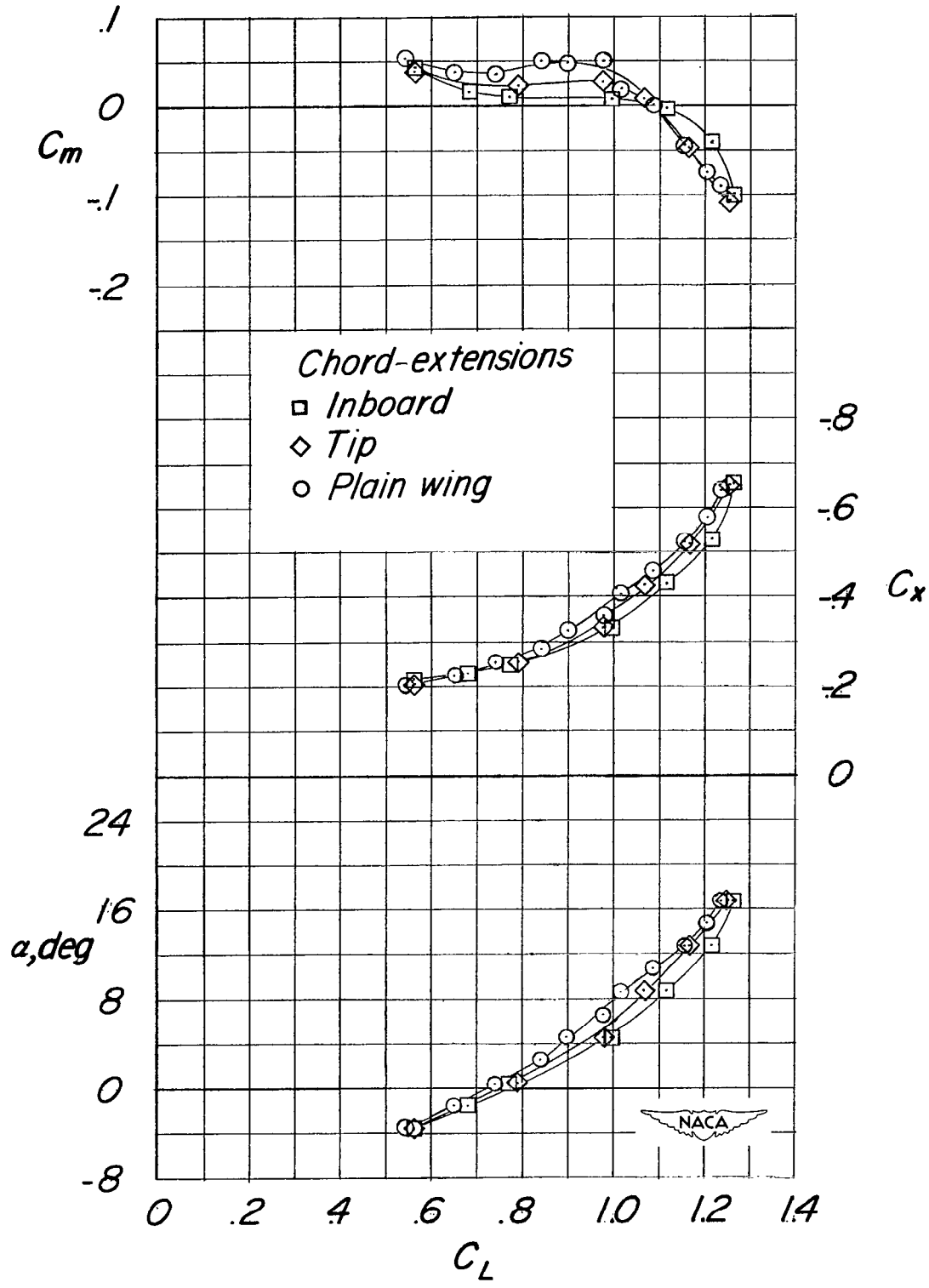

Figure 21.- The effect of chord-extensions on the aerodynamic characterist in pitch. Wing position A; $i_w = 4^\circ$; gear off; $\delta_f = 58^\circ$; tail 1.

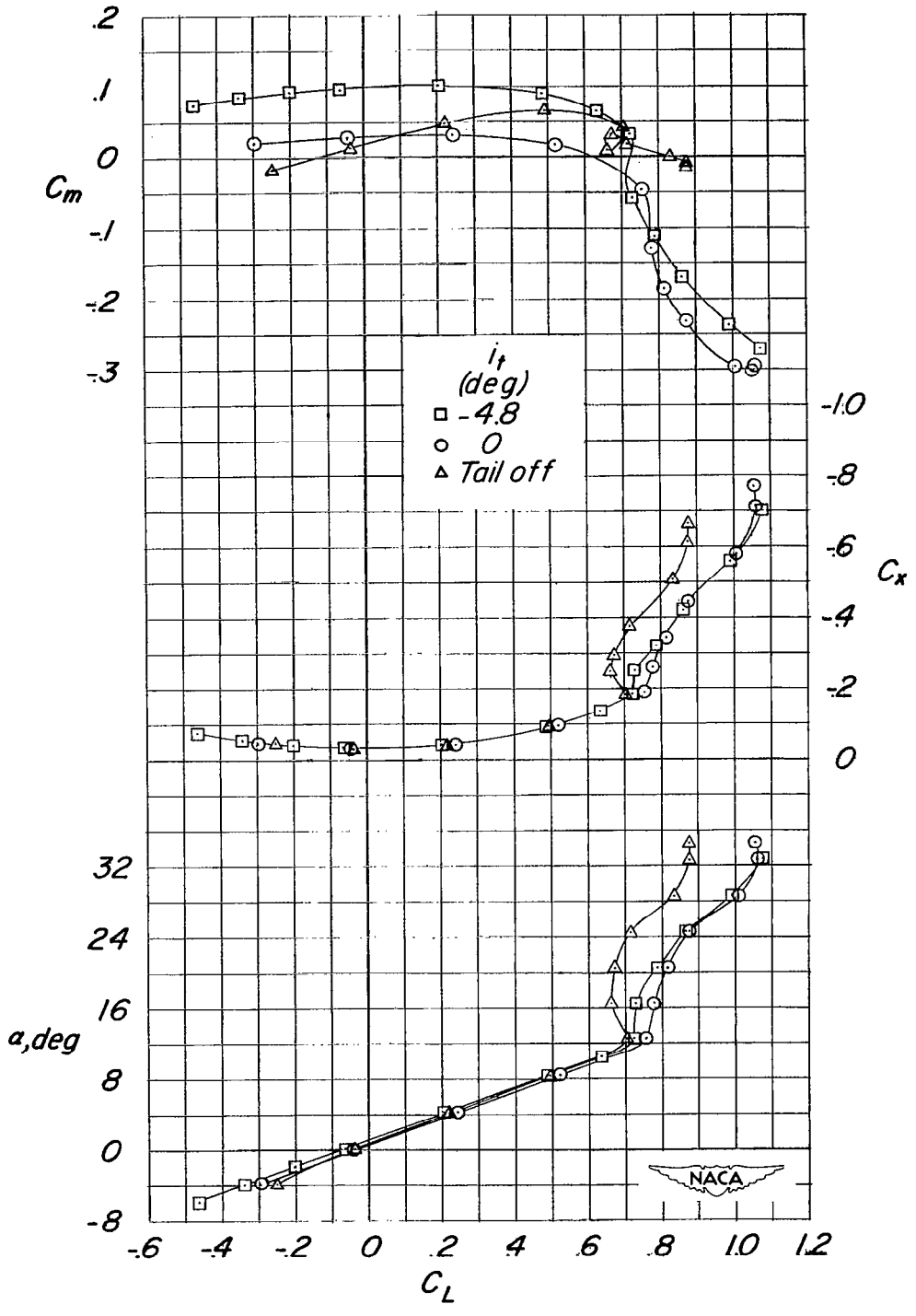

Figure 22.- The effect of the tail on the aerodynamic characteristics in pitch for the unswept-wing configuration. Wing position A; $i_w = 0^\circ$; tail 1; q = 101.5 lb/sq ft.

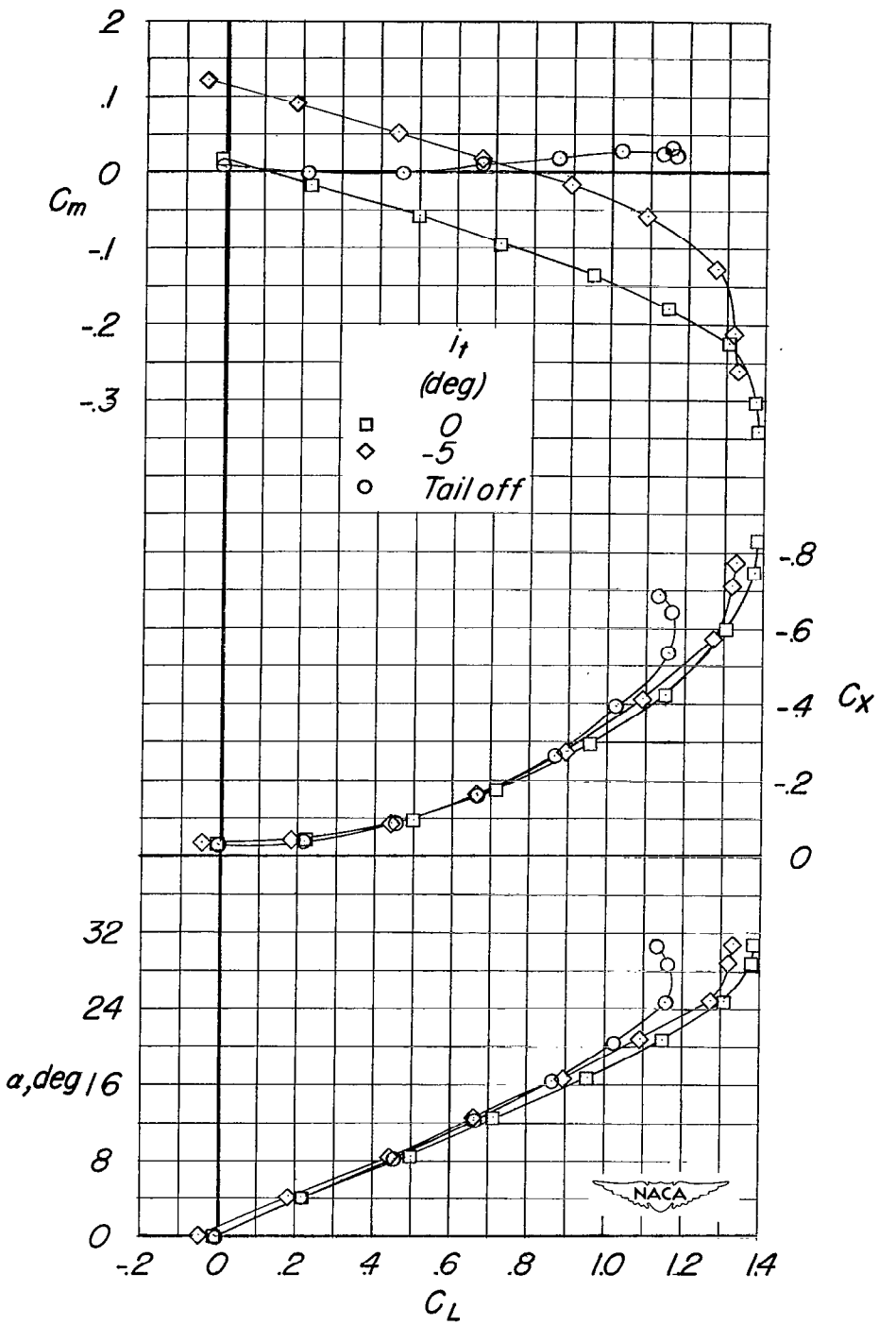

(a) $\delta_f = 0^\circ$.

Figure 23.- The effect of the large-span tail on the aerodynamic characteristics in pitch. Wing position C; tail 5; gear off.

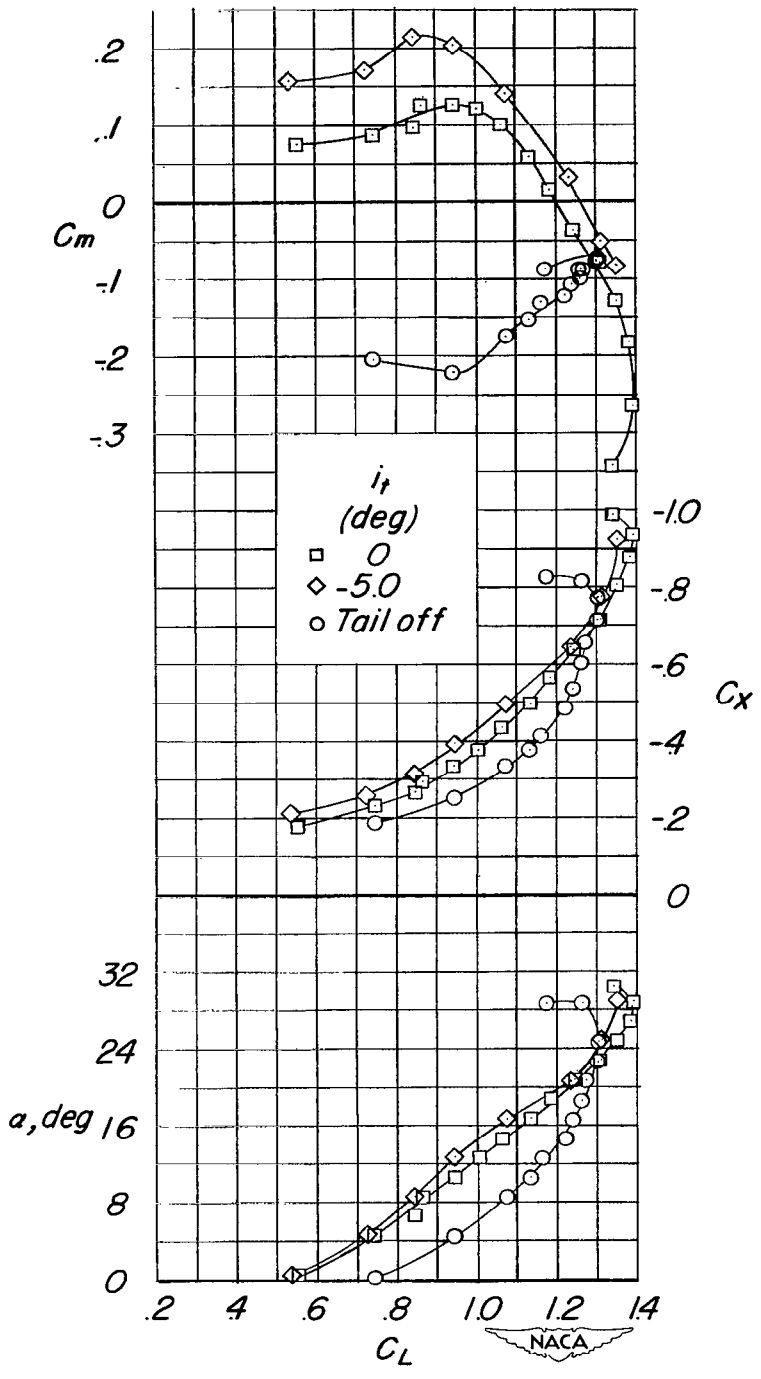

(b) $\delta_f = 52^\circ$.

Figure 23.- Concluded.

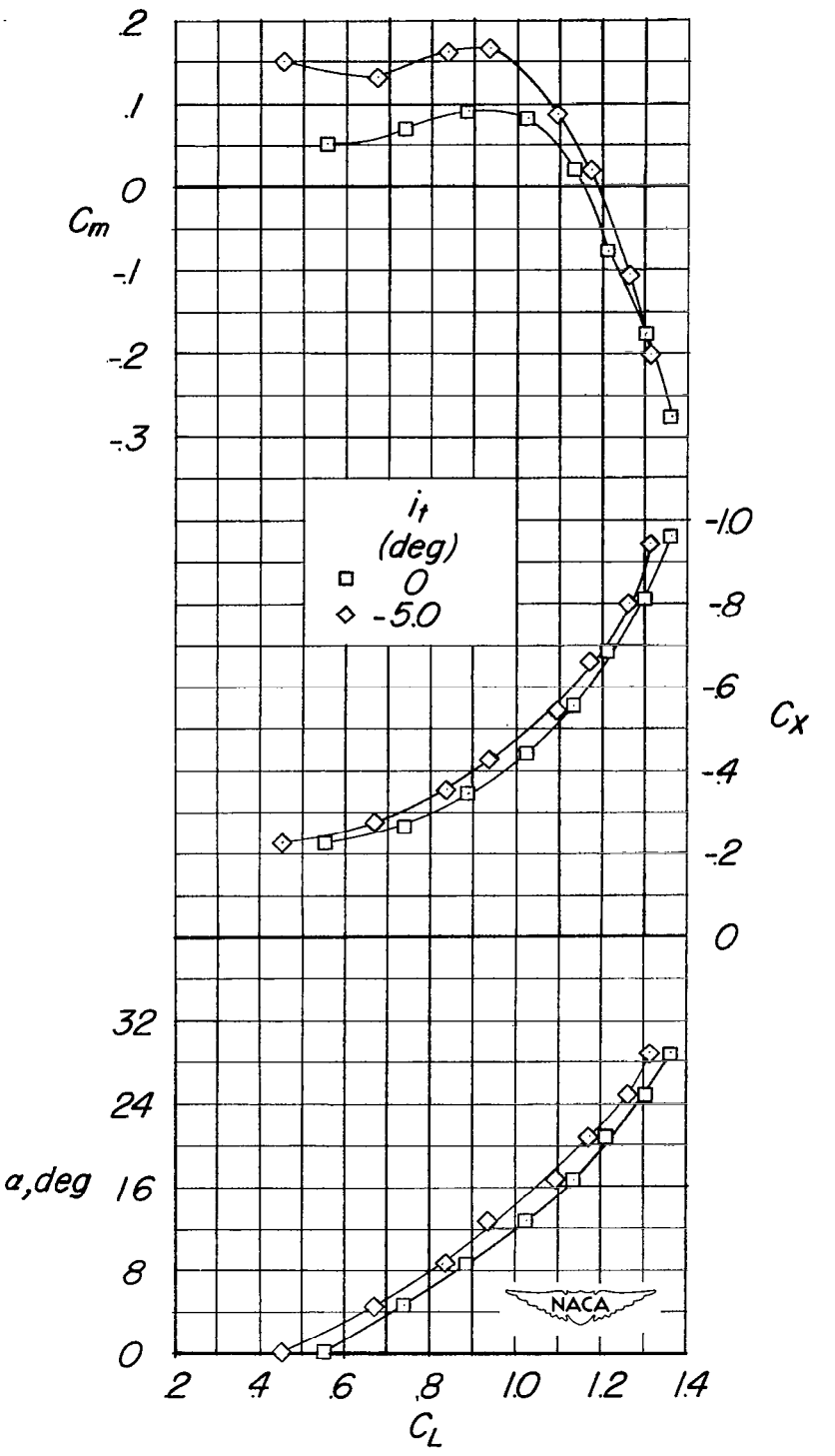

Figure 24.- The effect of the large-span tail on the aerodynamic characteristics in pitch. $\delta_f = 57^\circ$; gear on; doors open; wing position C; tail 5.

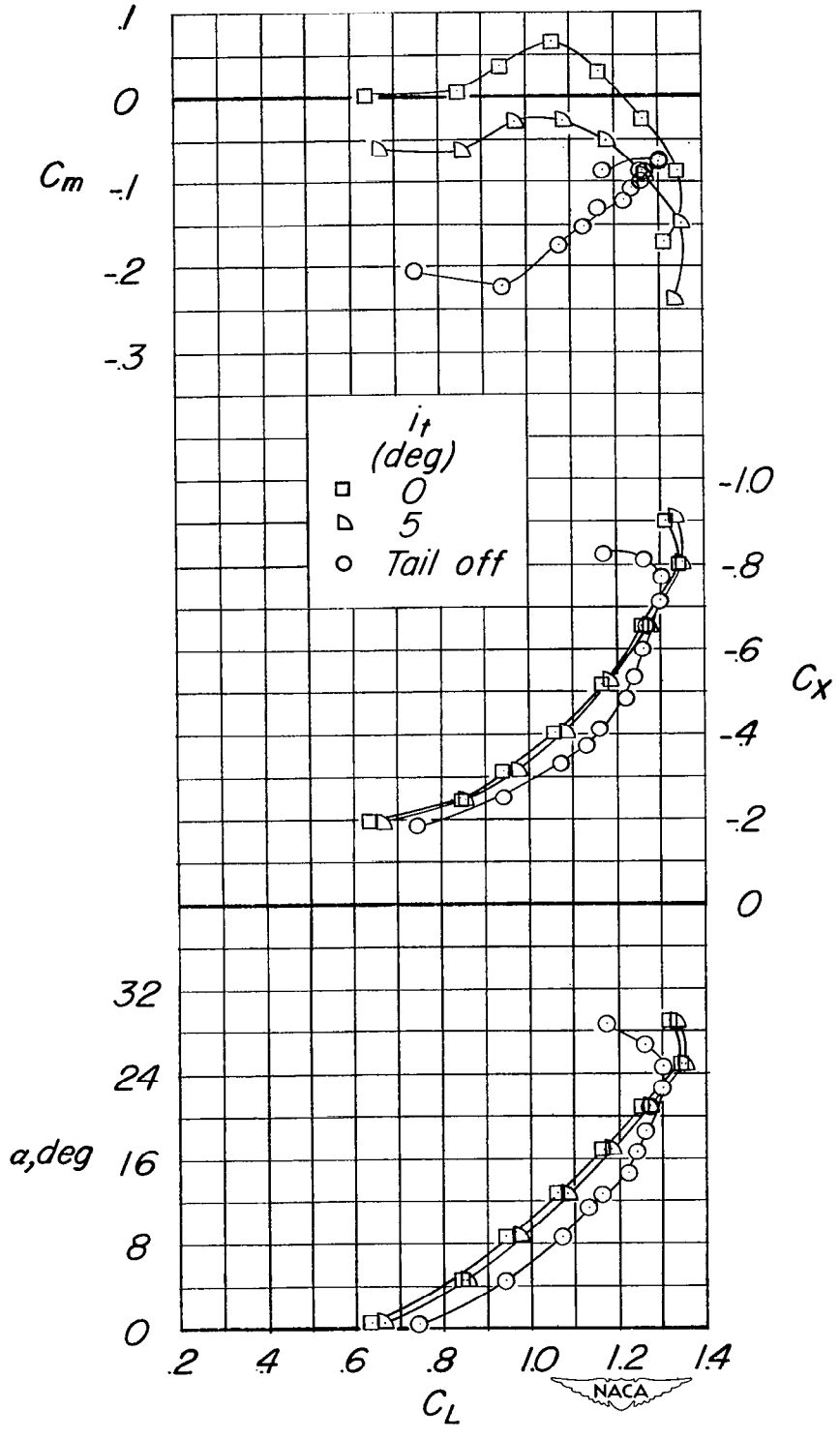

Figure 25.- The effect of the tail on the aerodynamic characteristics in pitch. Gear off; $\delta_f = 52^\circ$; wing position C; tail 4.

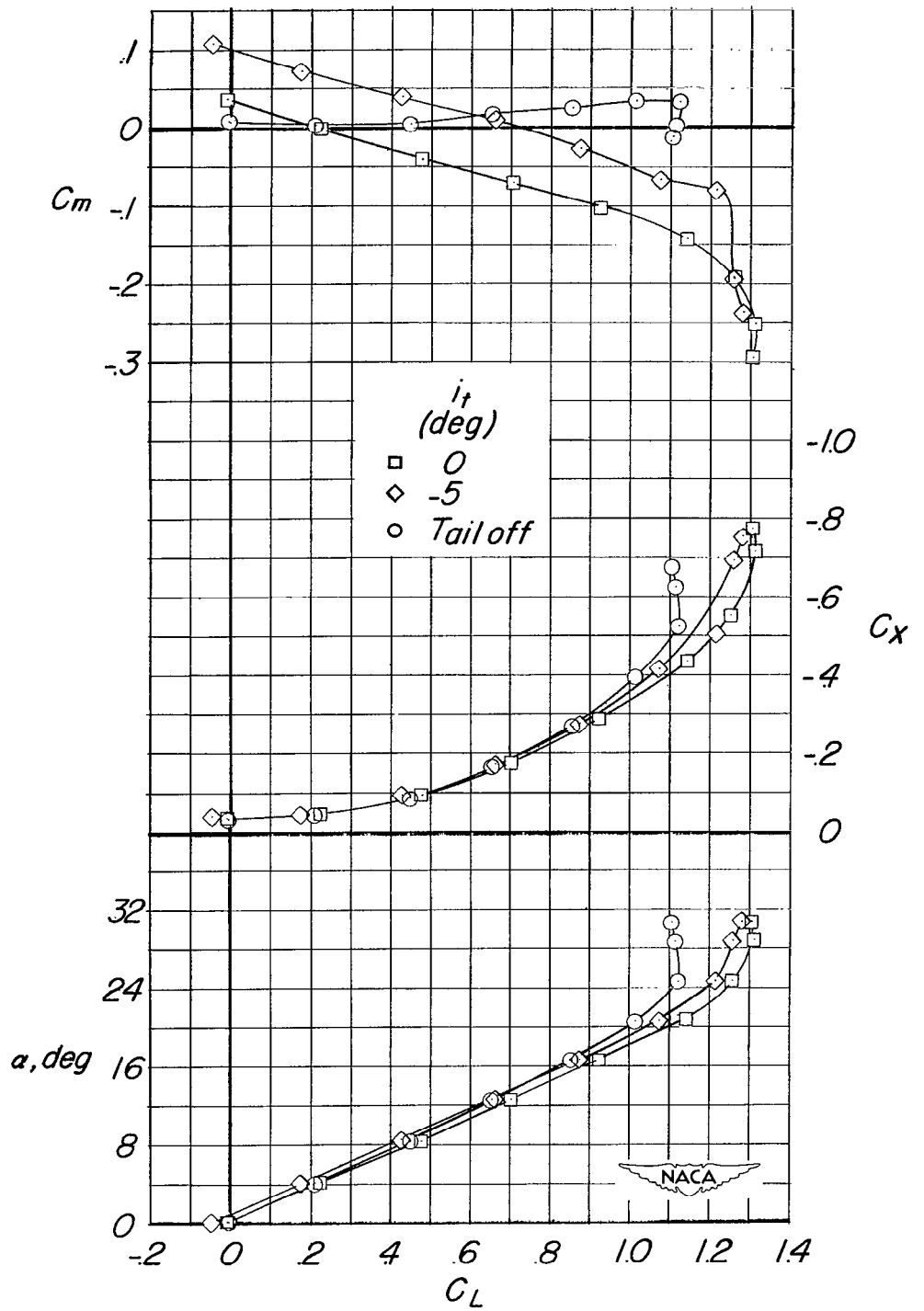

(a) $\delta_f = 0^\circ$; gear off.

Figure 26.- The effect of tail on the aerodynamic characteristics in pitch. Wing position B; tail 3.

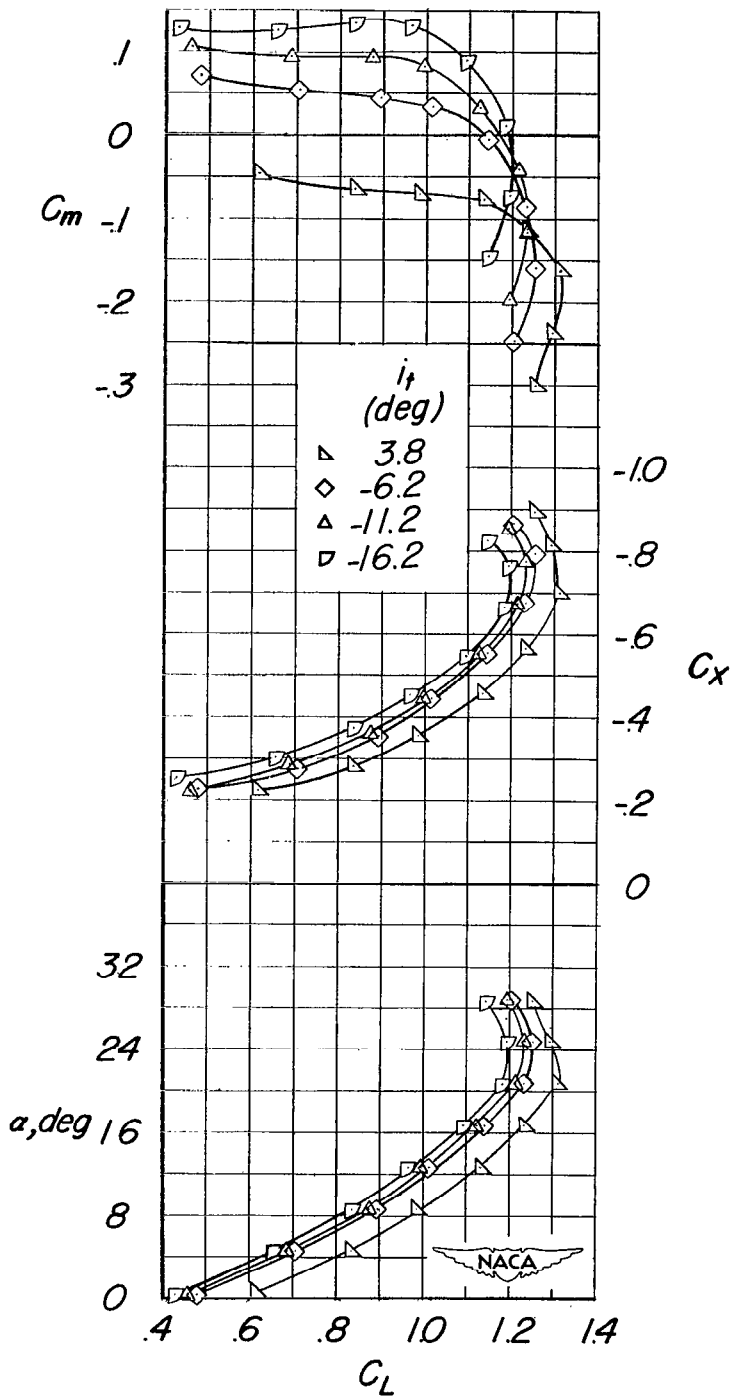

(b) $\delta_f = 57°$; gear on; doors closed.

Figure 26.- Concluded.

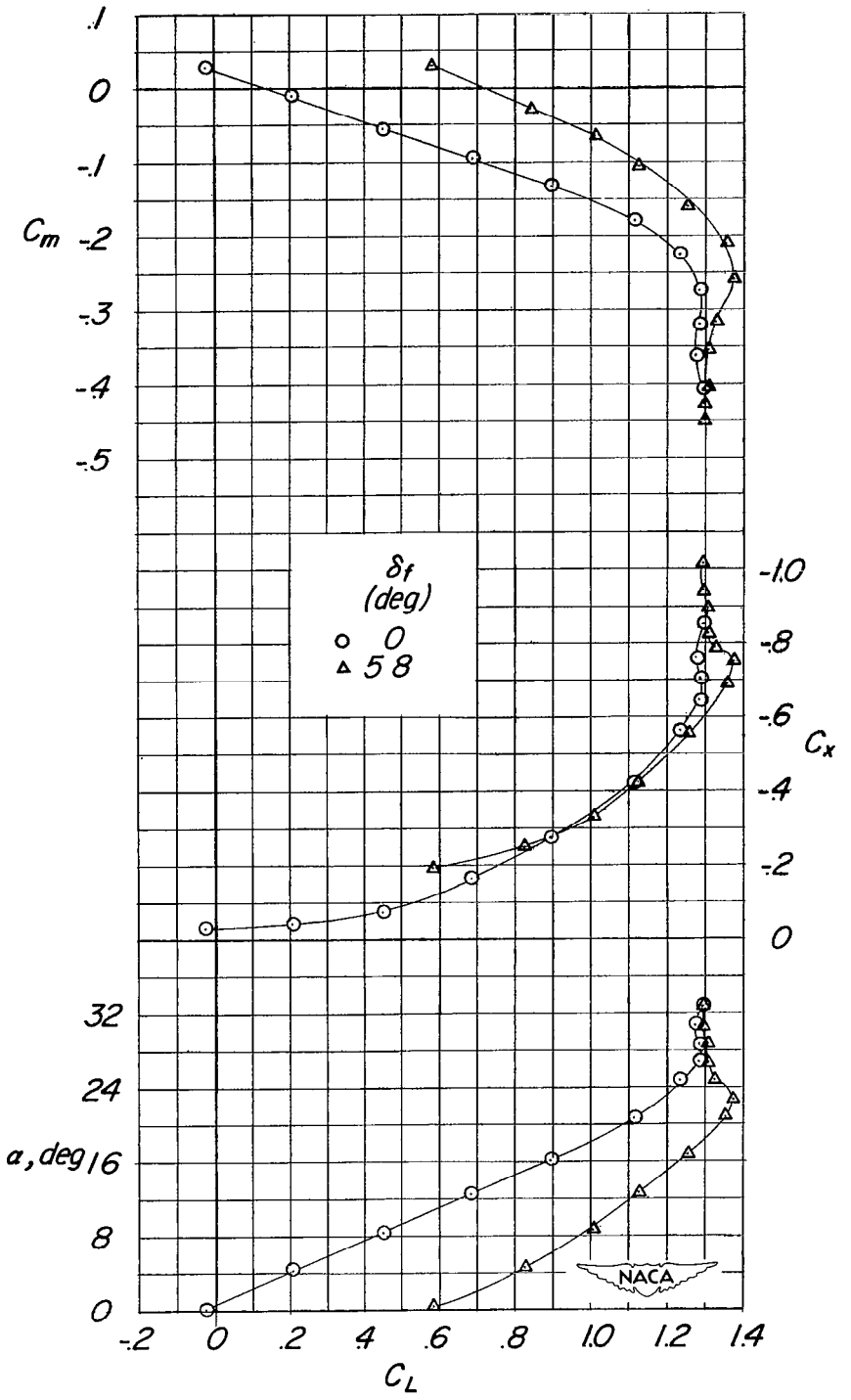

Figure 27.- The effect of optimum flap deflection on the aerodynamic characteristics in pitch. Wing position A; $i_w = 0^\circ$; tail 1; $i_t = 0^\circ$; gear off.

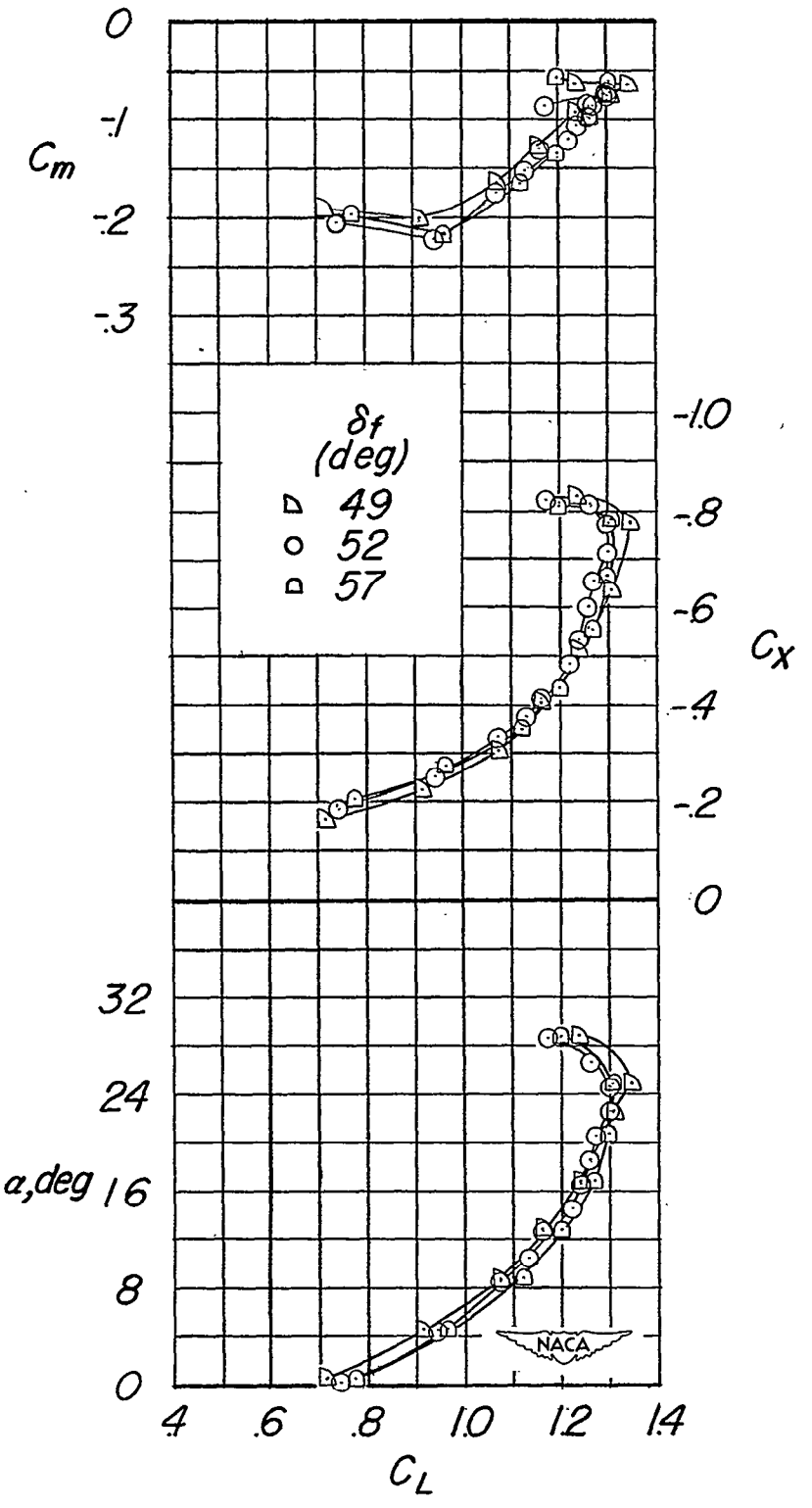

Figure 28.- The effect of flap deflection on the aerodynamic characteristics in pitch. Wing position C; tail off; gear off.

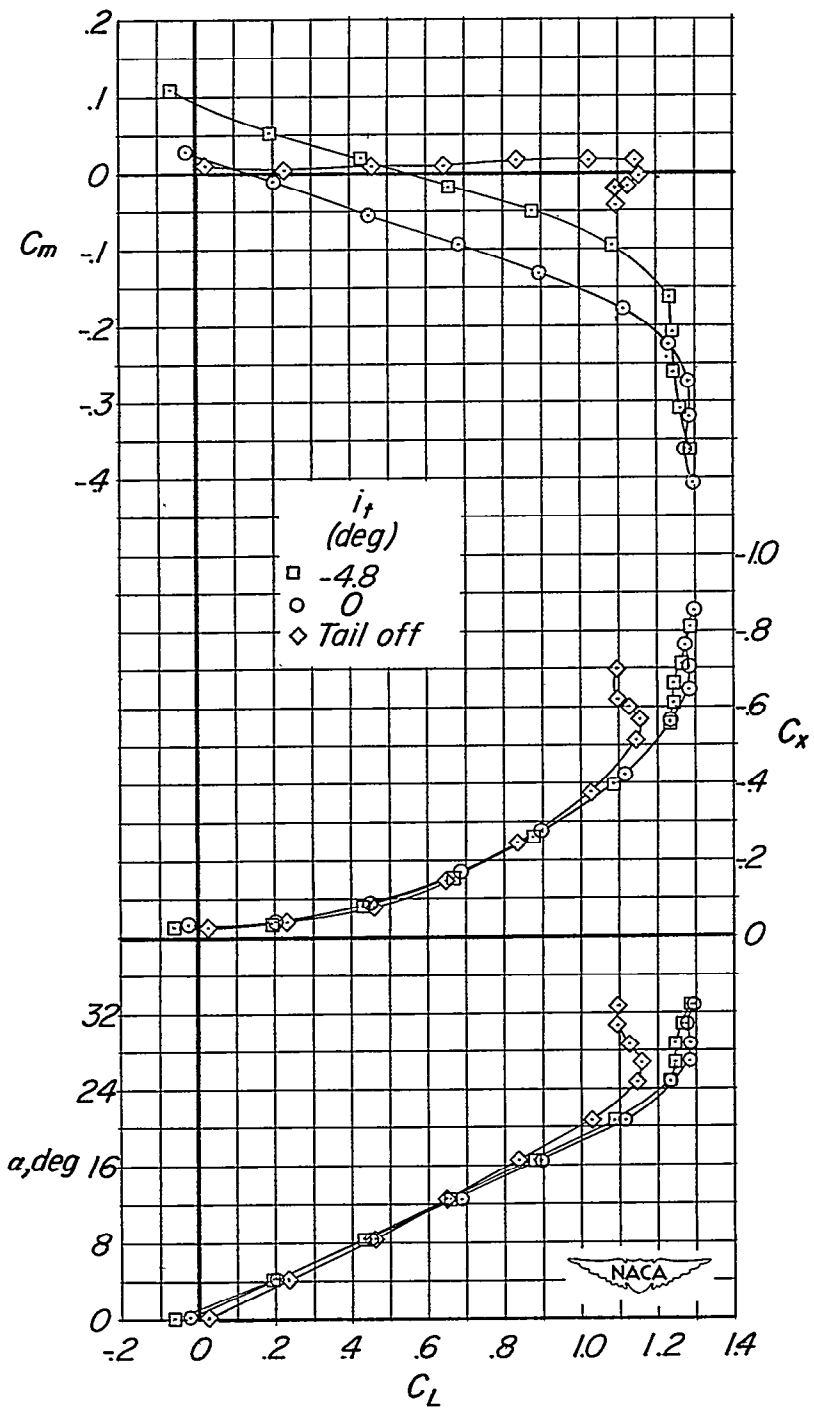

(a) $\delta_f = 0^\circ$.

Figure 29.- The effect of the tail on the aerodynamic characteristics in pitch. Gear off; wing position A; $i_w = 0^\circ$; tail 1.

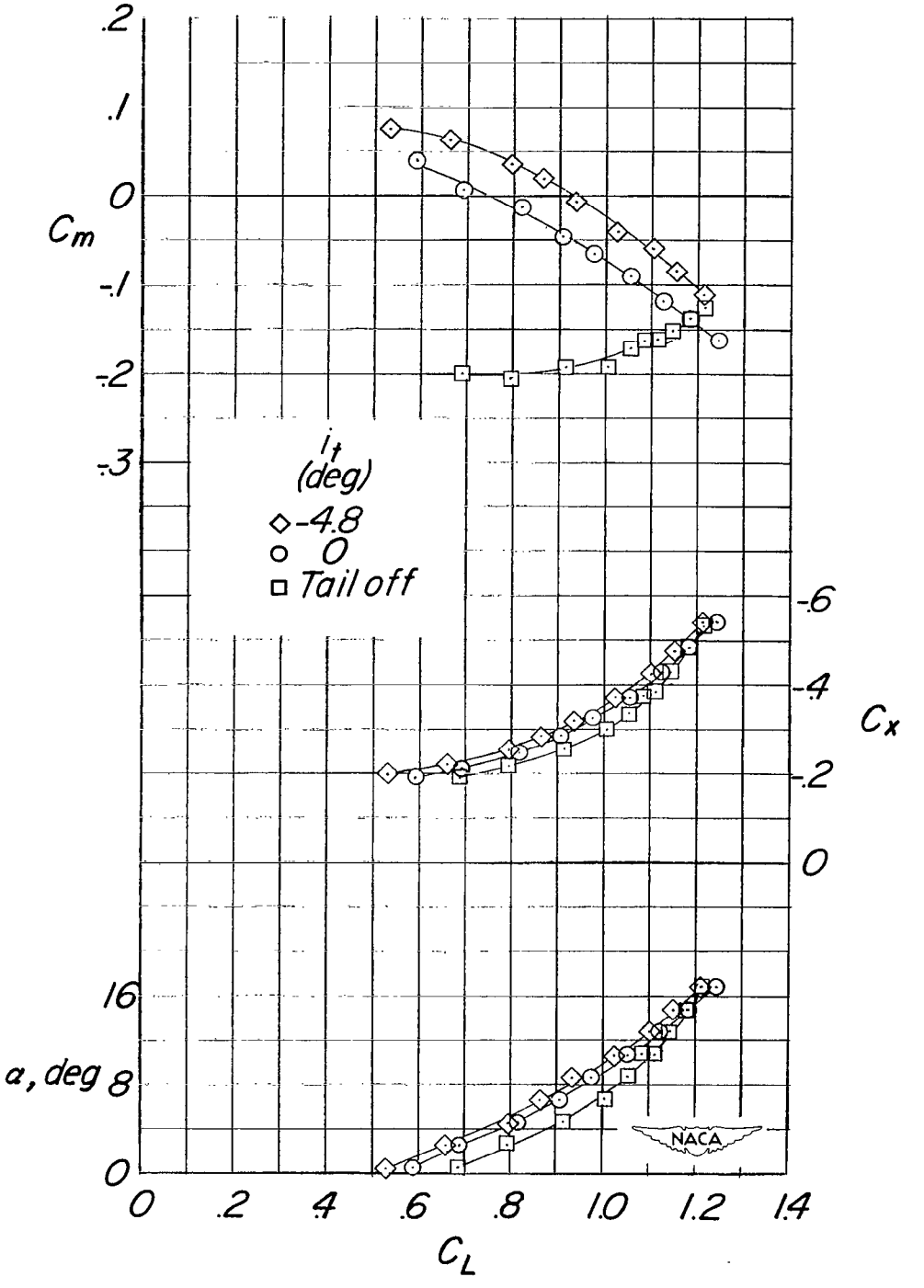

(b) $\delta_f = 58^\circ$.

Figure 29.- Concluded.

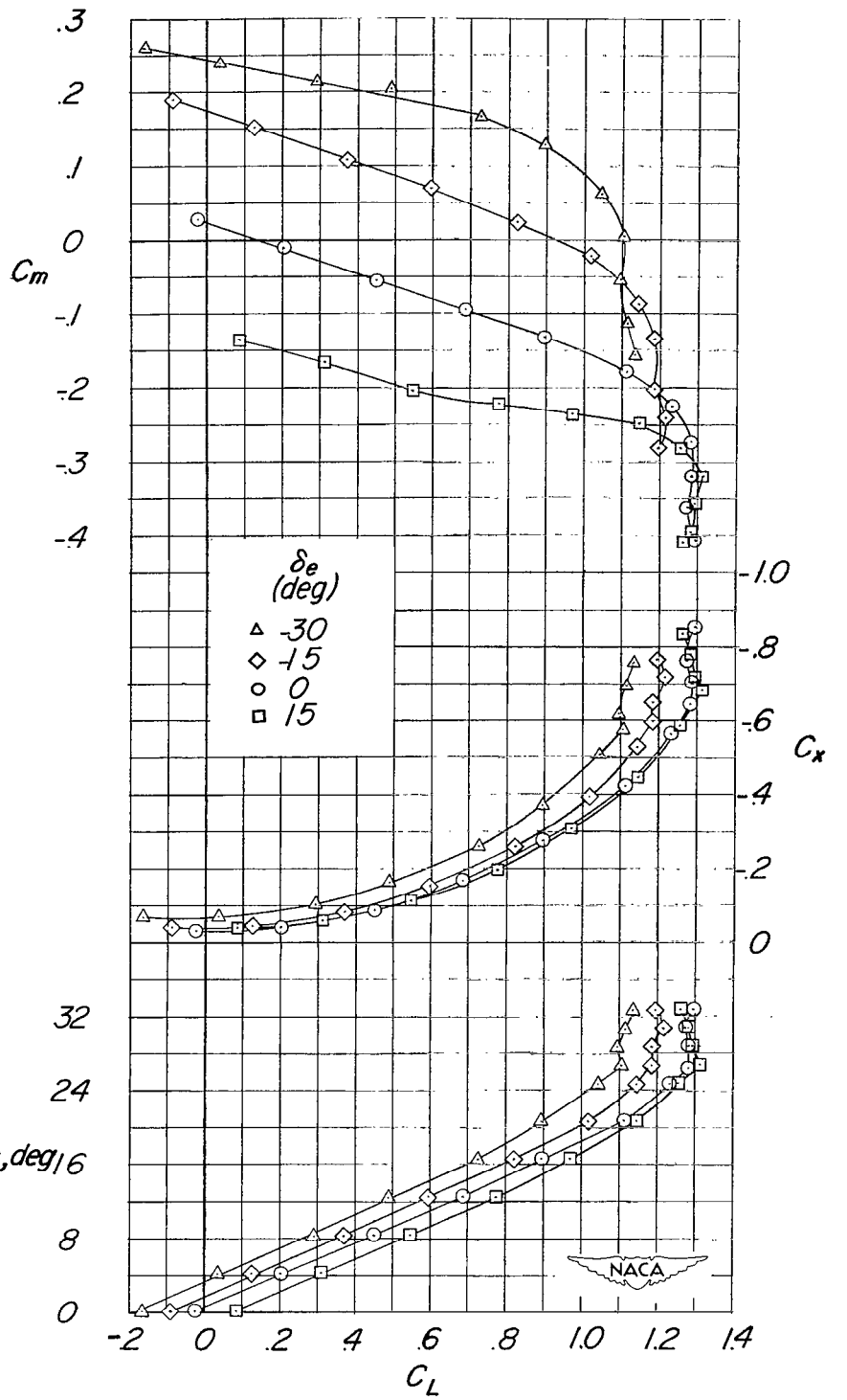

Figure 30.- The effect of elevator deflection on the aerodynamic characteristics in pitch. $\delta_f = 0^\circ$; wing position A; $i_w = 0^\circ$; tail 1; q = 25 lb/sq ft.

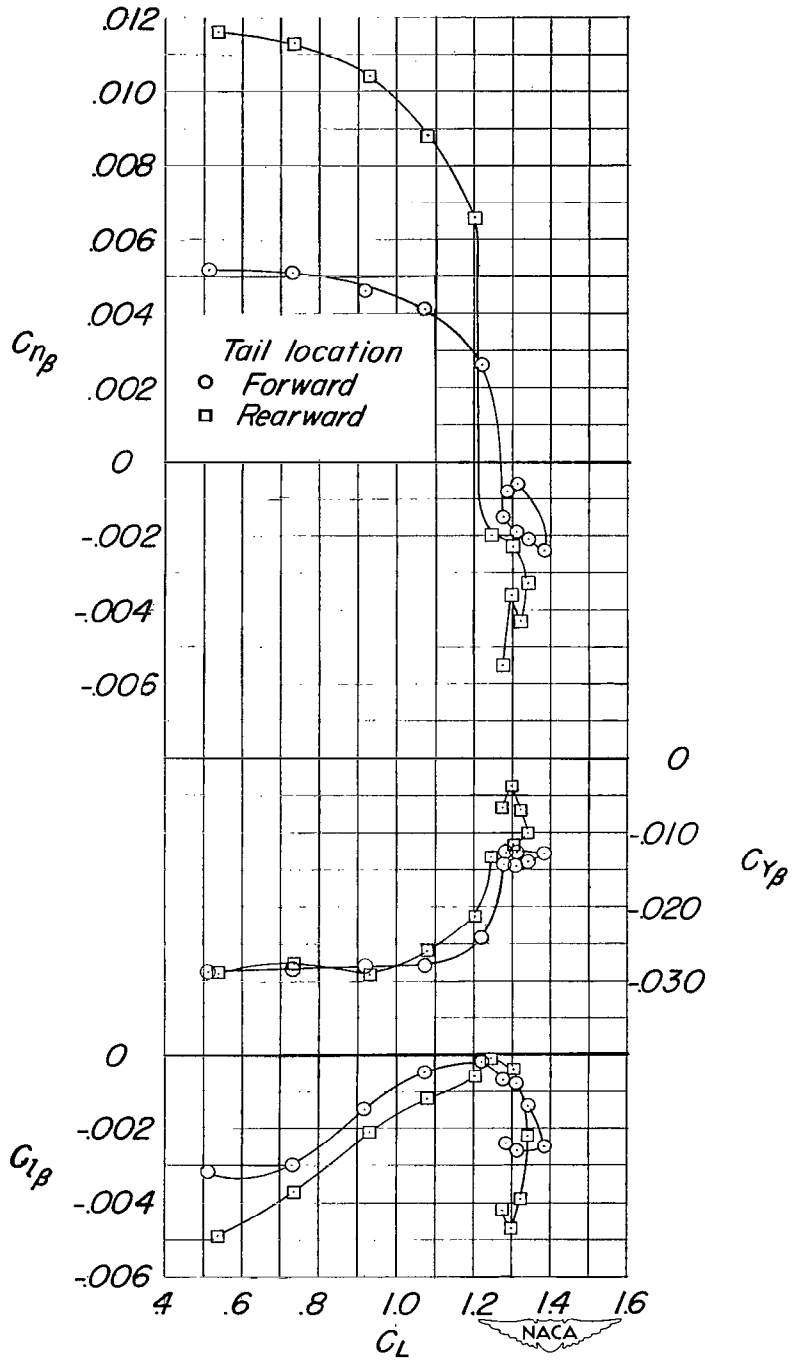

(a) $i_w = 0^\circ$; $\delta_f = 58^\circ$.

Figure 31.- Effect of vertical-tail location on the variation of the lateral-stability parameters with lift coefficient. Wing position A; tail 1; $i_t = 0^\circ$.

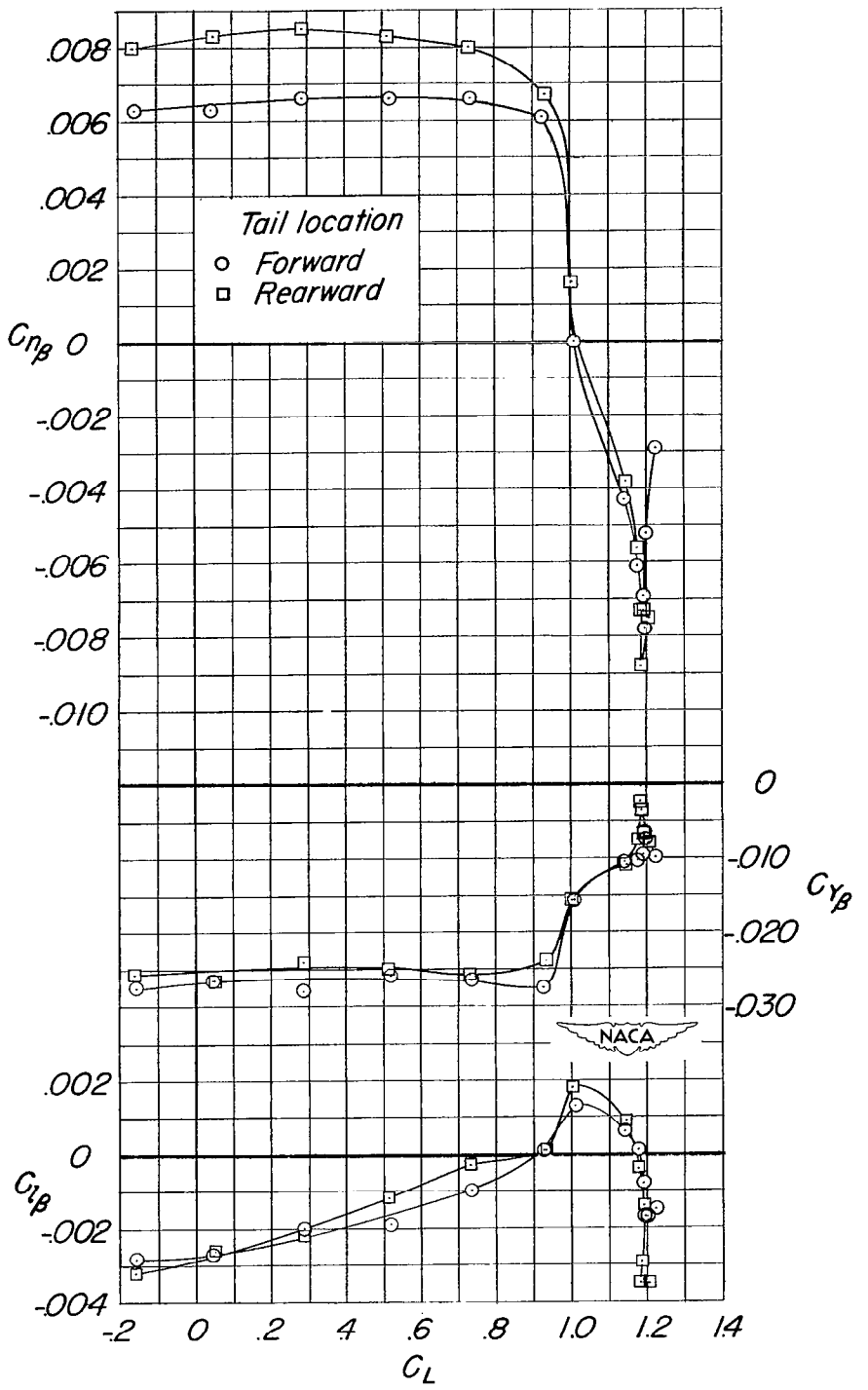

(b) $i_w = 8^\circ$; $\delta_f = 0^\circ$.

Figure 31.- Concluded.

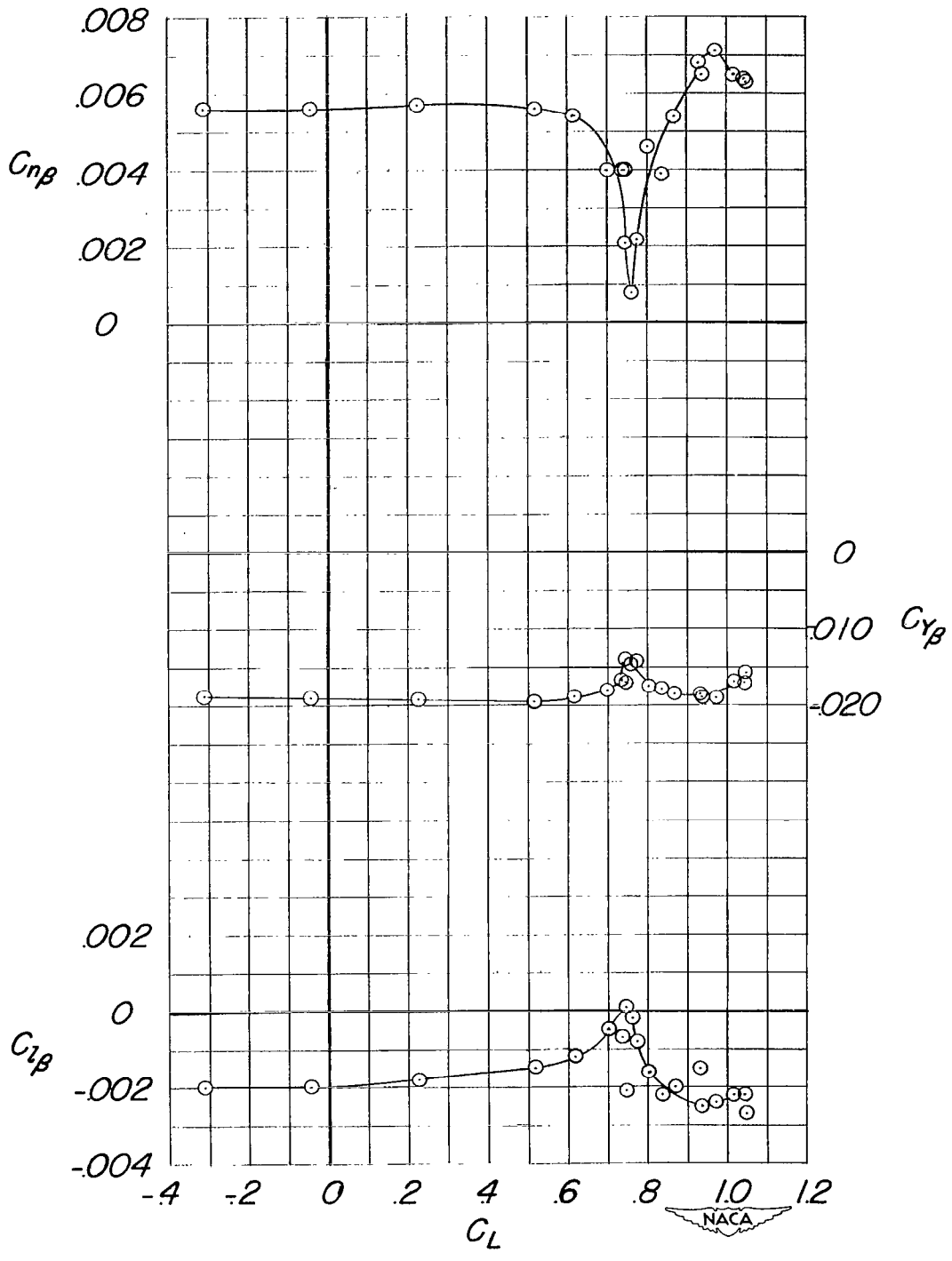

Figure 32.- Variation of the lateral-stability parameters with lift coefficient for the unswept-wing configuration. Wing position A; $i_w = 0^\circ$; tail 1; $i_t = 0^\circ$.

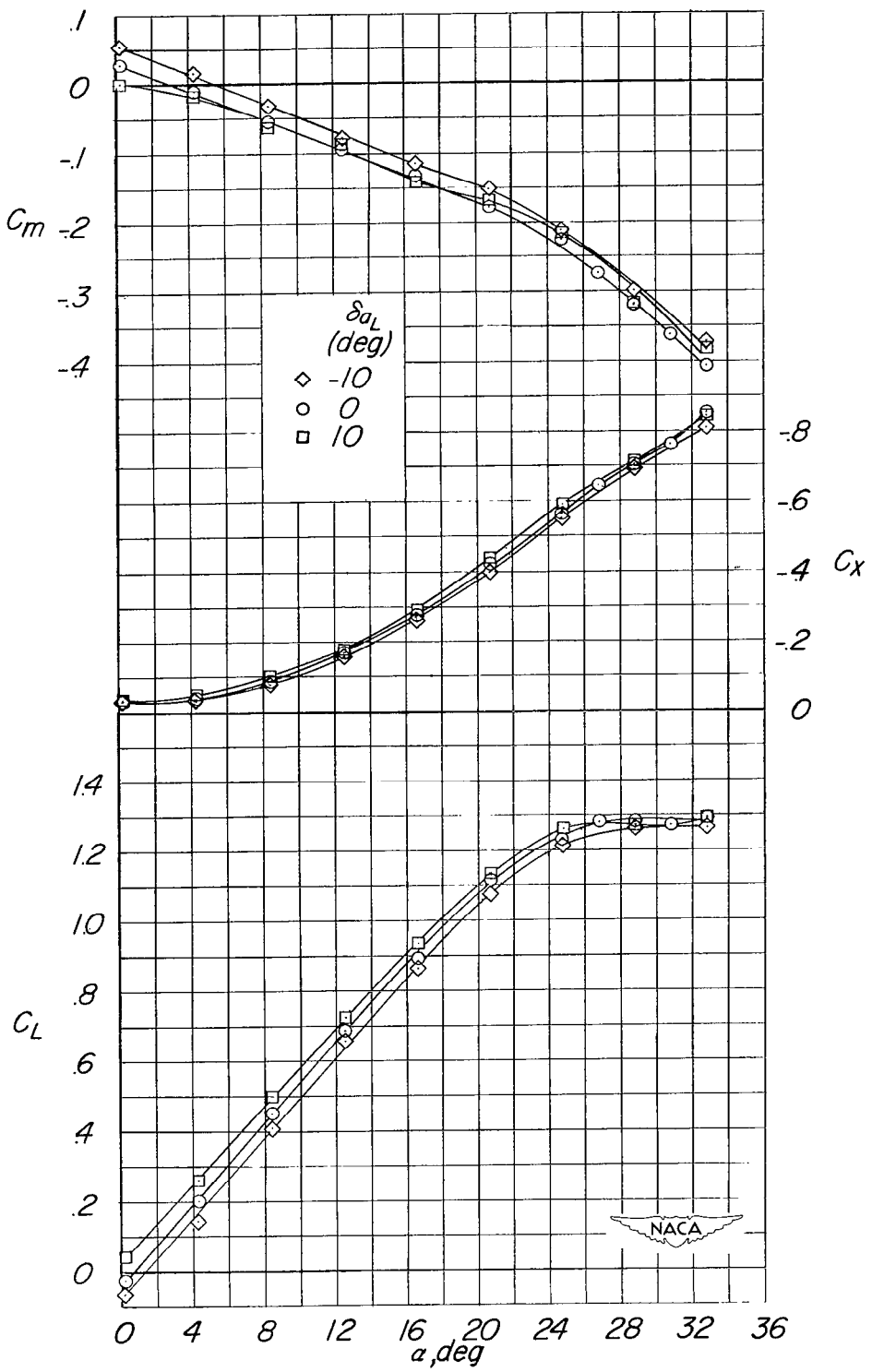

Figure 33.- Effect of aileron deflection on the aerodynamic characteristics in pitch. $\delta_f = 0^\circ$; wing position A; $i_w = 0^\circ$; tail 1; $i_t = 0^\circ$.

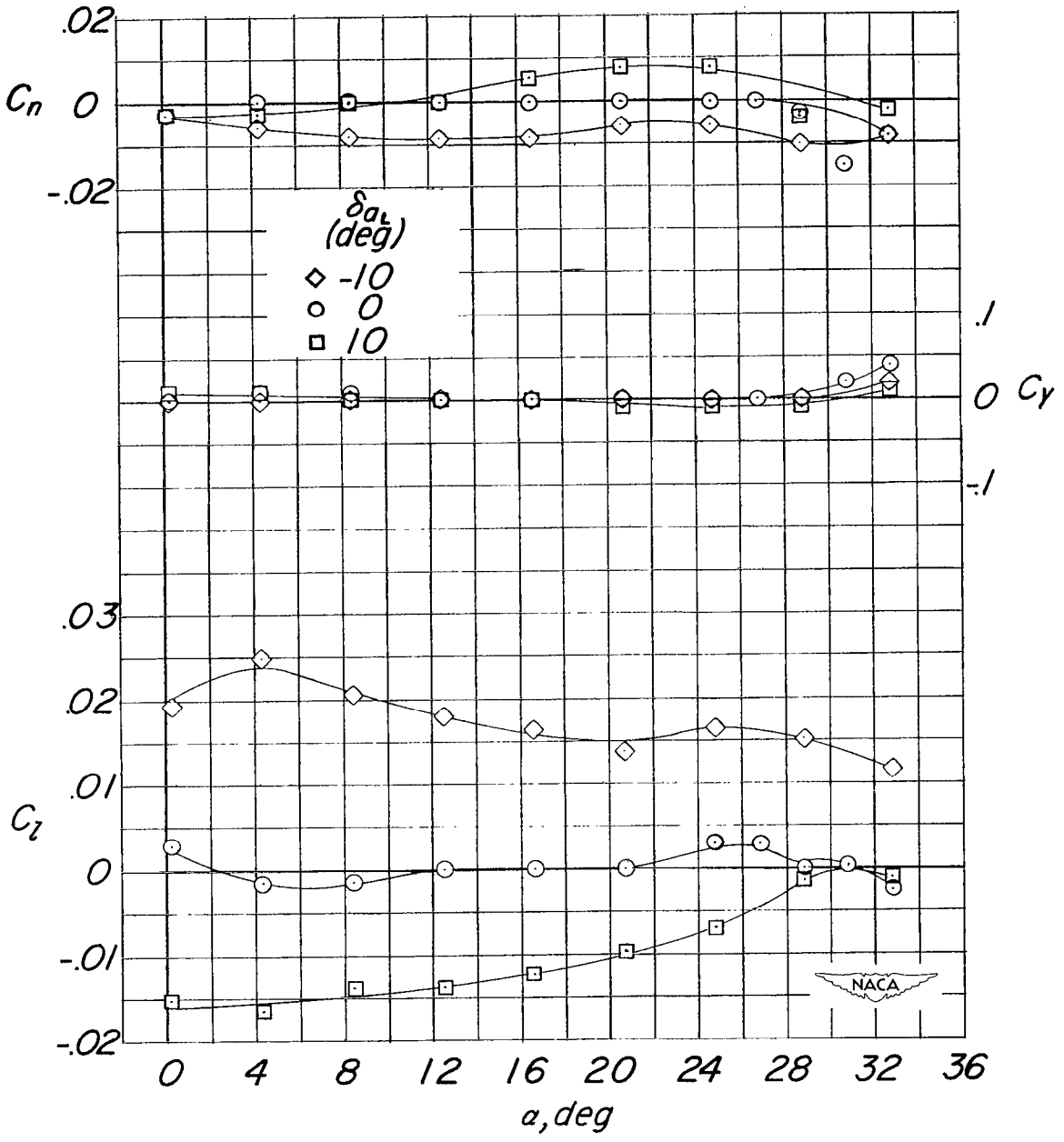

Figure 33.- Concluded.

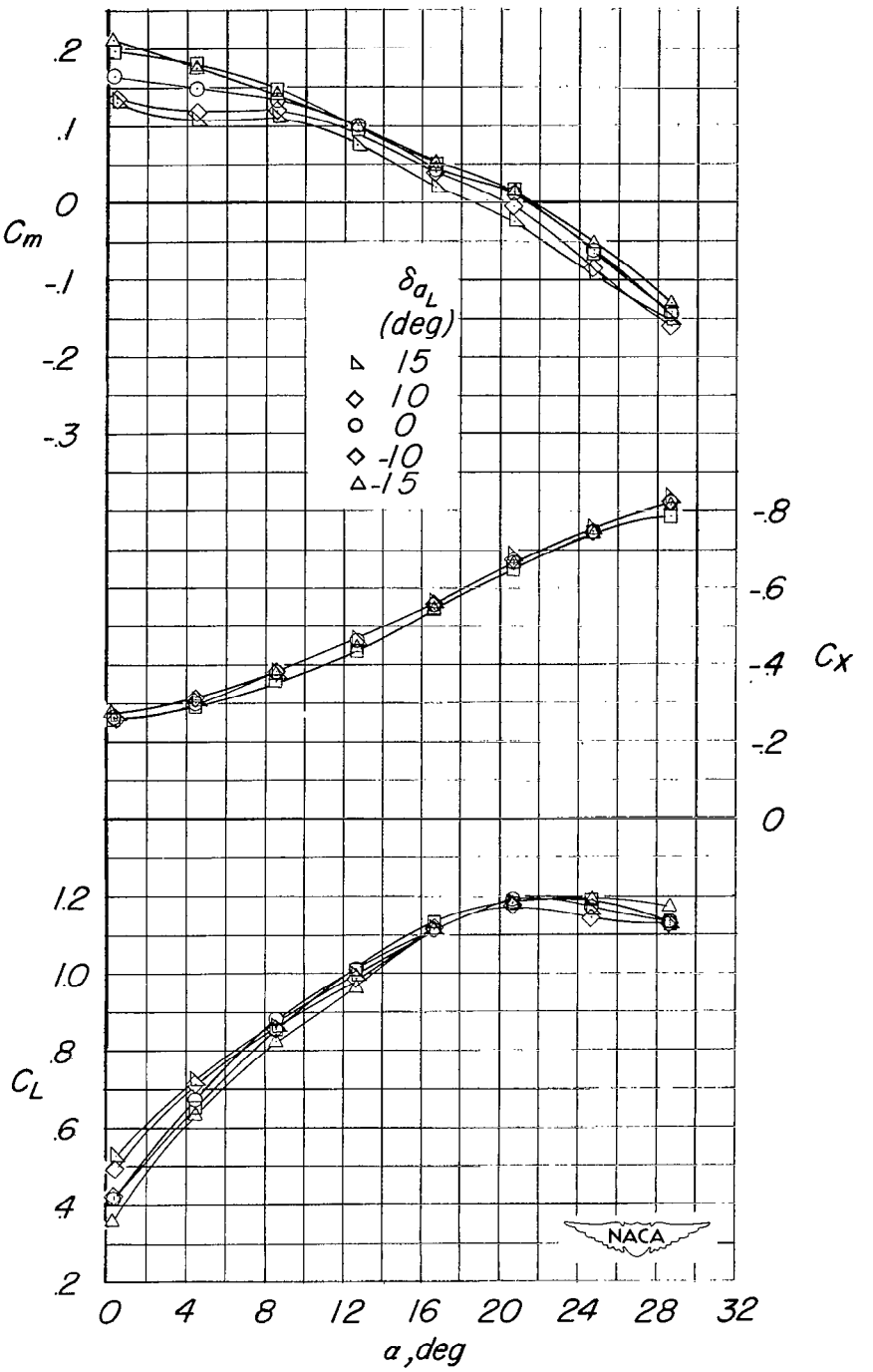

(a) $i_t = -20.2°$.

Figure 34.- Effect of aileron deflection on the aerodynamic characteristics in pitch. Gear on; doors closed; $\delta_f = 57°$; wing position B; tail 2.

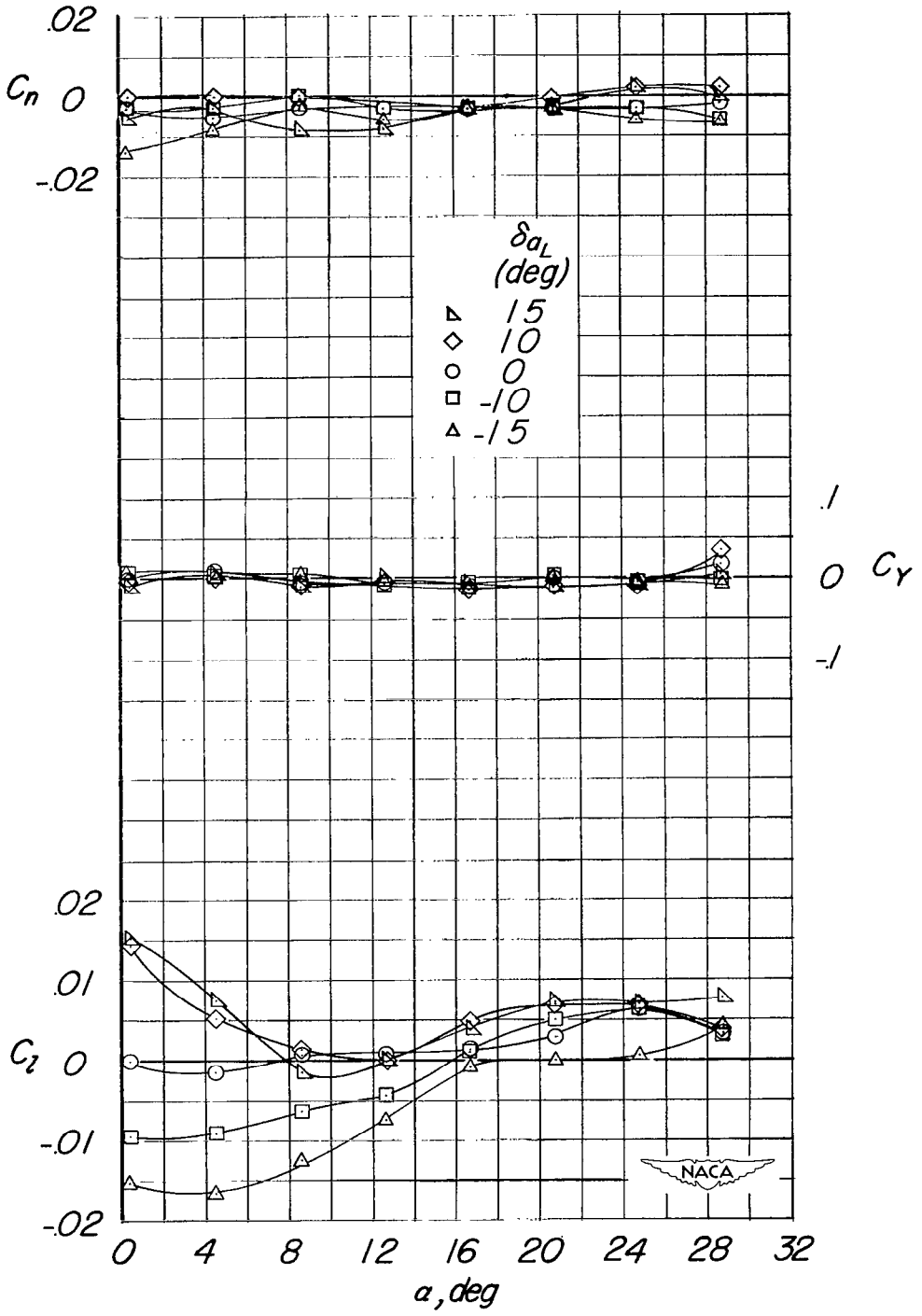

(a) Concluded.

Figure 34.- Continued.

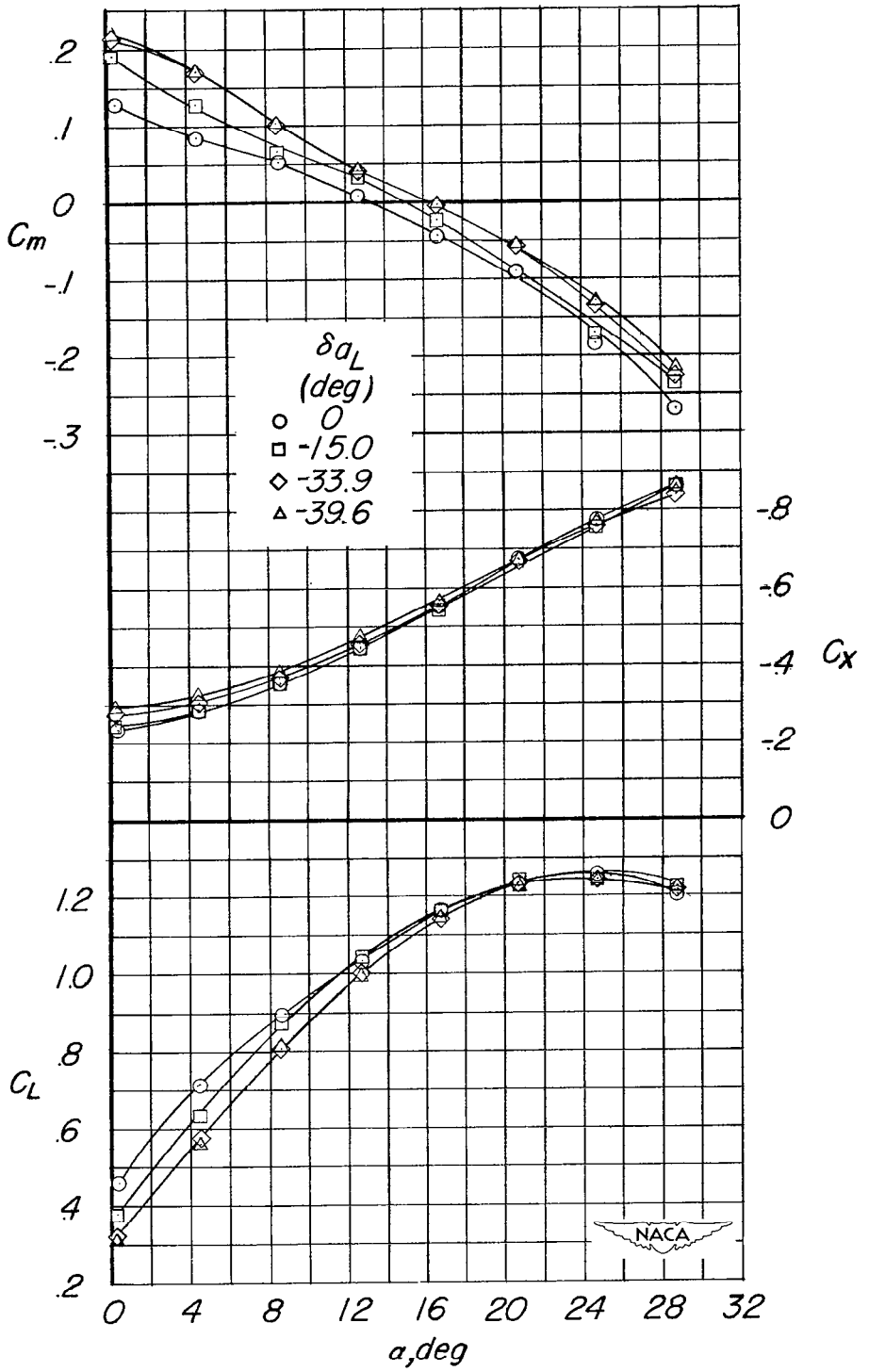

(b) $i_t = -11.1^\circ$.

Figure 34.- Continued.

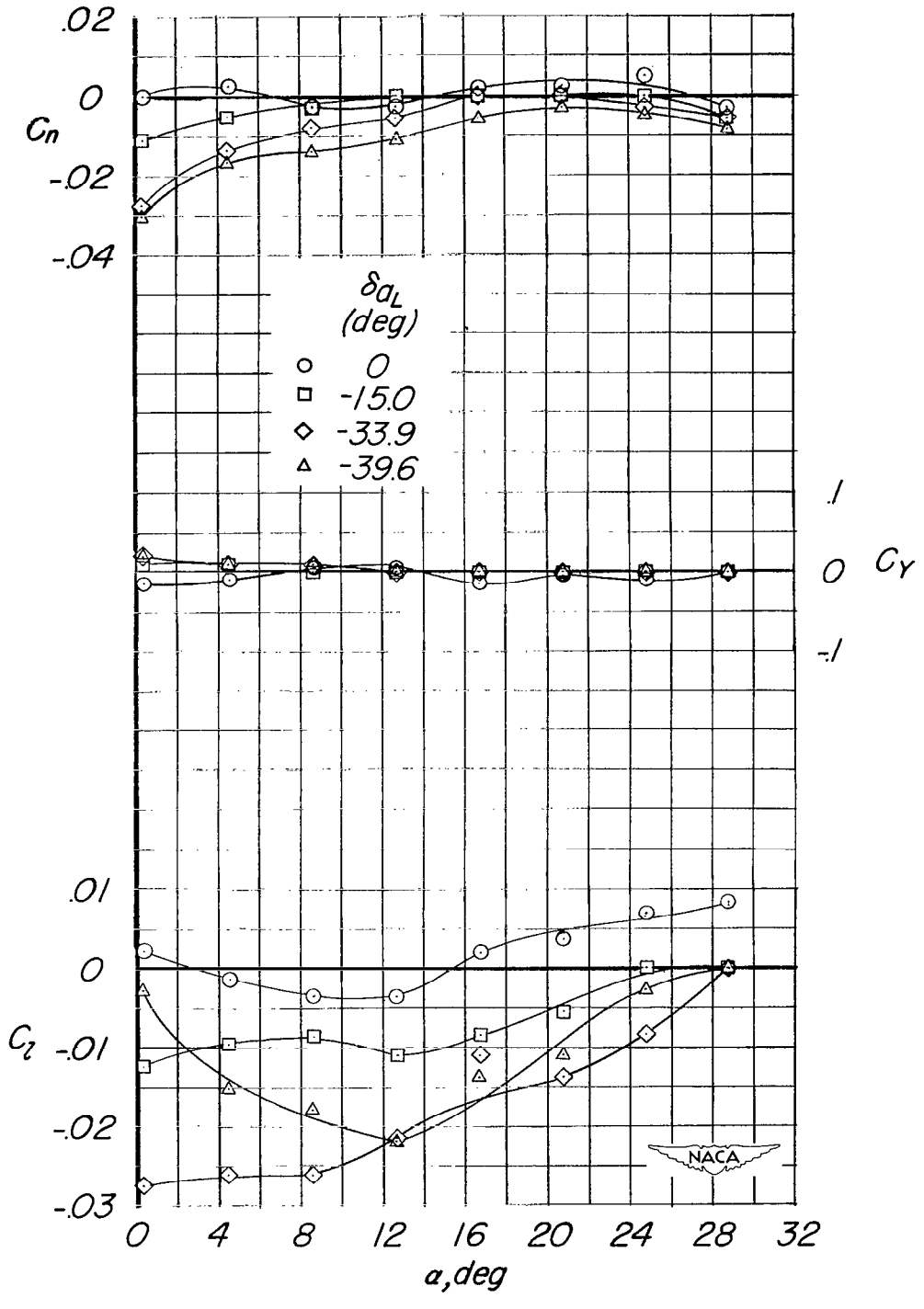

(b) Concluded.

Figure 34.- Concluded.

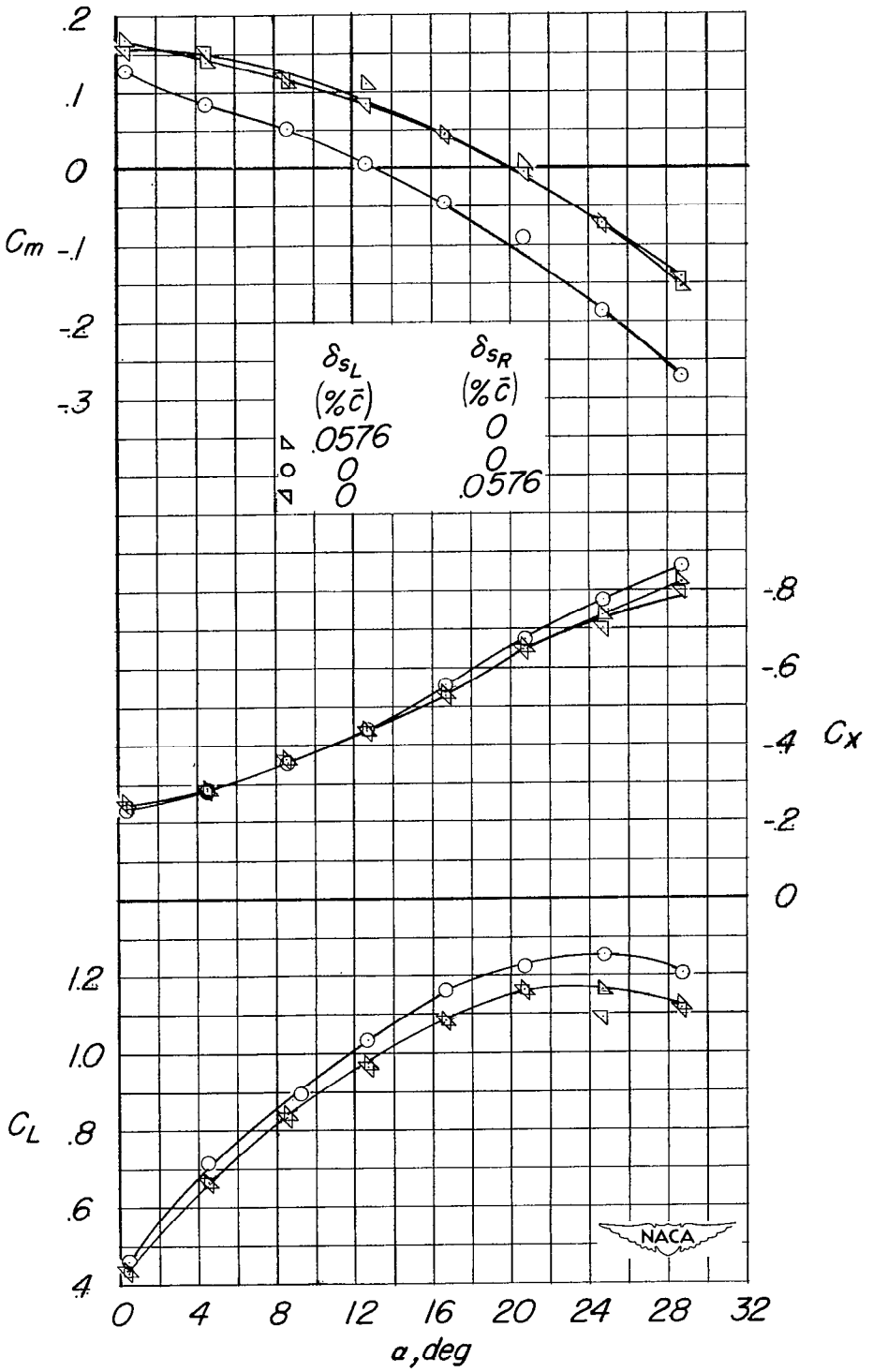

Figure 35.- Effect of spoiler deflection on the aerodynamic characteristics in pitch. Gear on; doors closed; $\delta_f = 57^\circ$; spoilers located on flap; wing position B; tail 2.

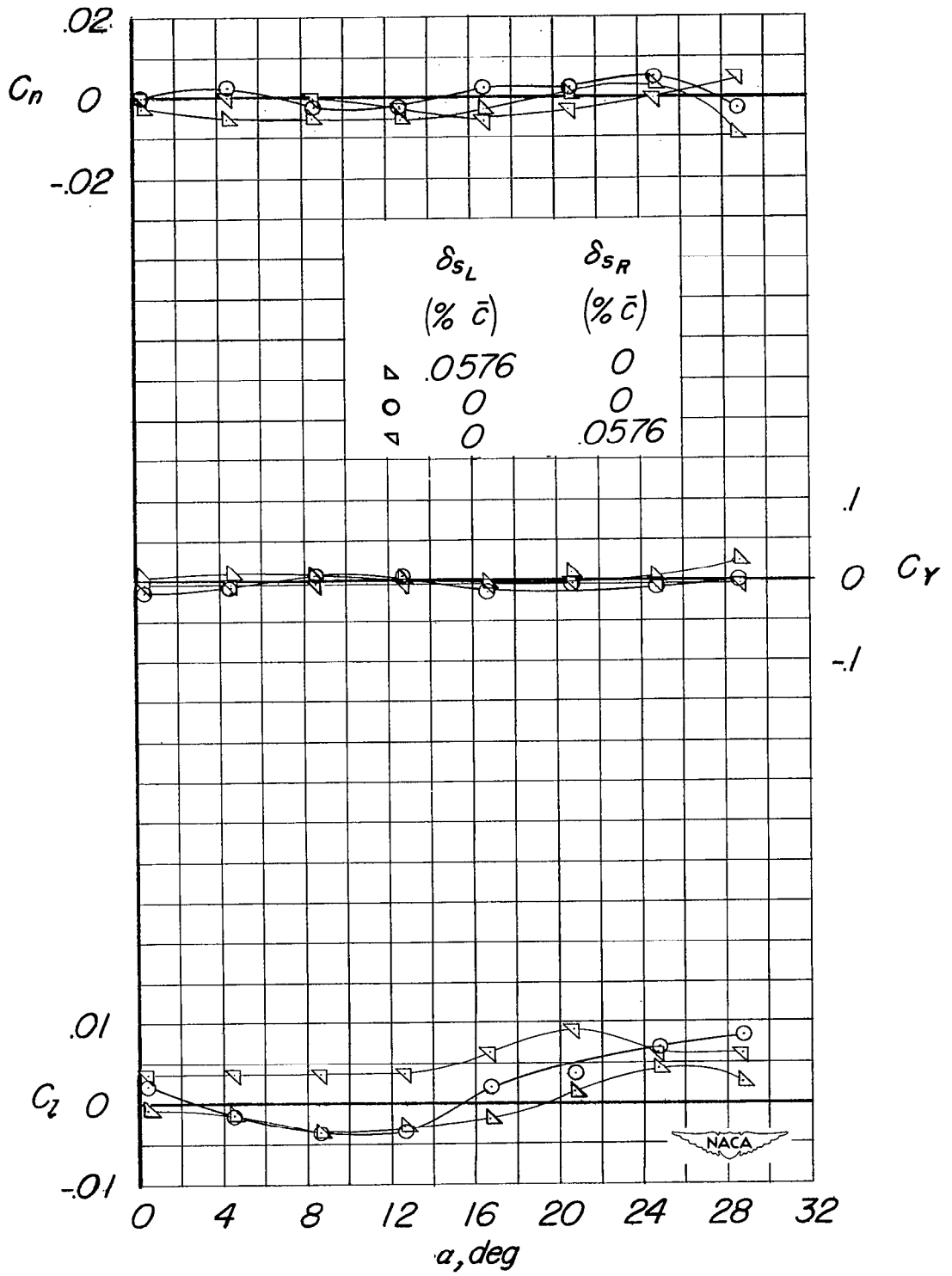

Figure 35.- Concluded.

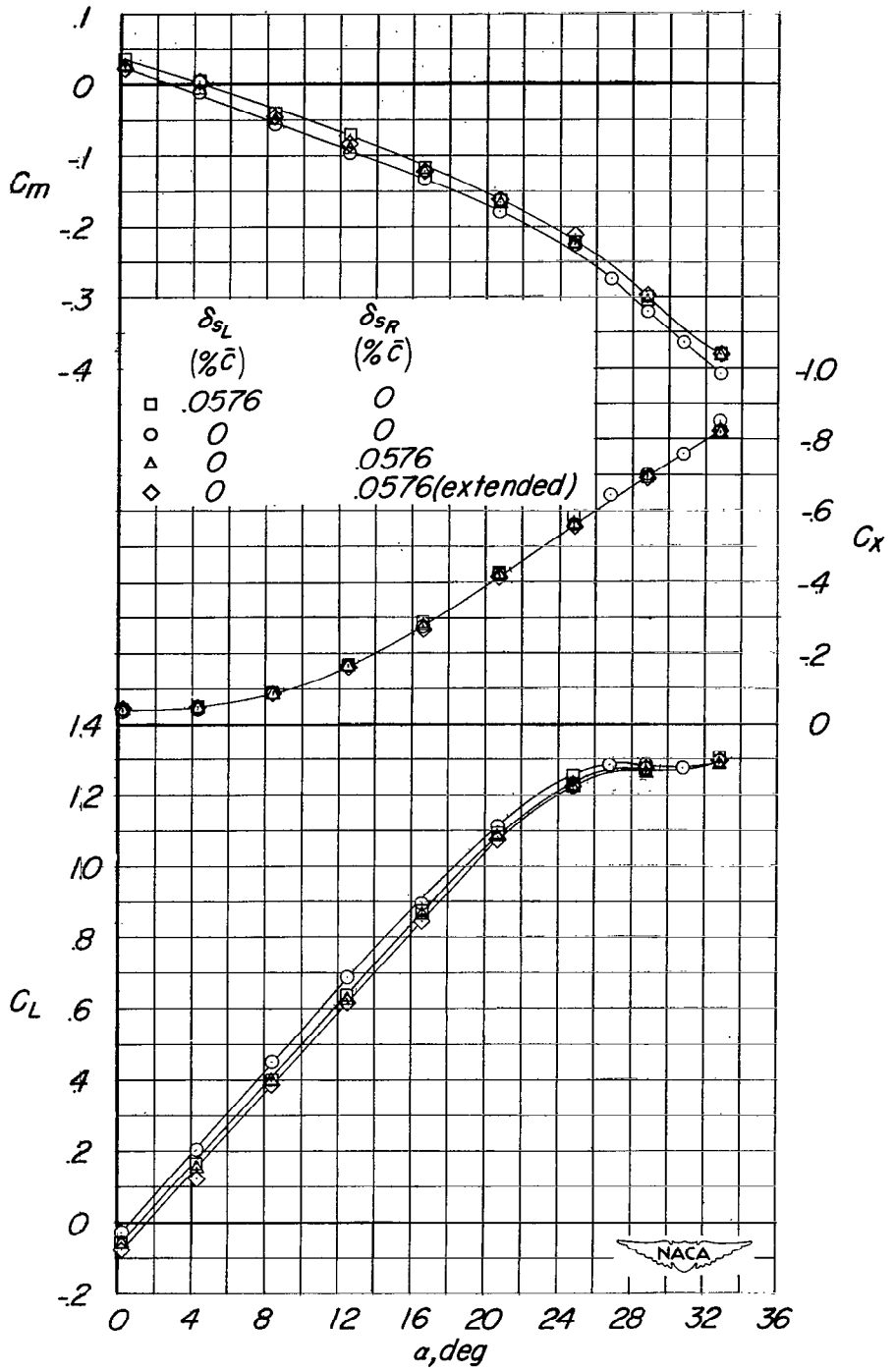

(a) $\delta_f = 0^\circ$; wing positon A; $i_w = 0$; tail 1.

Figure 36.- Effect of spoiler deflection on the aerodynamic characteristics in pitch. Spoilers on wing.

[redacted]

	δ_{s_L} (% $\bar{c}$)	δ_{s_R} (% $\bar{c}$)
□	.0576	0
○	0	0
△	0	.0576
◇	0	.0576 (extended)

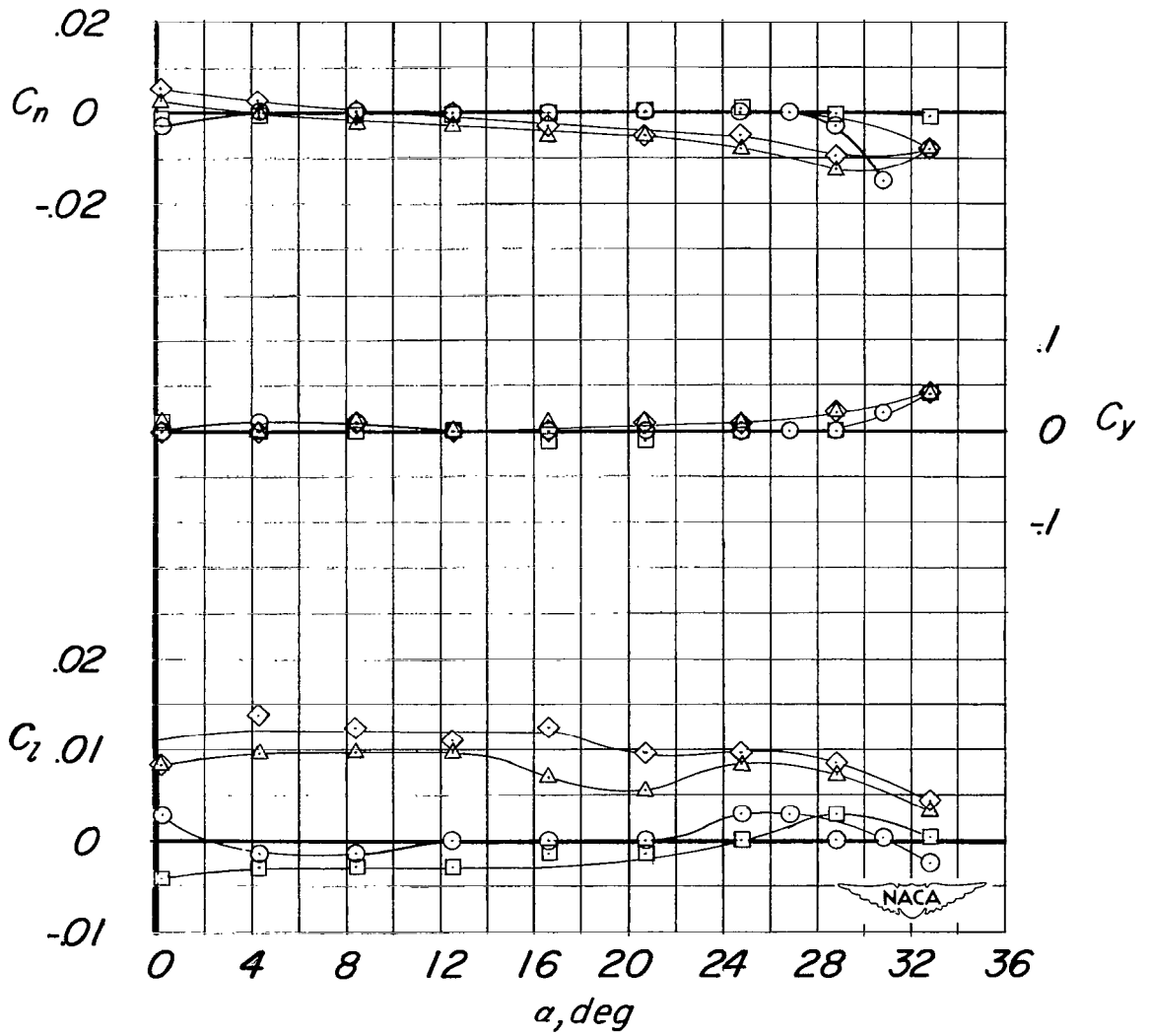

(a) Concluded.

Figure 36.- Continued.

[redacted]

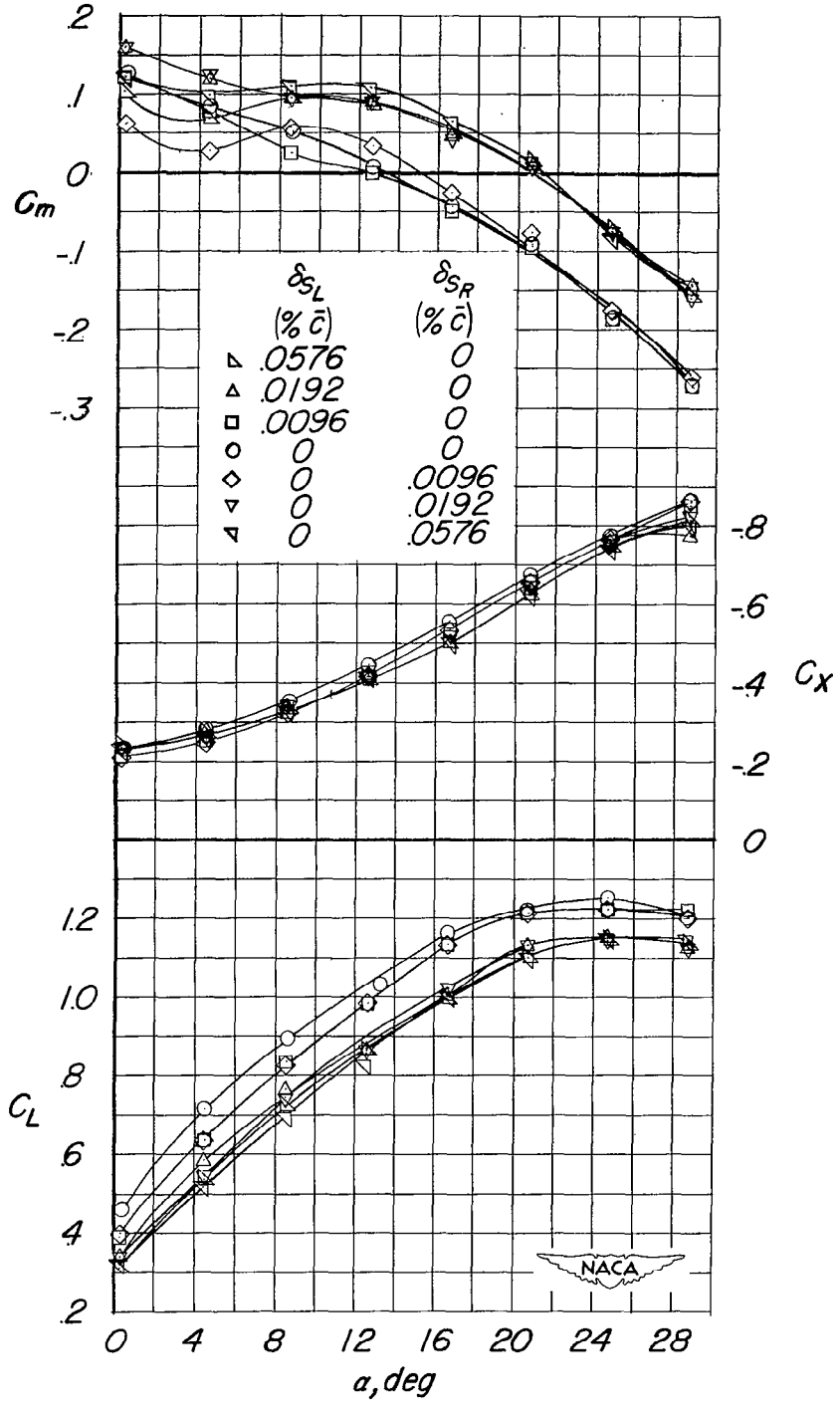

(b) $\delta_f = 57^\circ$; wing position B; $i_w = 0^\circ$; tail 2; gear on; doors closed.

Figure 36.- Continued.

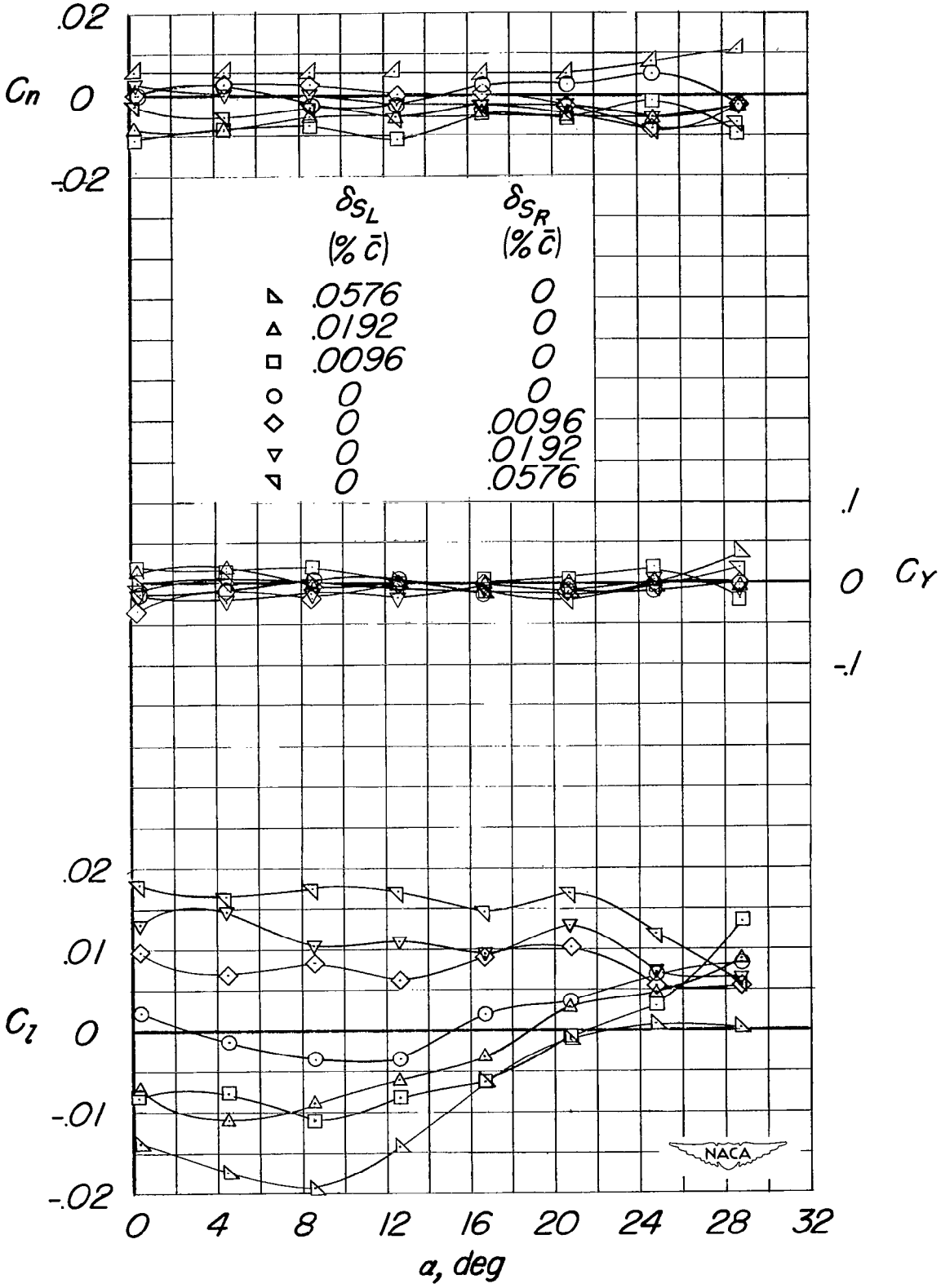

(b) Concluded.

Figure 36.- Concluded.

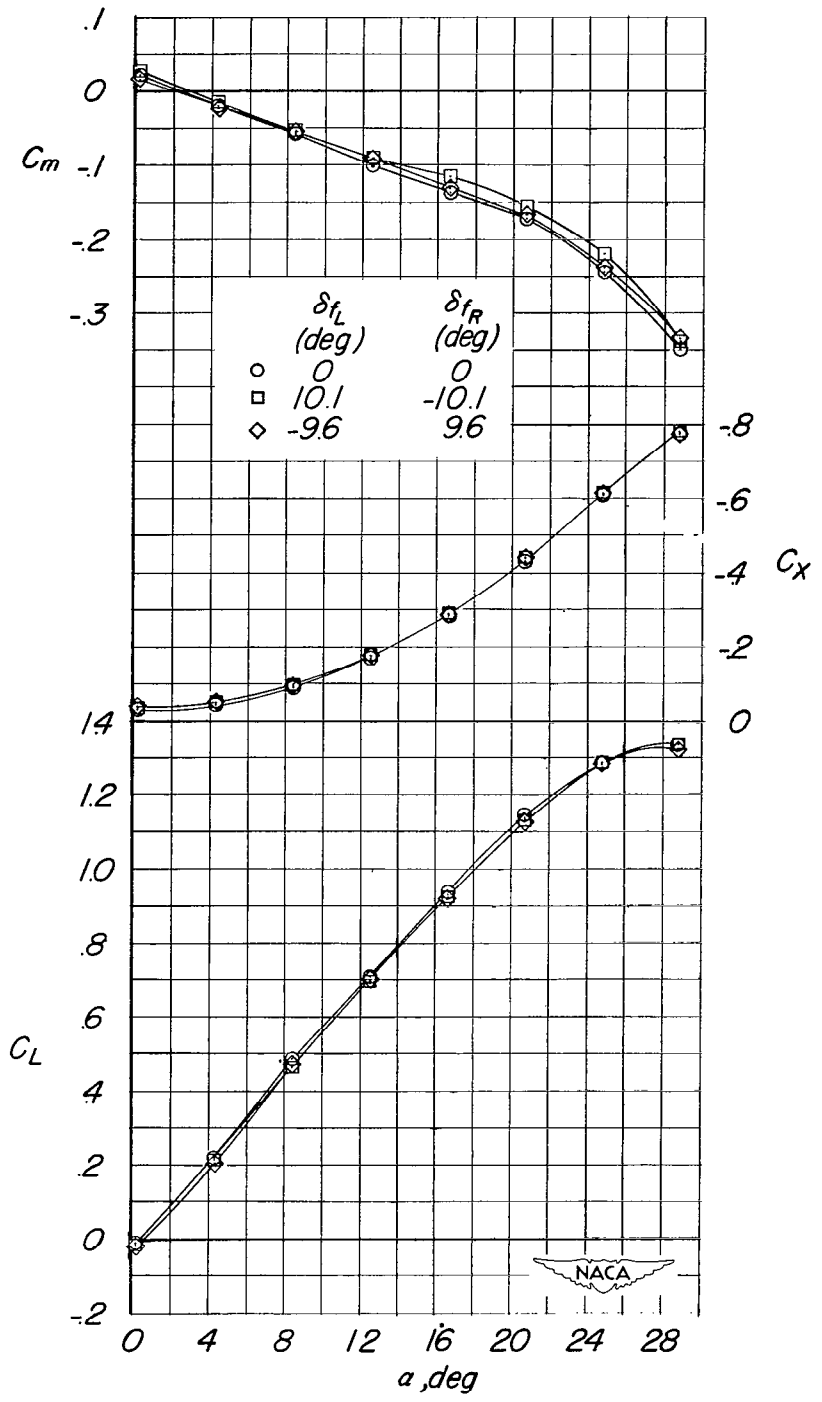

(a) $\delta_f = 0^\circ$.

Figure 37.- Effect of differential flap deflection on the aerodynamic characteristics in pitch. Wing position B; tail 2; gear off.

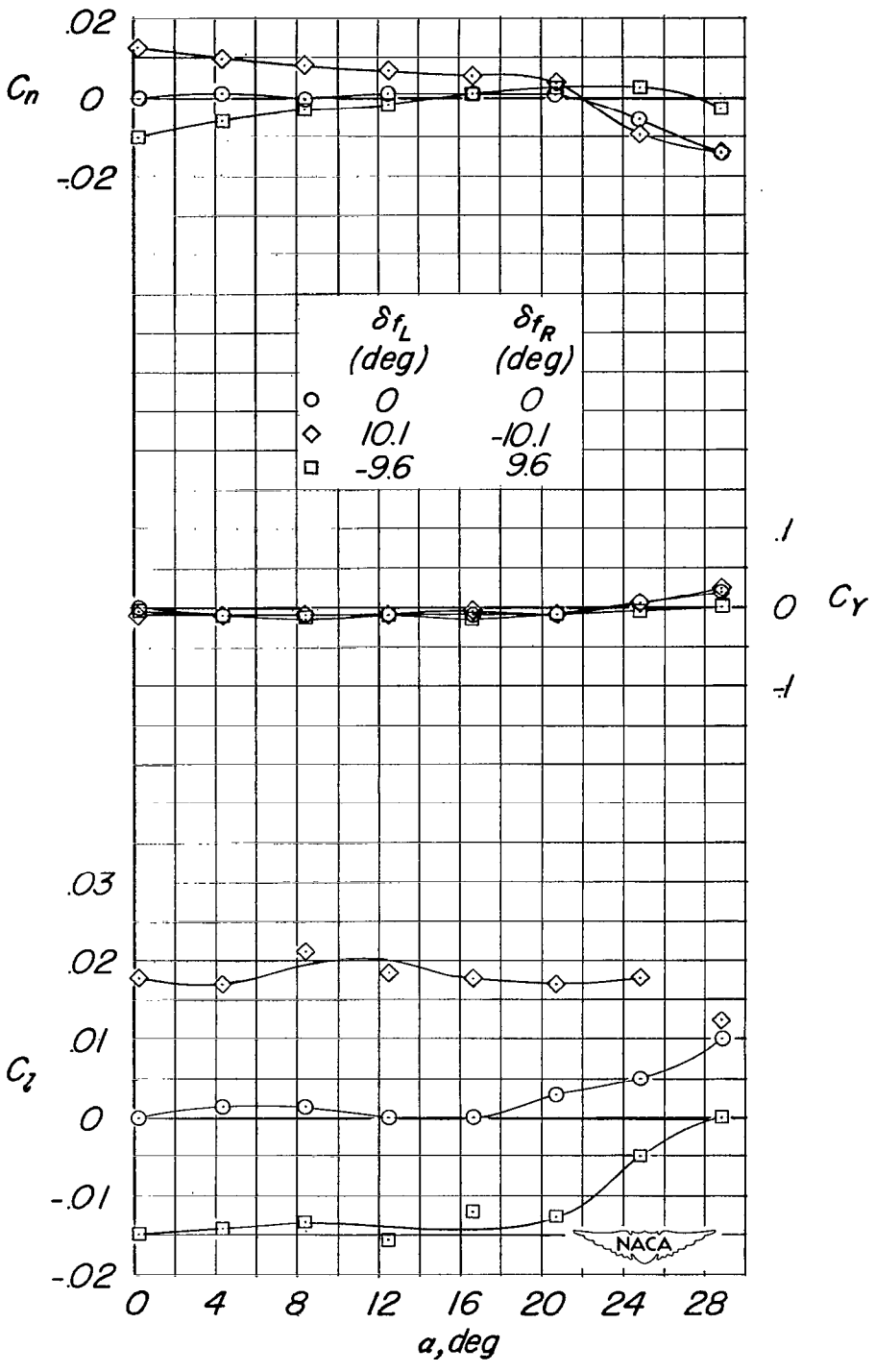

(a) Concluded.

Figure 37.- Continued.

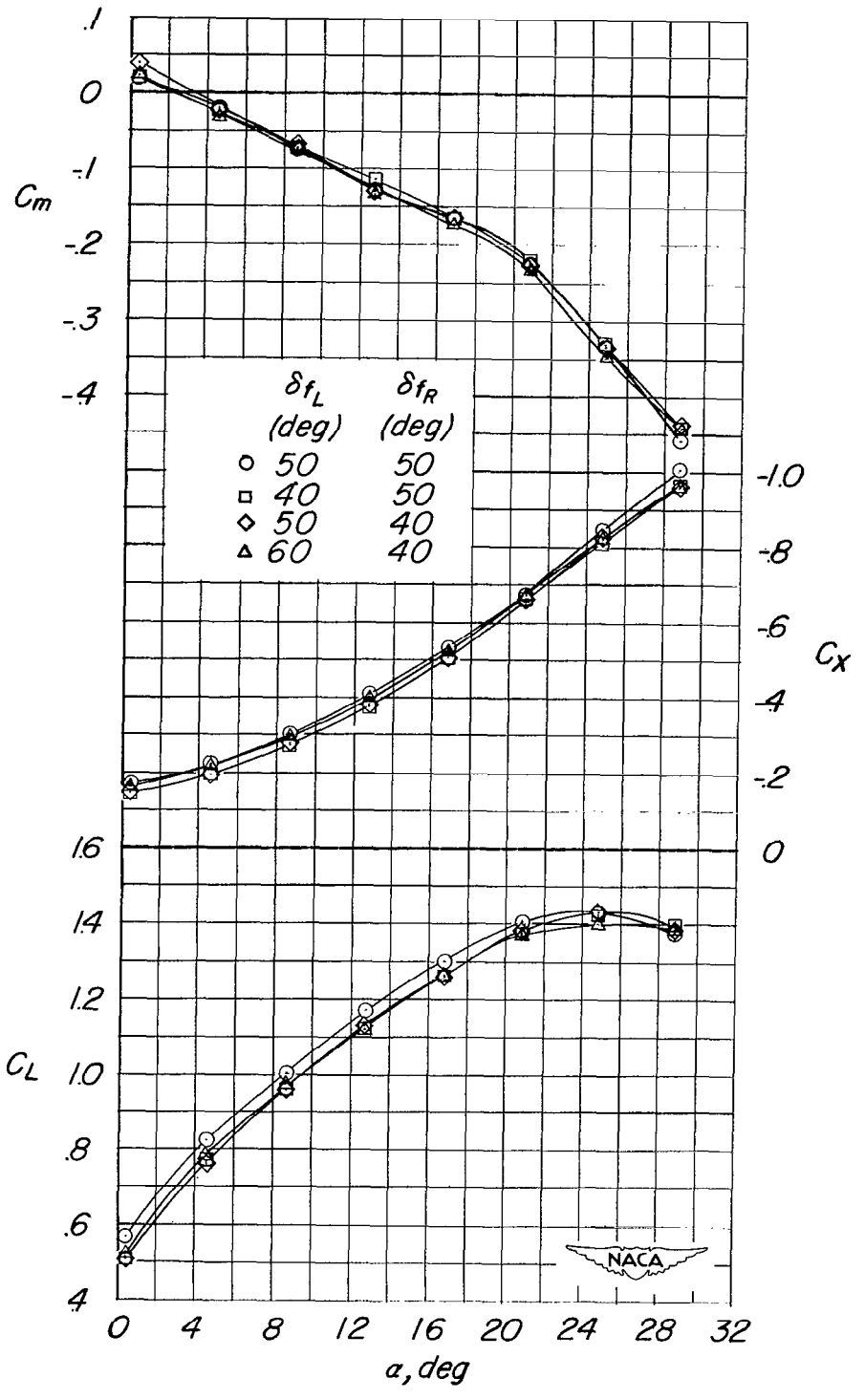

(b) $\delta_f = 50°$.

Figure 37.- Continued.

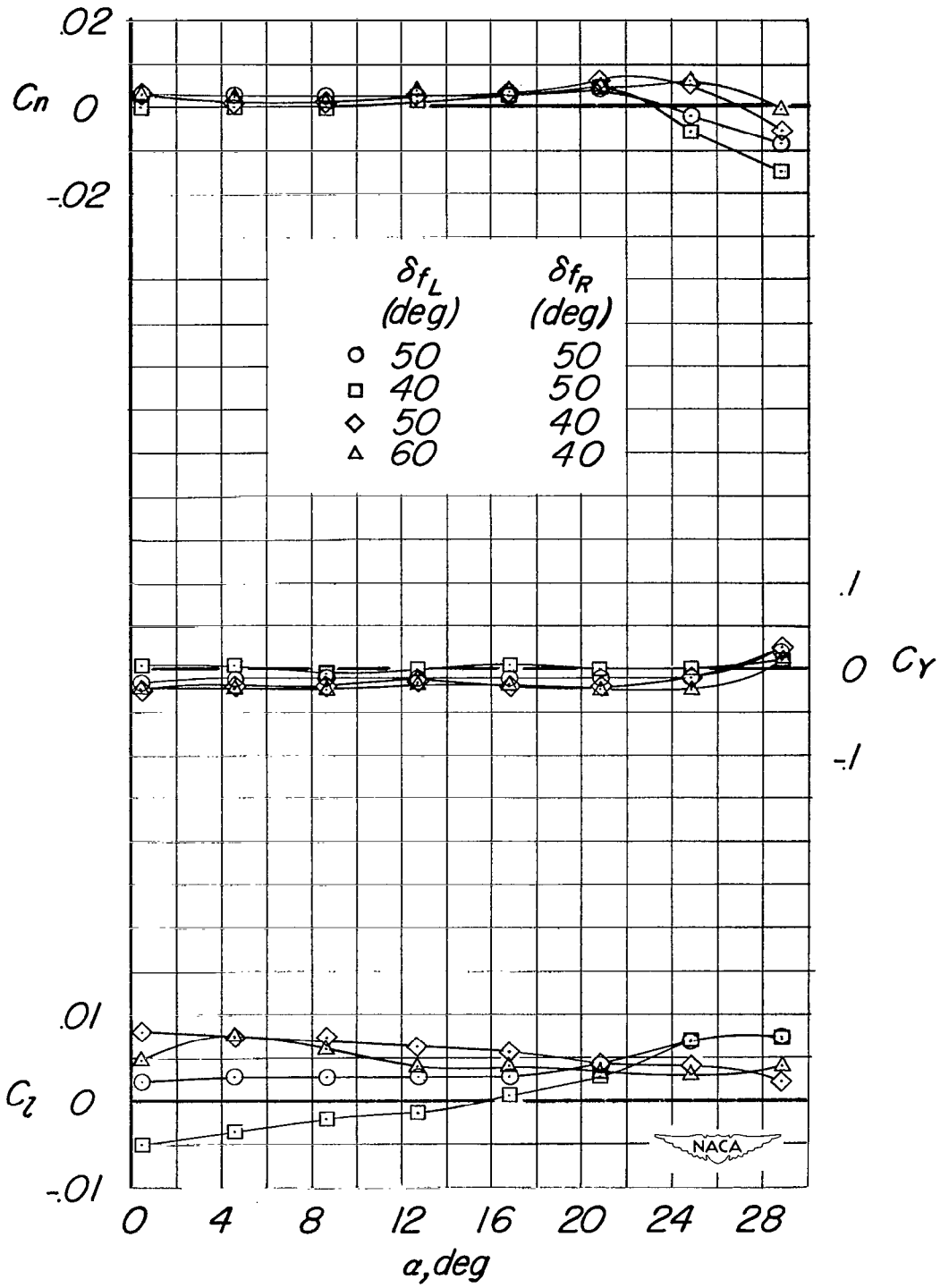

(b) Concluded.

Figure 37.- Concluded.

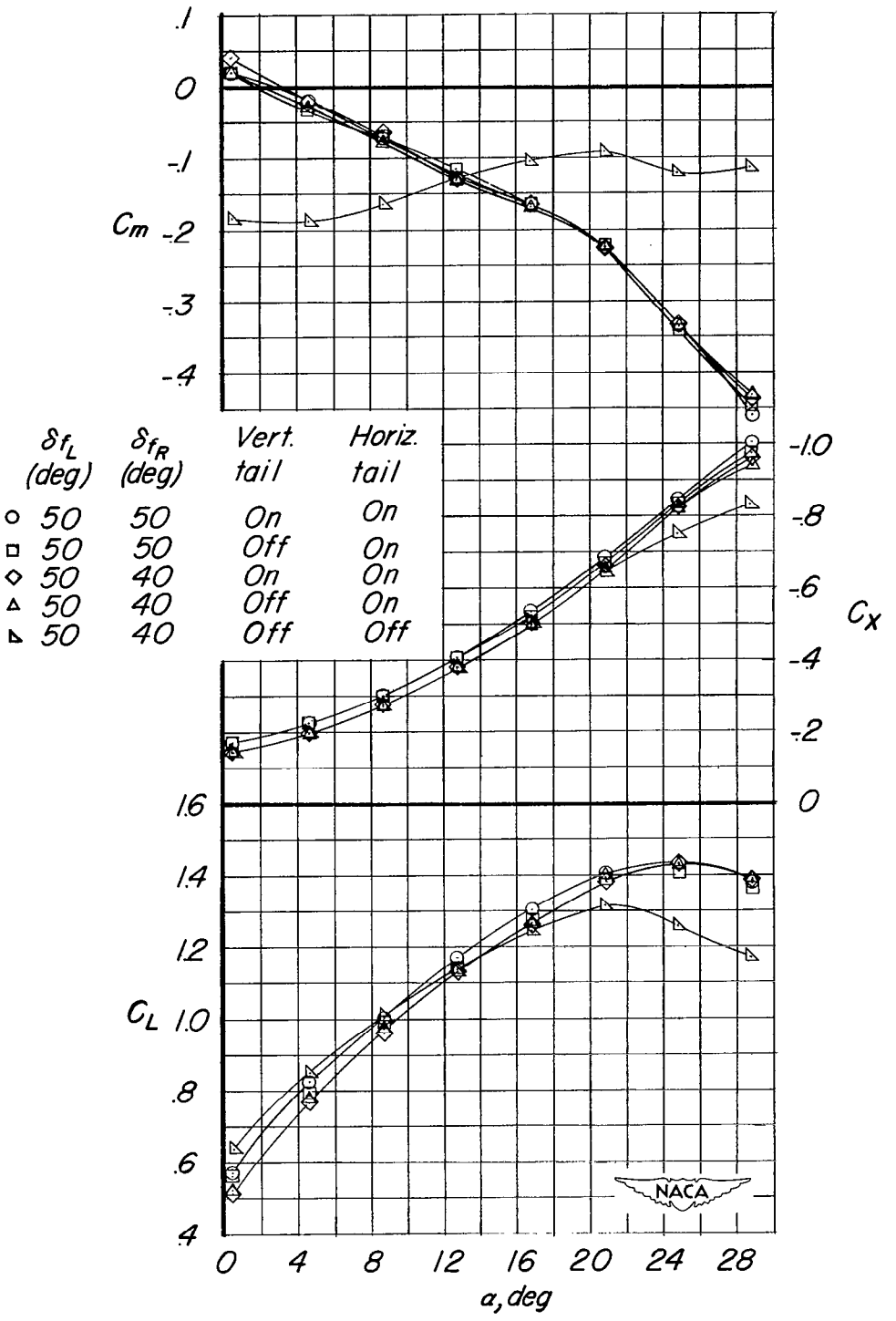

Figure 38.- Effect of the tail planes on the aerodynamic characteristics with the flaps differentially deflected. Wing position B; tail 2; gear off.

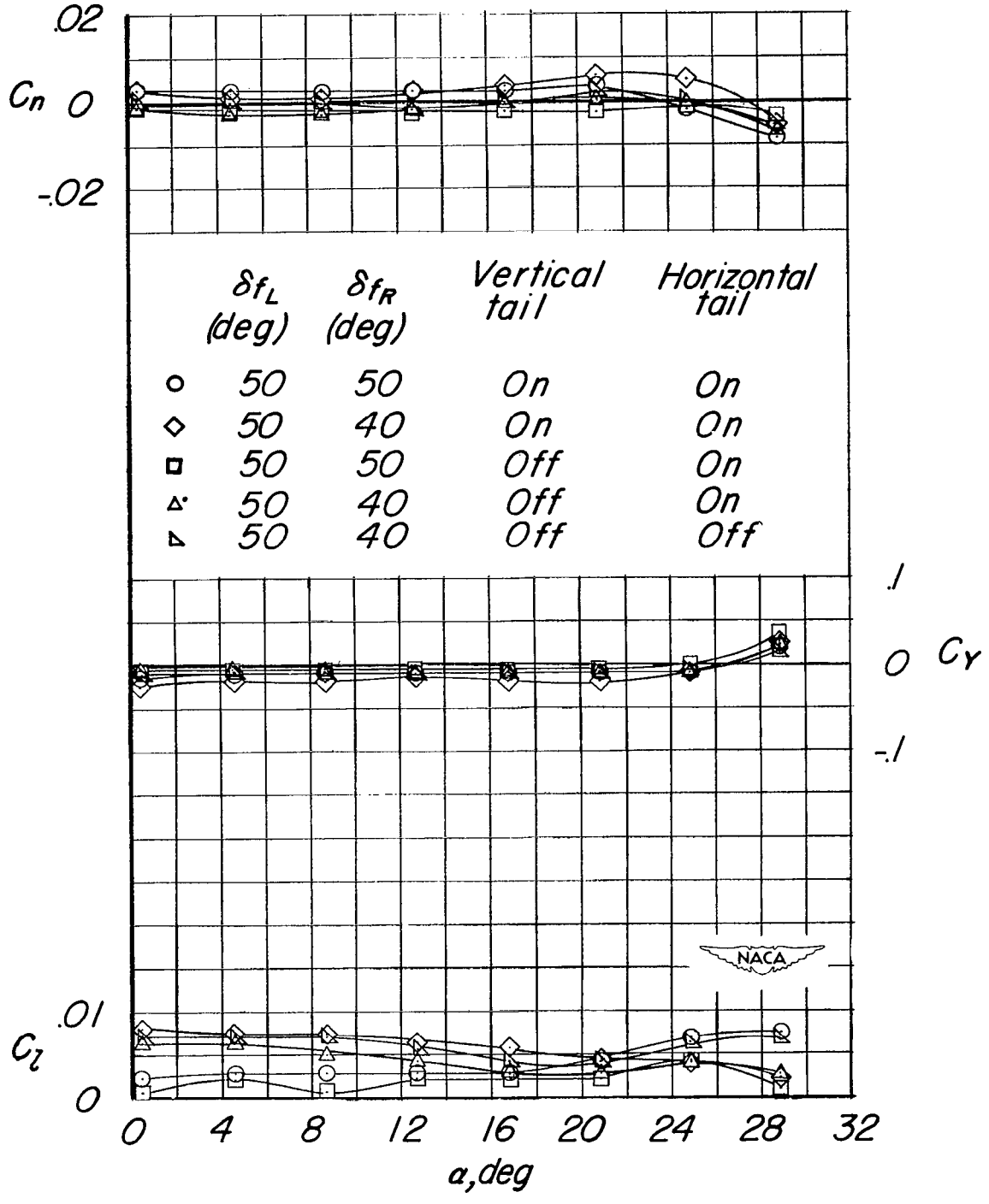

Figure 38.- Concluded.

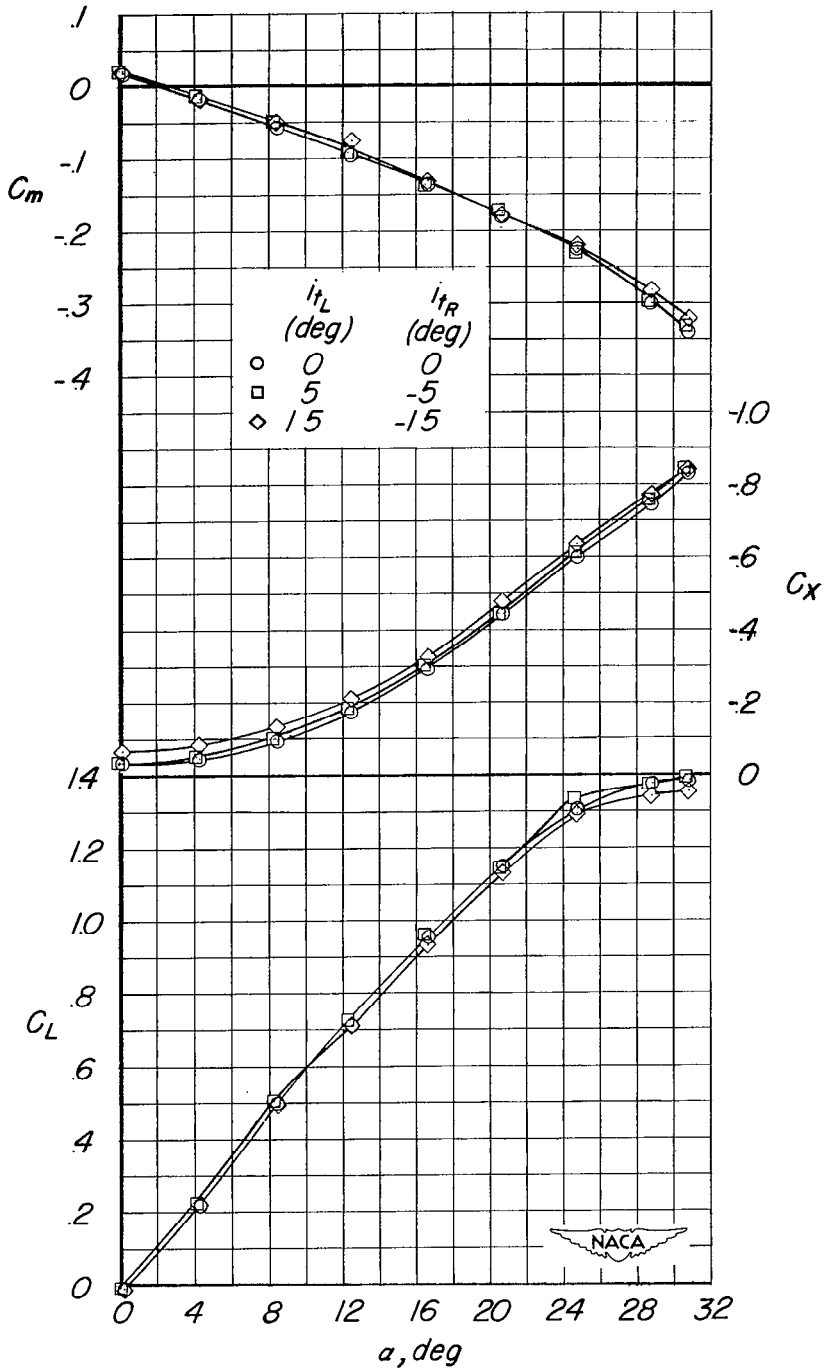

(a) $\delta_f = 0°$.

Figure 39.- Effect of differential deflection of the large-span horizontal on the aerodynamic characteristics in pitch. Wing position C; tail 5; gear off.

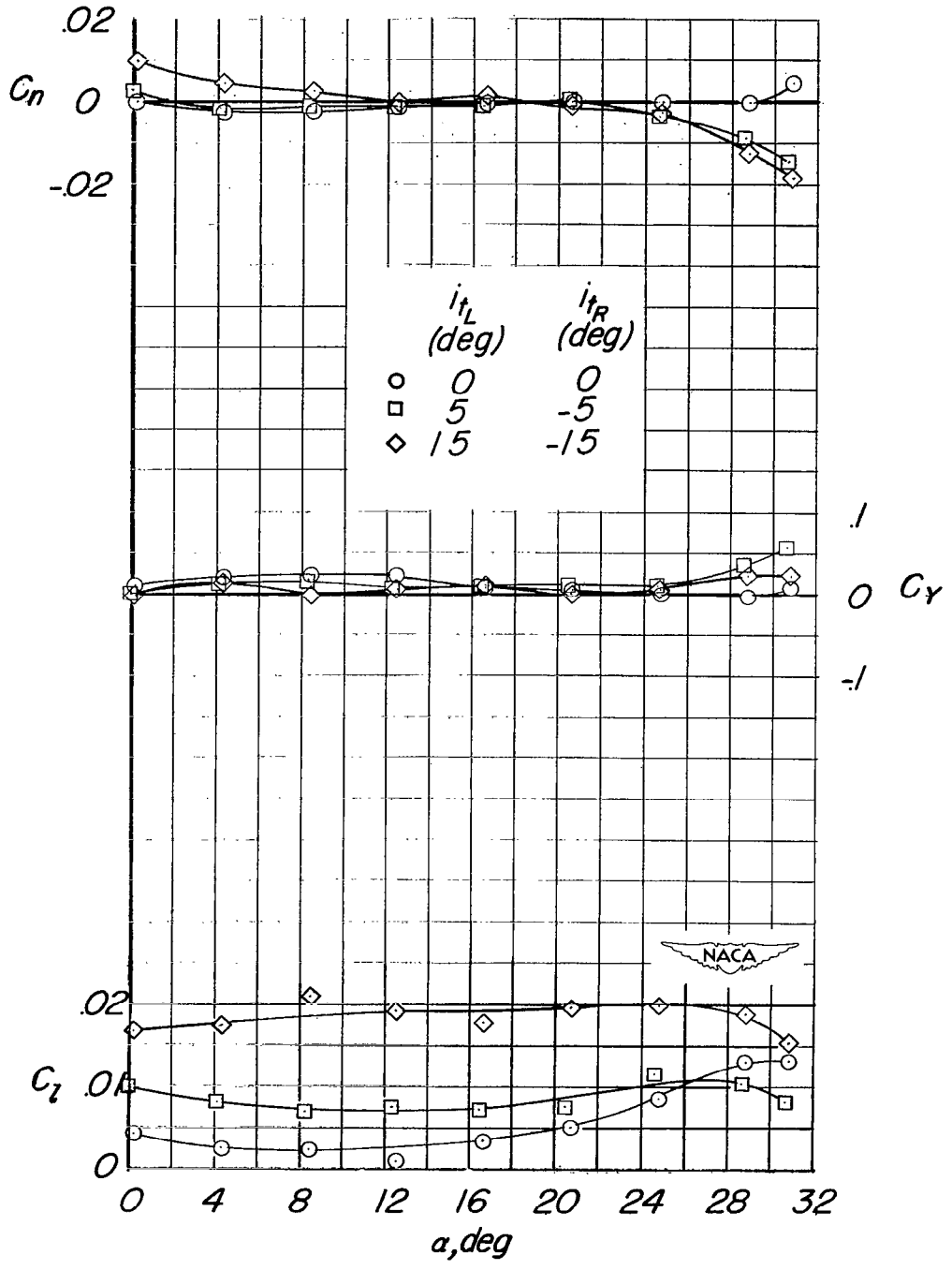

(a) Concluded.

Figure 39.- Continued.

[redacted]

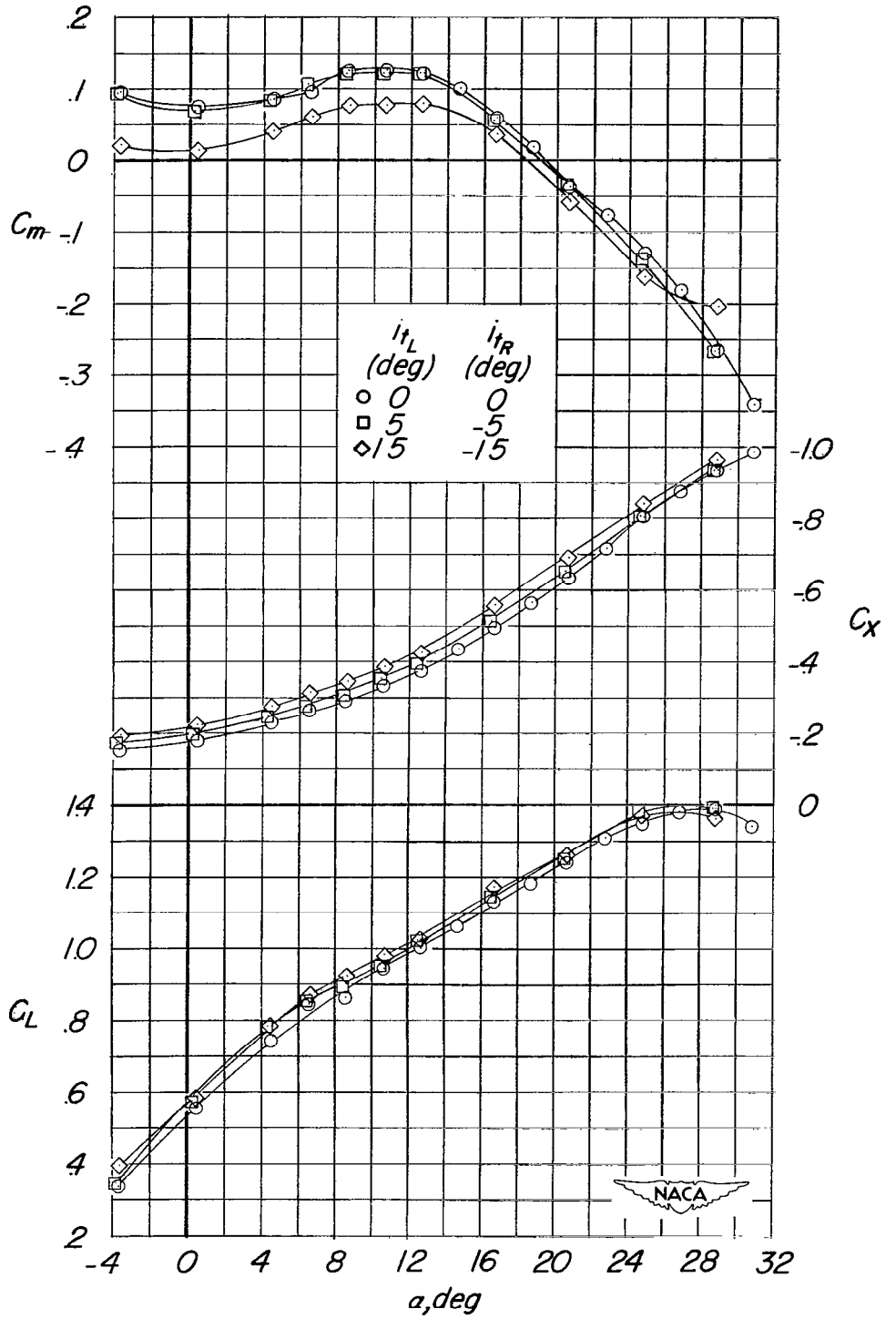

(b) $\delta_f = 52^\circ$.

Figure 39.- Continued.

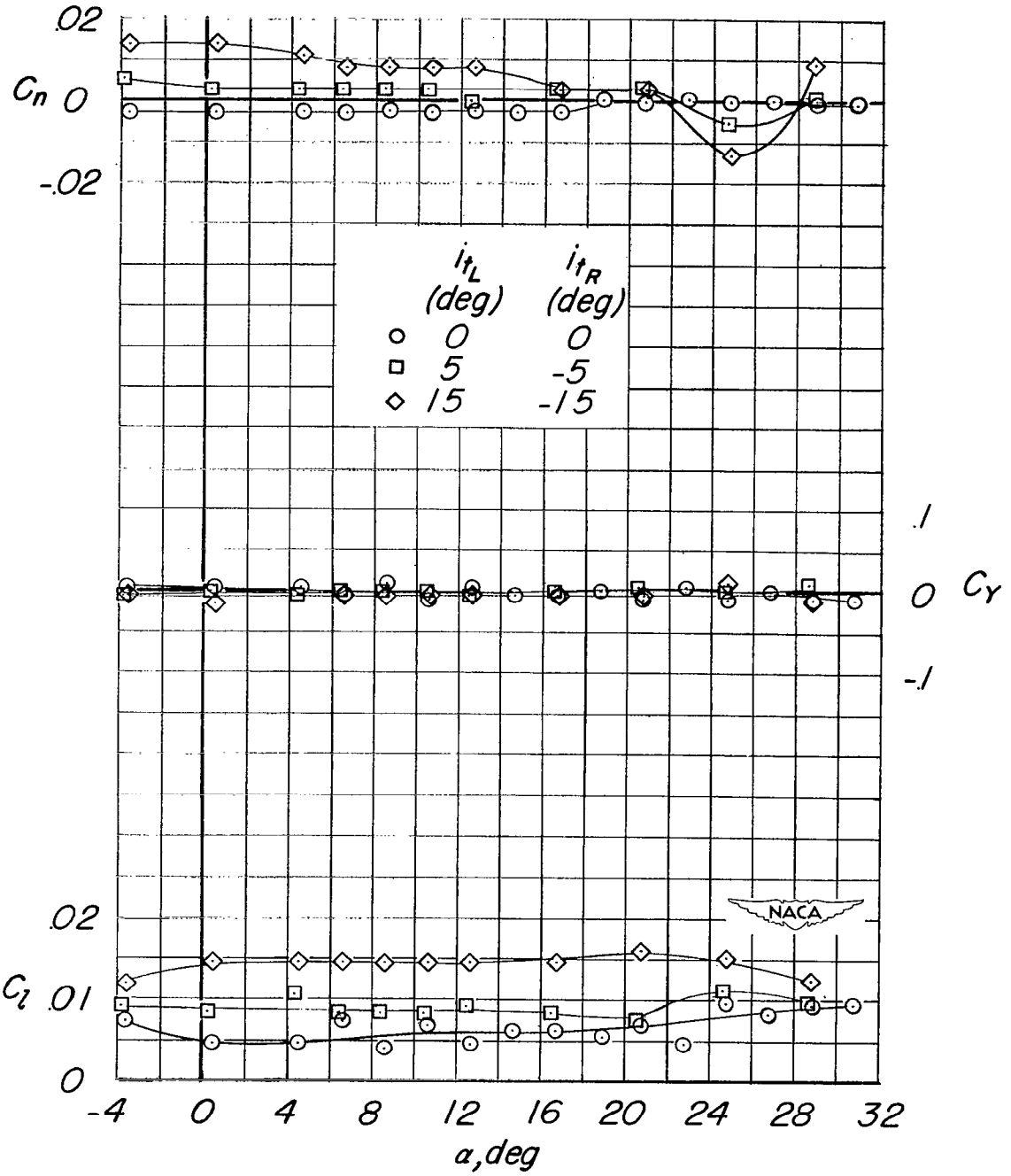

(b) Concluded.

Figure 39.- Concluded.

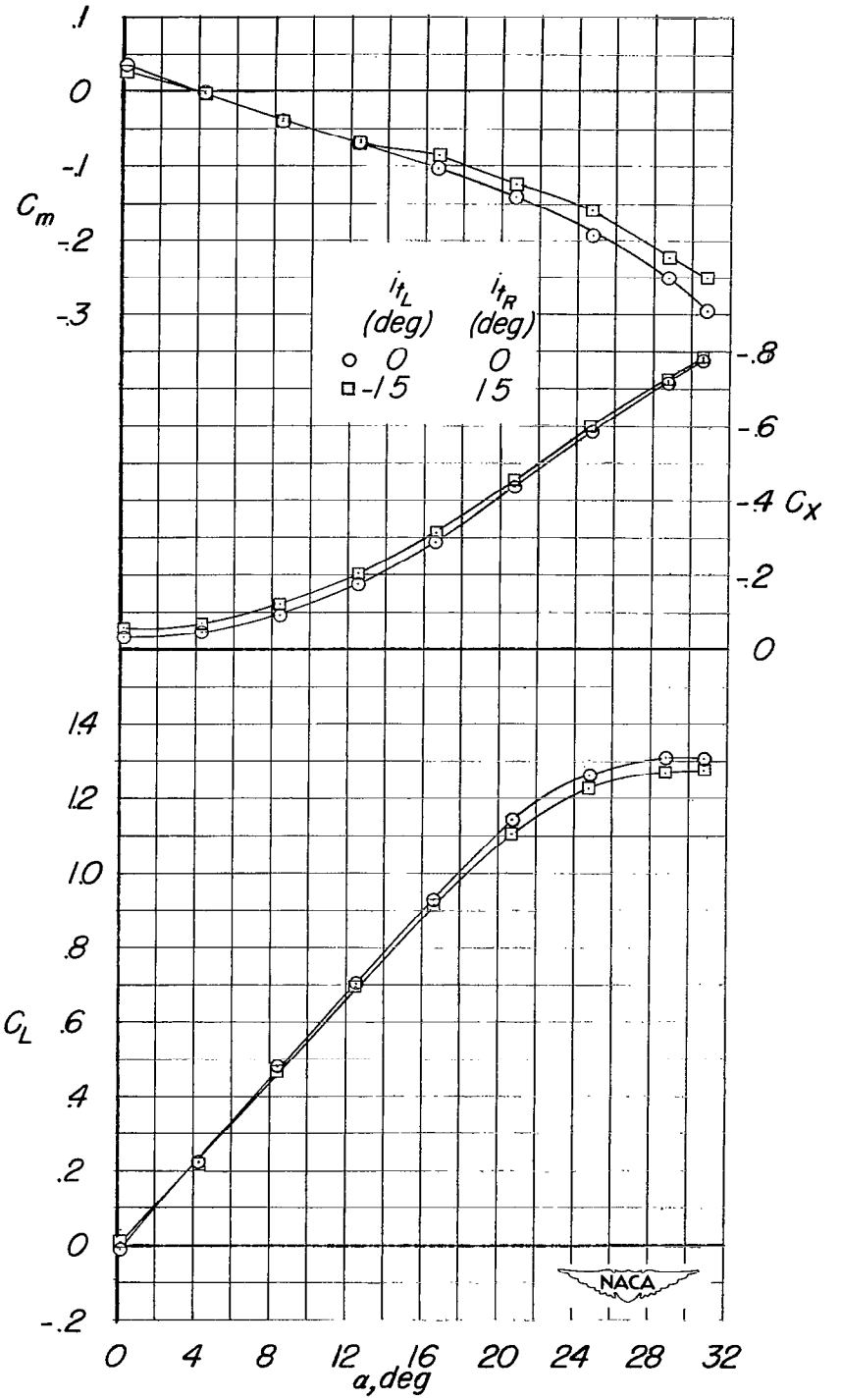

(a) $\delta_f = 0^\circ$; gear off.

Figure 40.- Effect of differential deflection of the horizontal tail on the aerodynamic characteristics in pitch. Wing position B; tail 3.

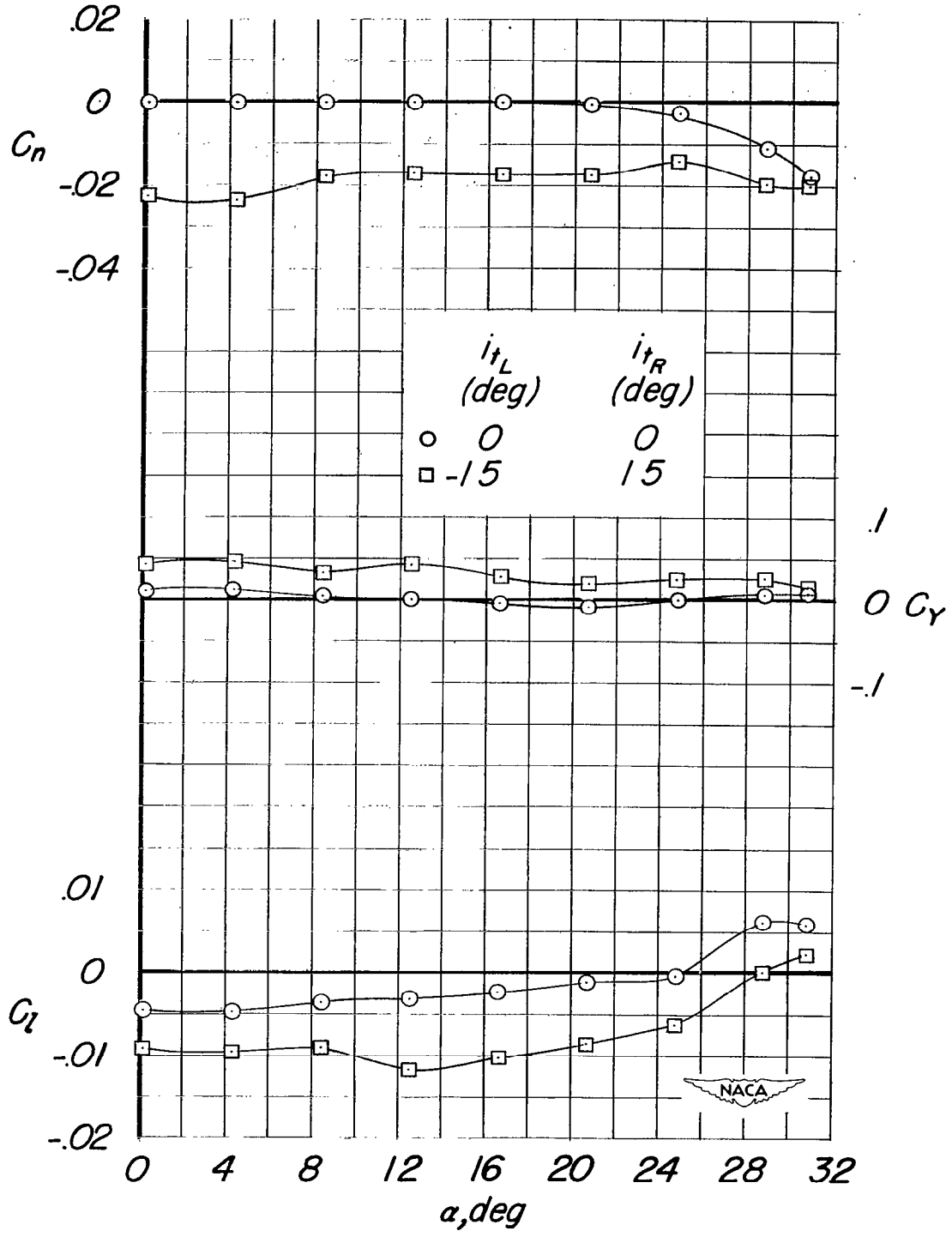

(a) Concluded.

Figure 40.- Continued.

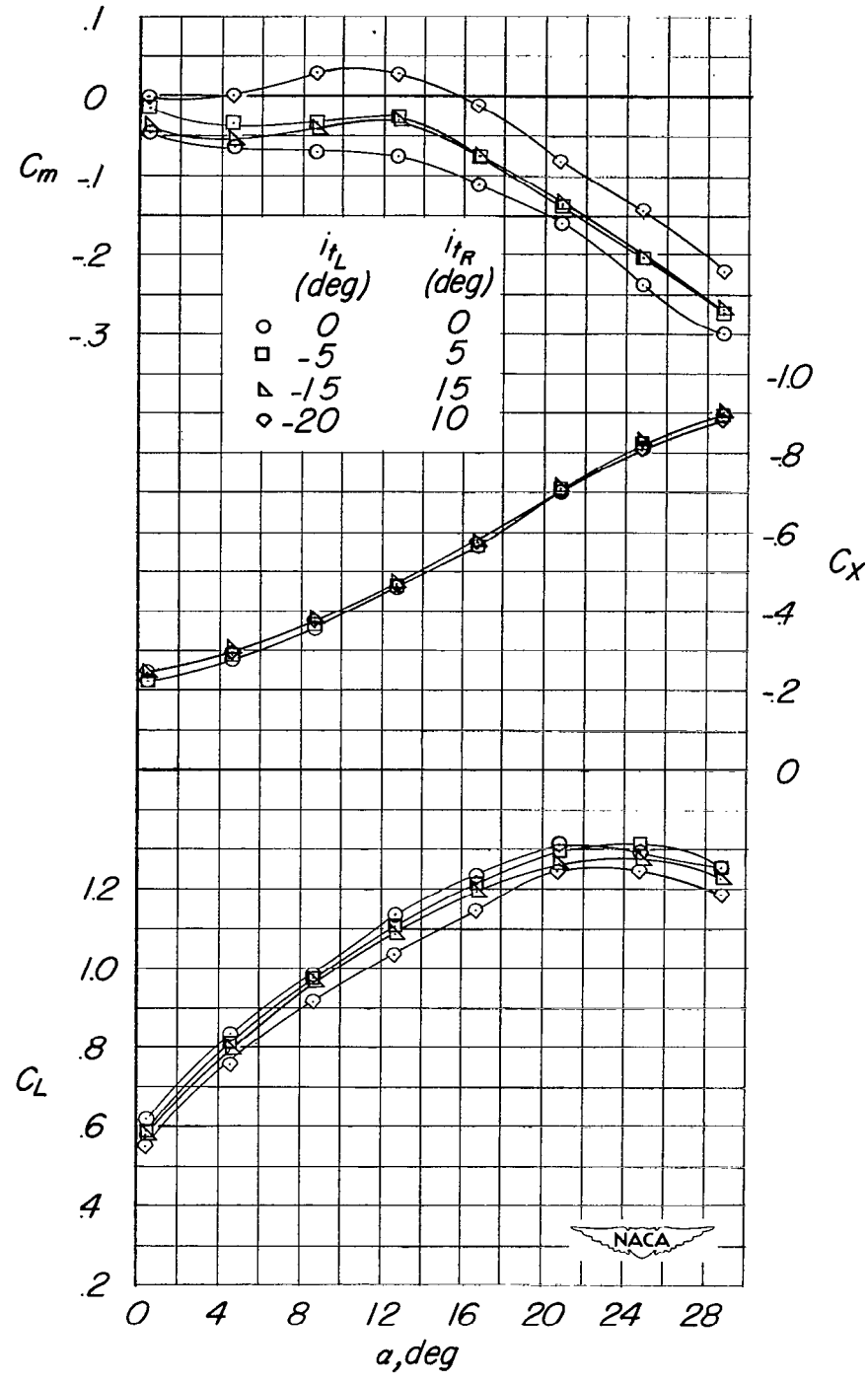

(b) $\delta_f = 57^\circ$; gear on; doors closed.

Figure 40.- Continued.

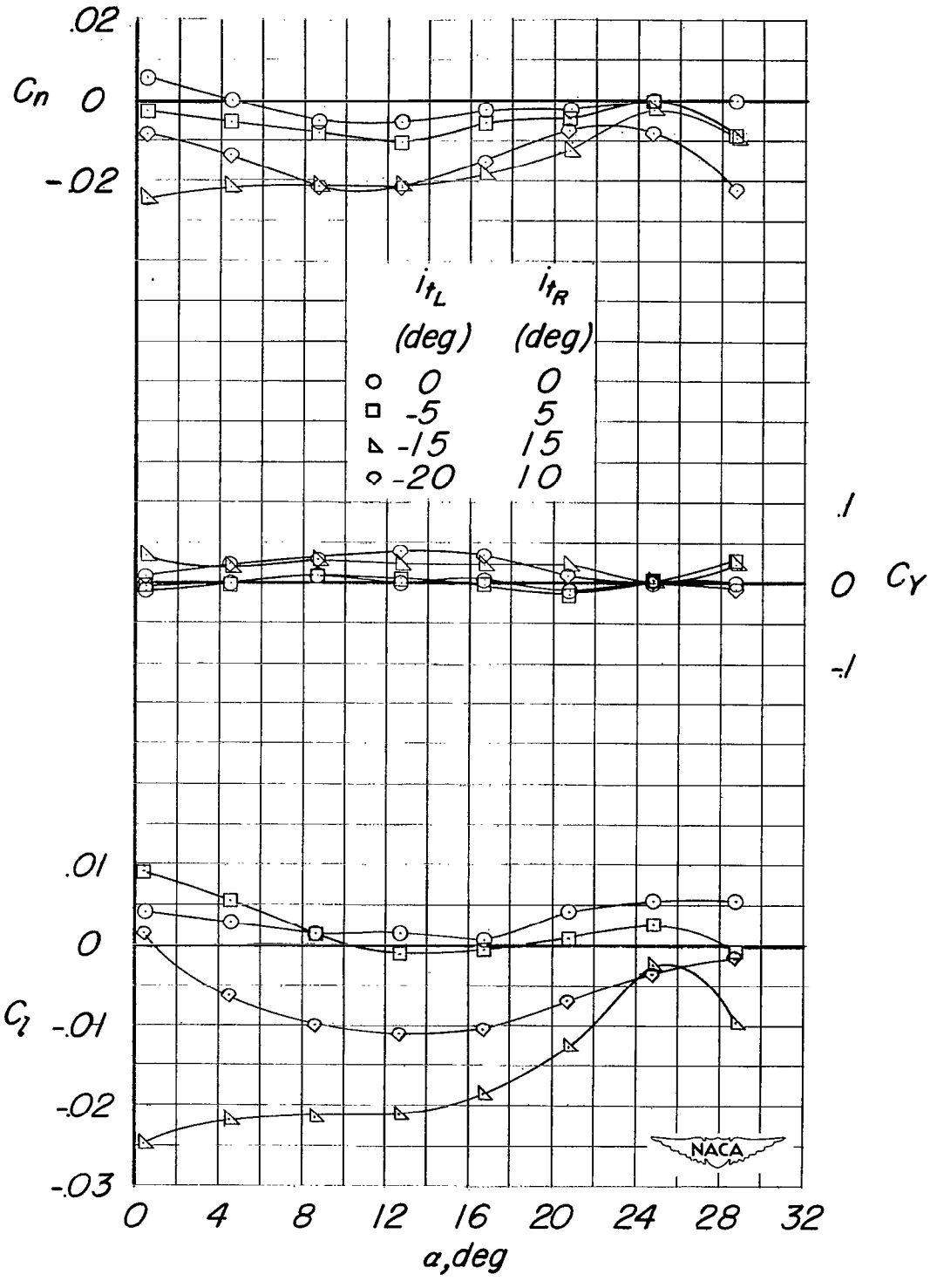

(b) Concluded.

Figure 40.- Concluded.

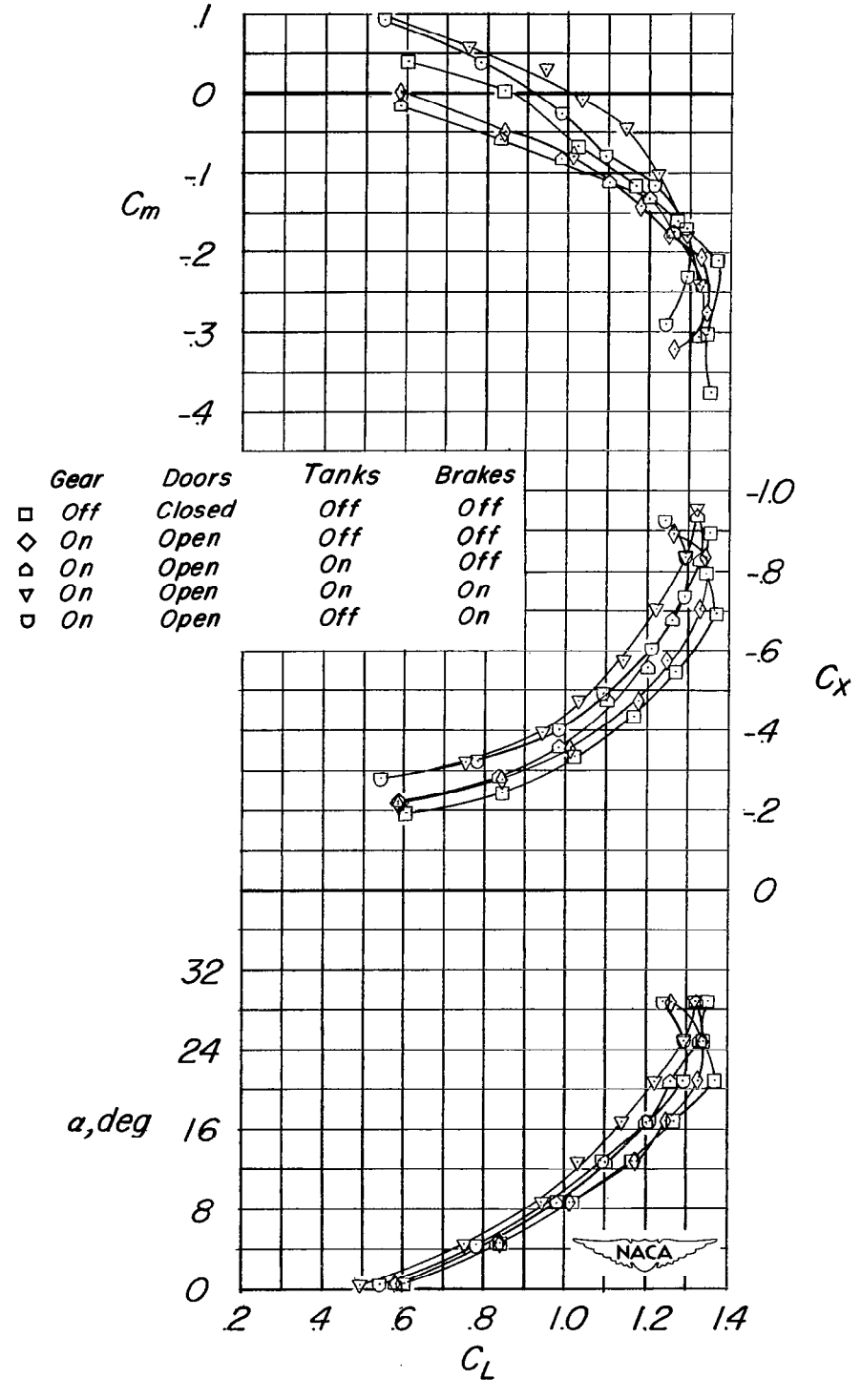

Figure 41.- The effect of external tanks, speed brakes, landing gear, and landing-gear doors on the aerodynamic characteristics in pitch. Wing position B; tail 2; $i_t = 0°$; $\delta_f = 57°$.

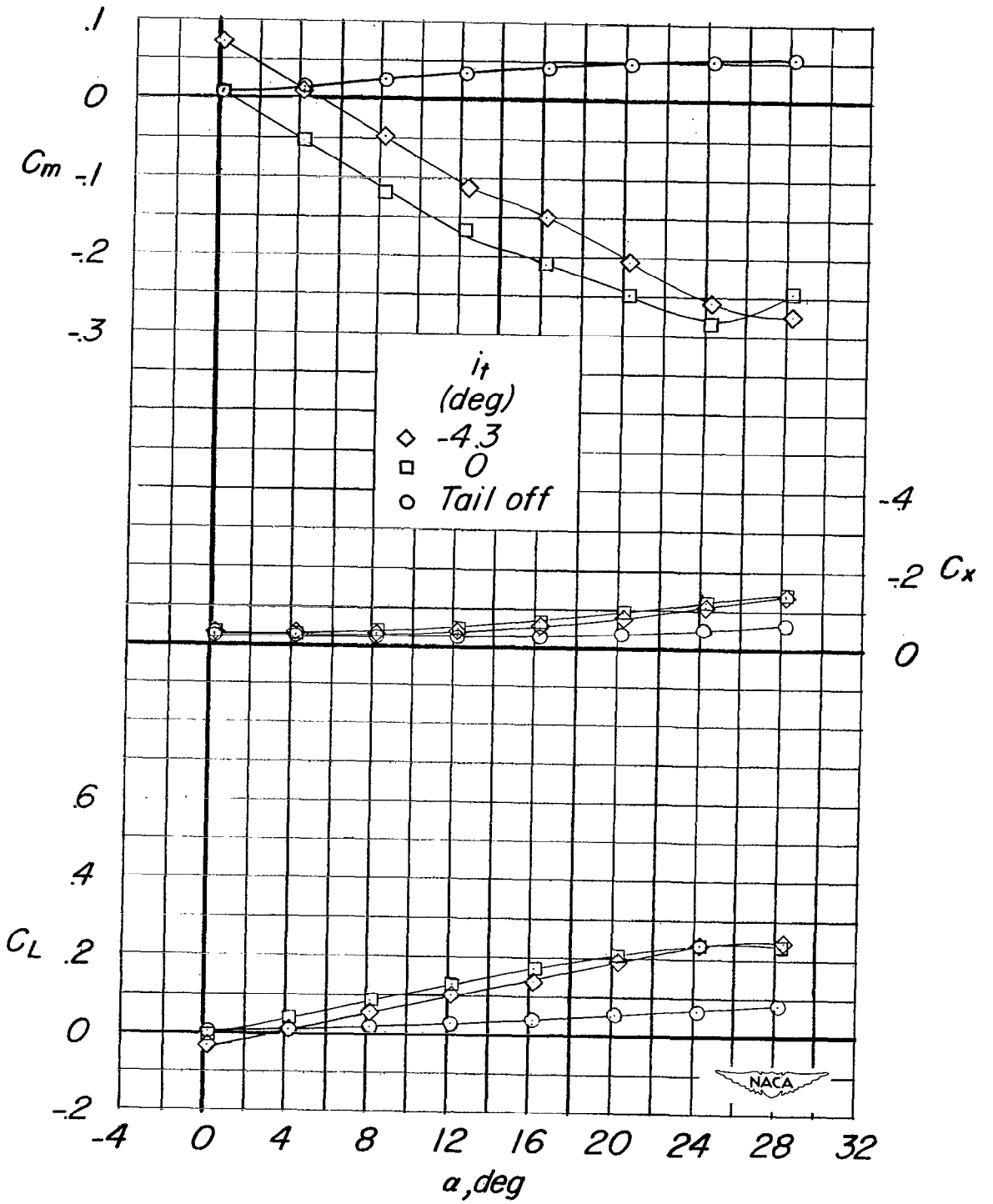

Figure 42.- The effect of the tail on the aerodynamic characteristics of the fuselage in pitch. Tail 2.

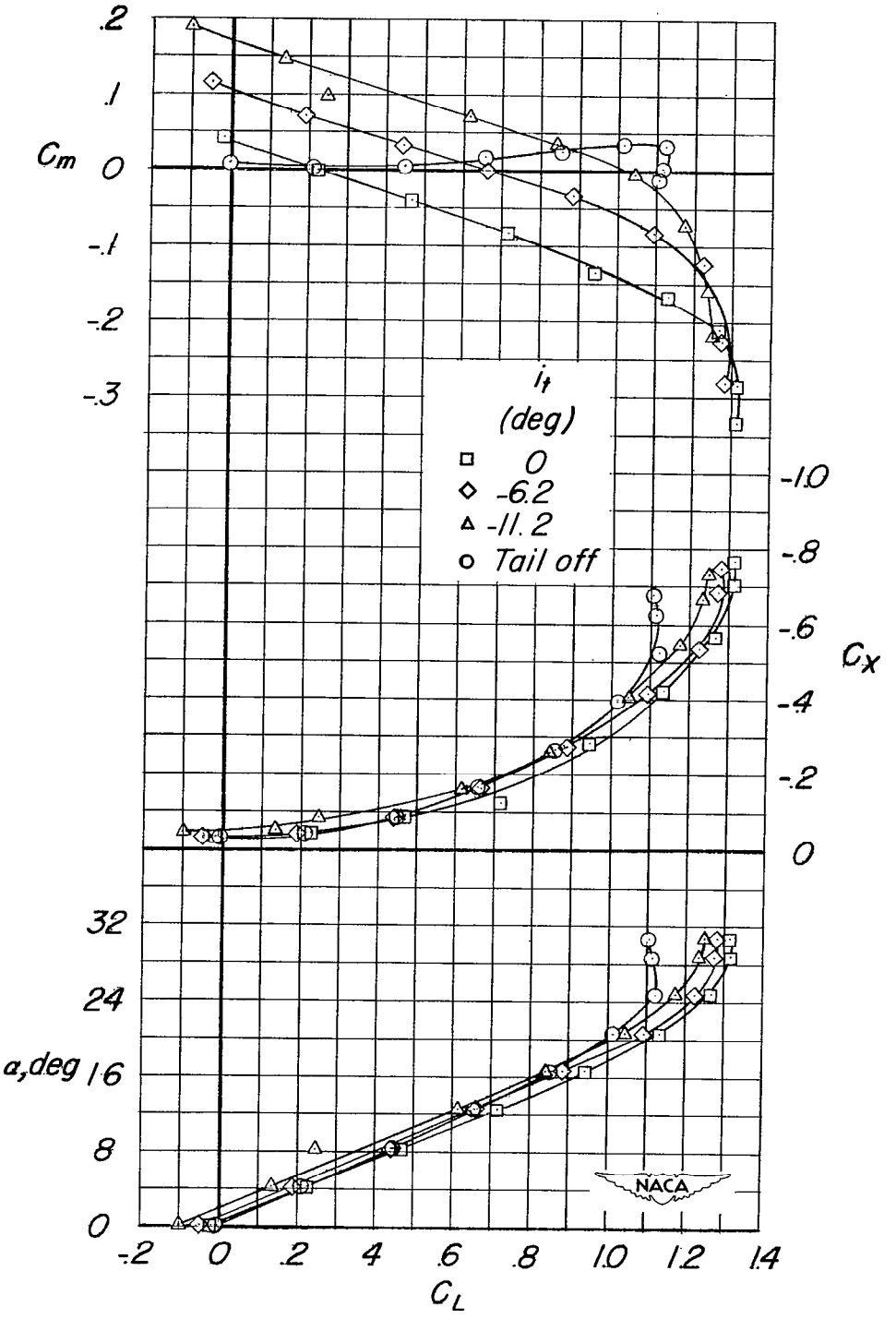

(a) Tanks off; brakes off.

Figure 43.- The effect of the tail on the aerodynamic characteristics in pitch. $\delta_f = 0^\circ$; wing position B; tail 2.

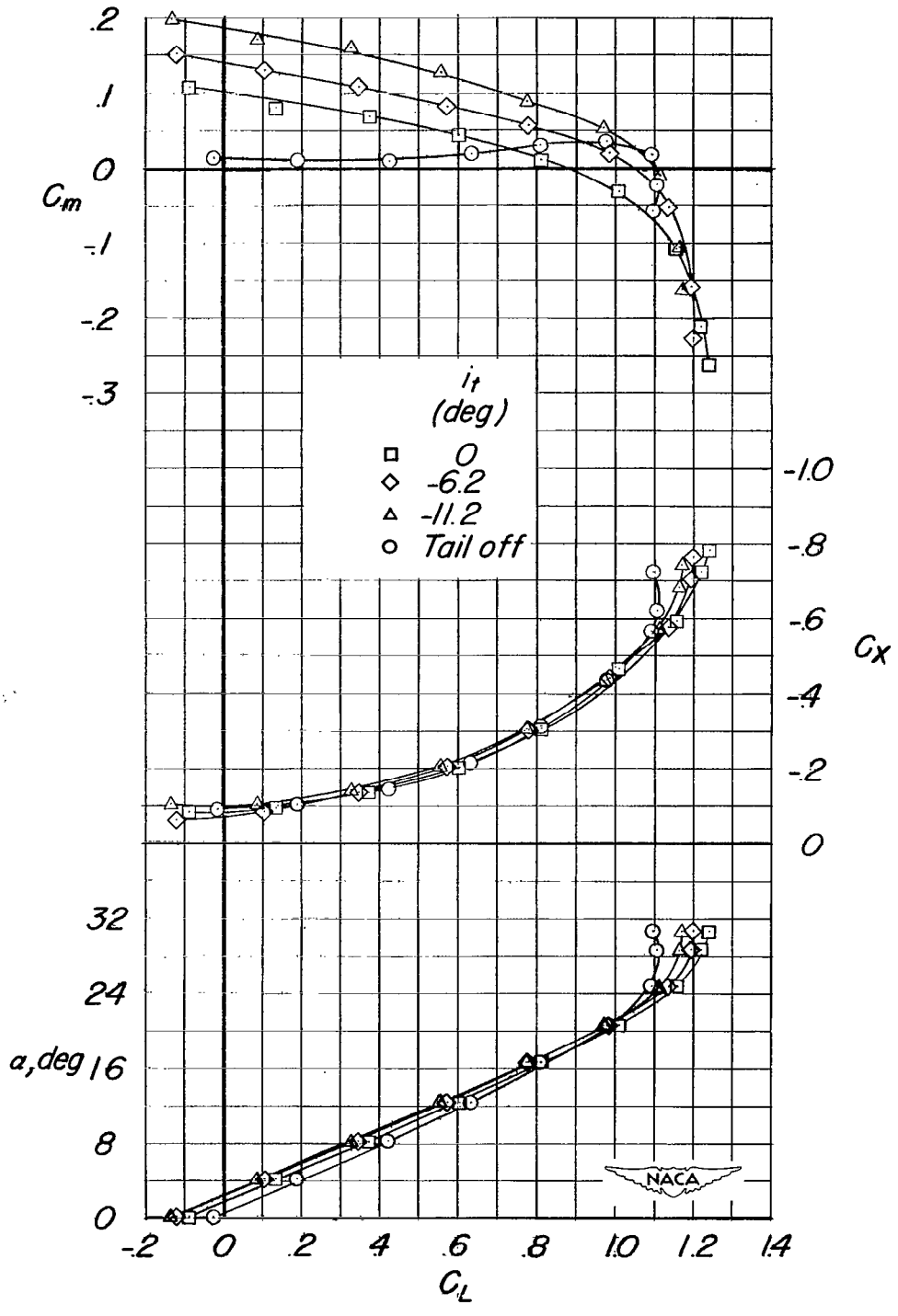

(b) Tanks on; brakes on.

Figure 43.- Concluded.

[redacted]

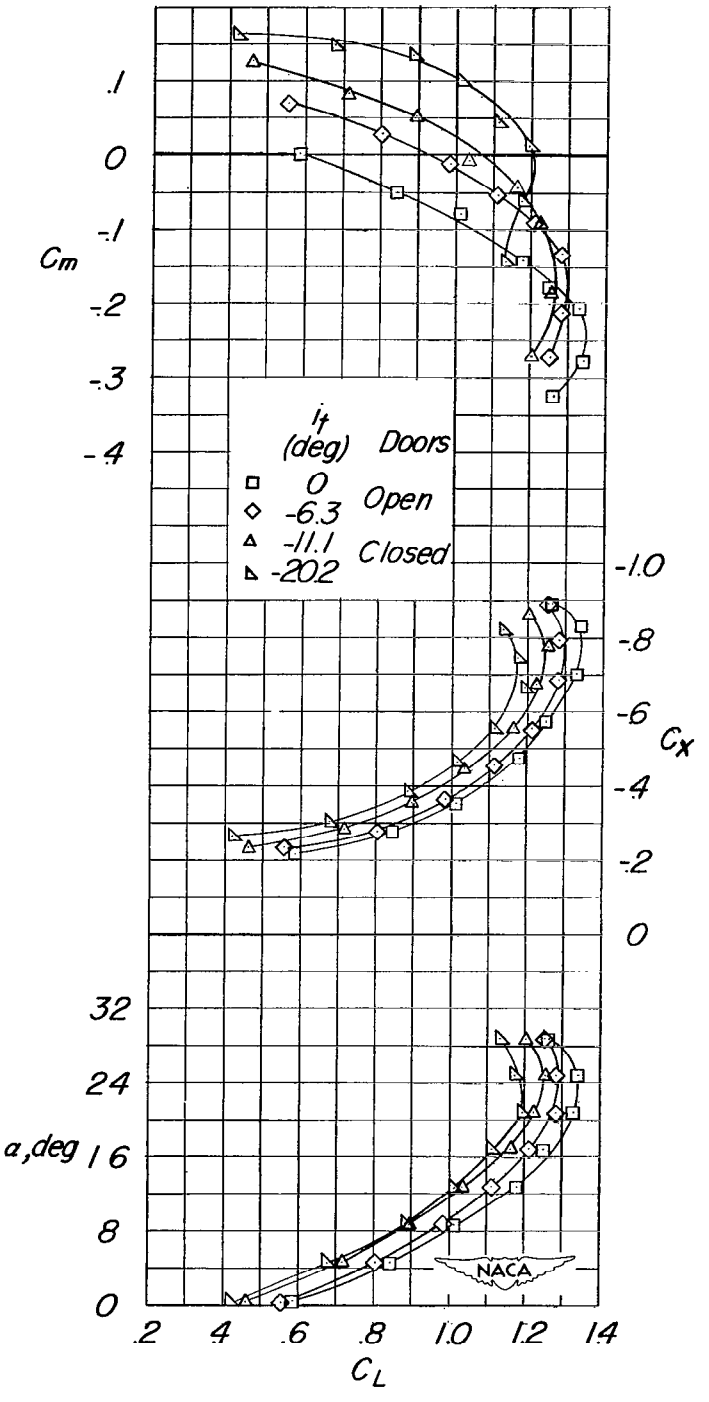

(a) Tanks off; brakes off.

Figure 44.- The effect of the tail on the aerodynamic characteristics in pitch. Gear on; $\delta_f = 57^\circ$; wing position B; tail 2.

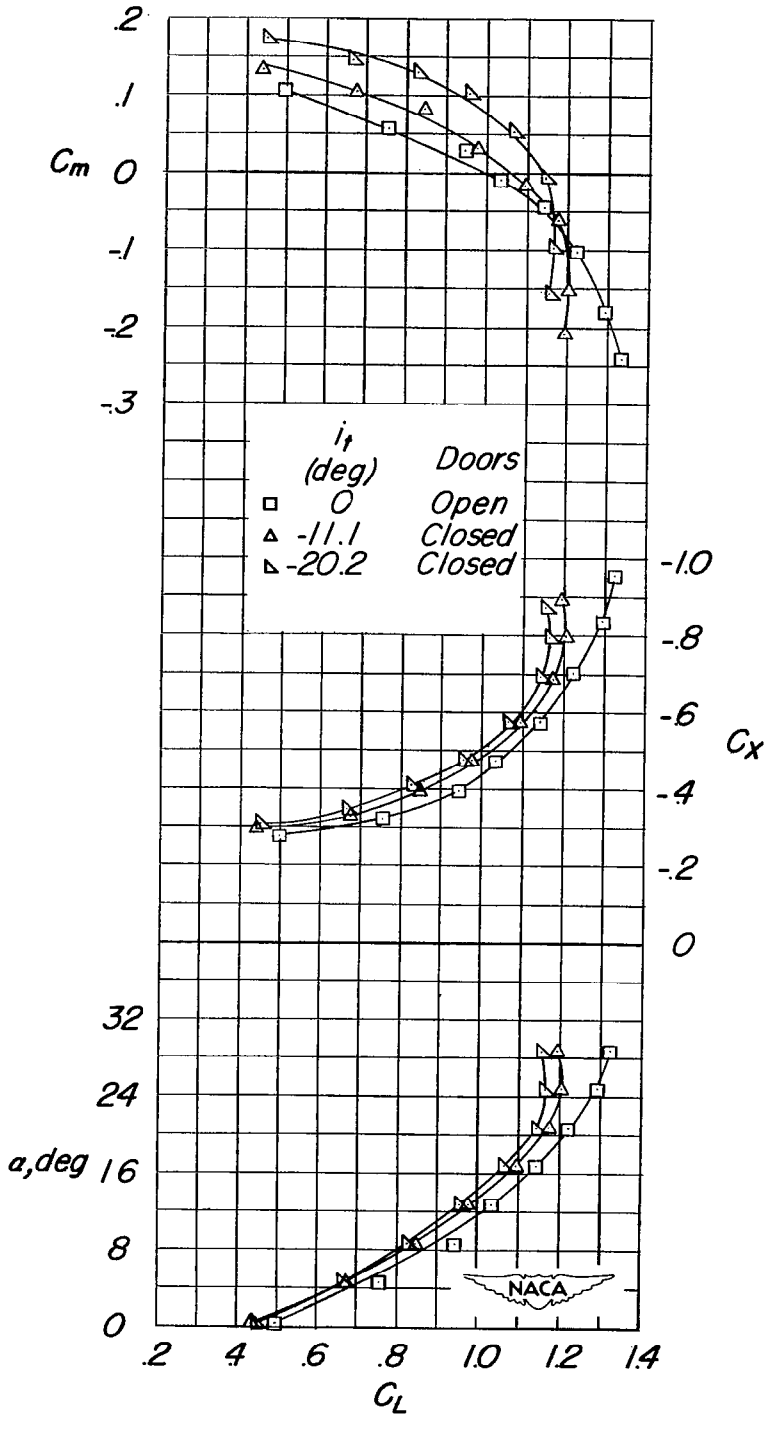

(b) Tanks on; brakes on.

Figure 44.- Continued.

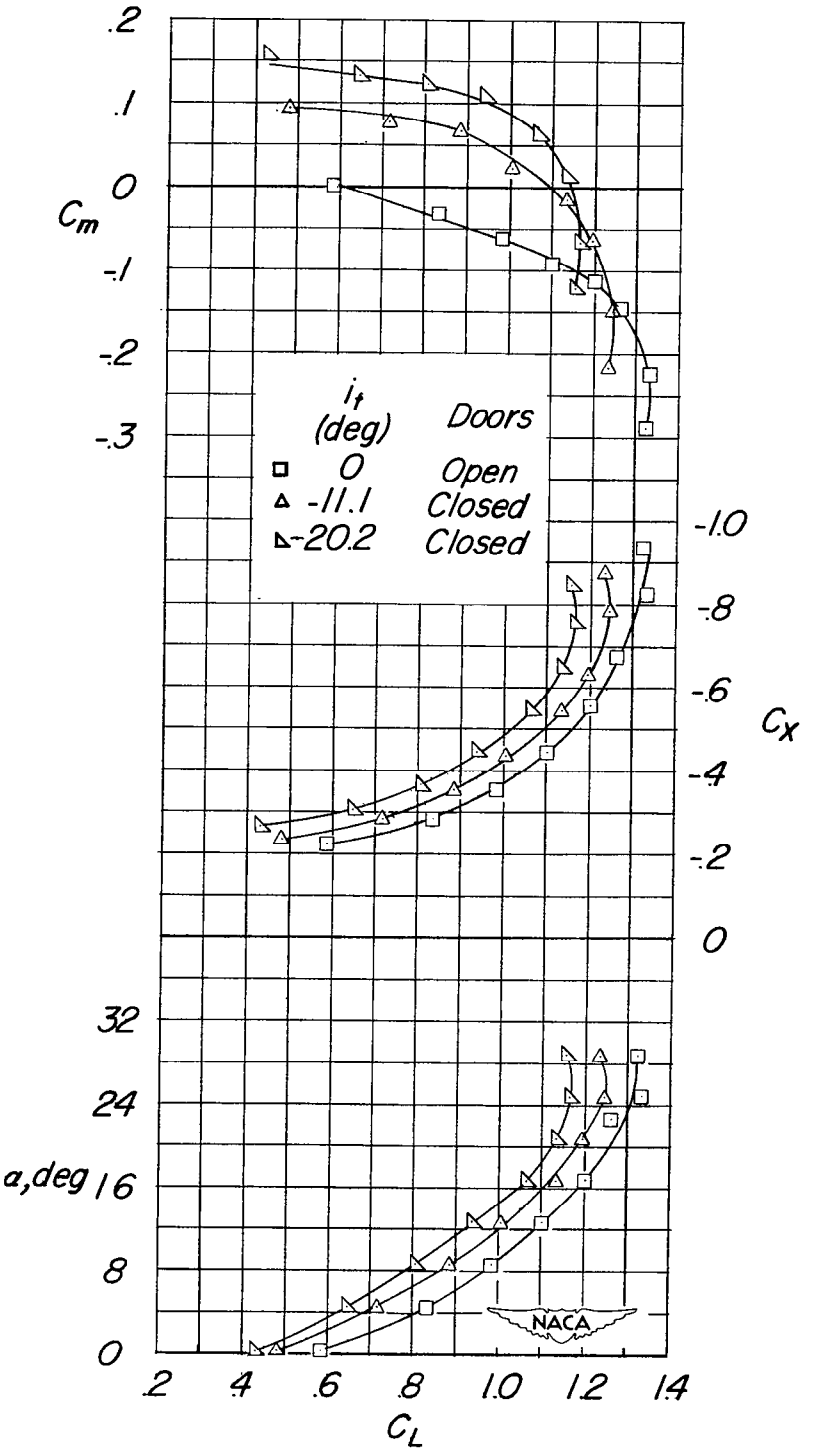

(c) Tanks on; brakes off.

Figure 44.- Continued.

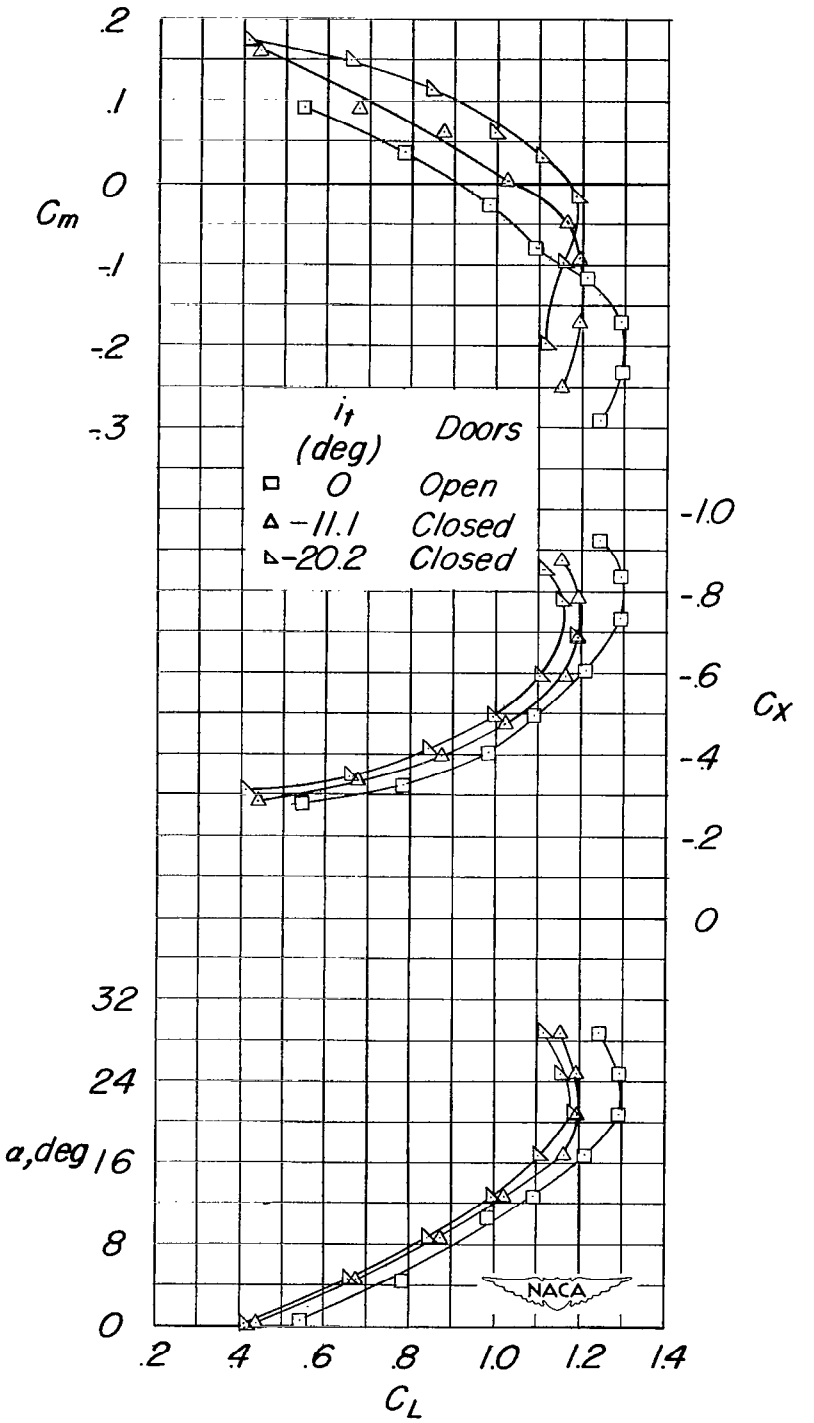

(d) Tanks off; brakes on.

Figure 44.- Concluded.

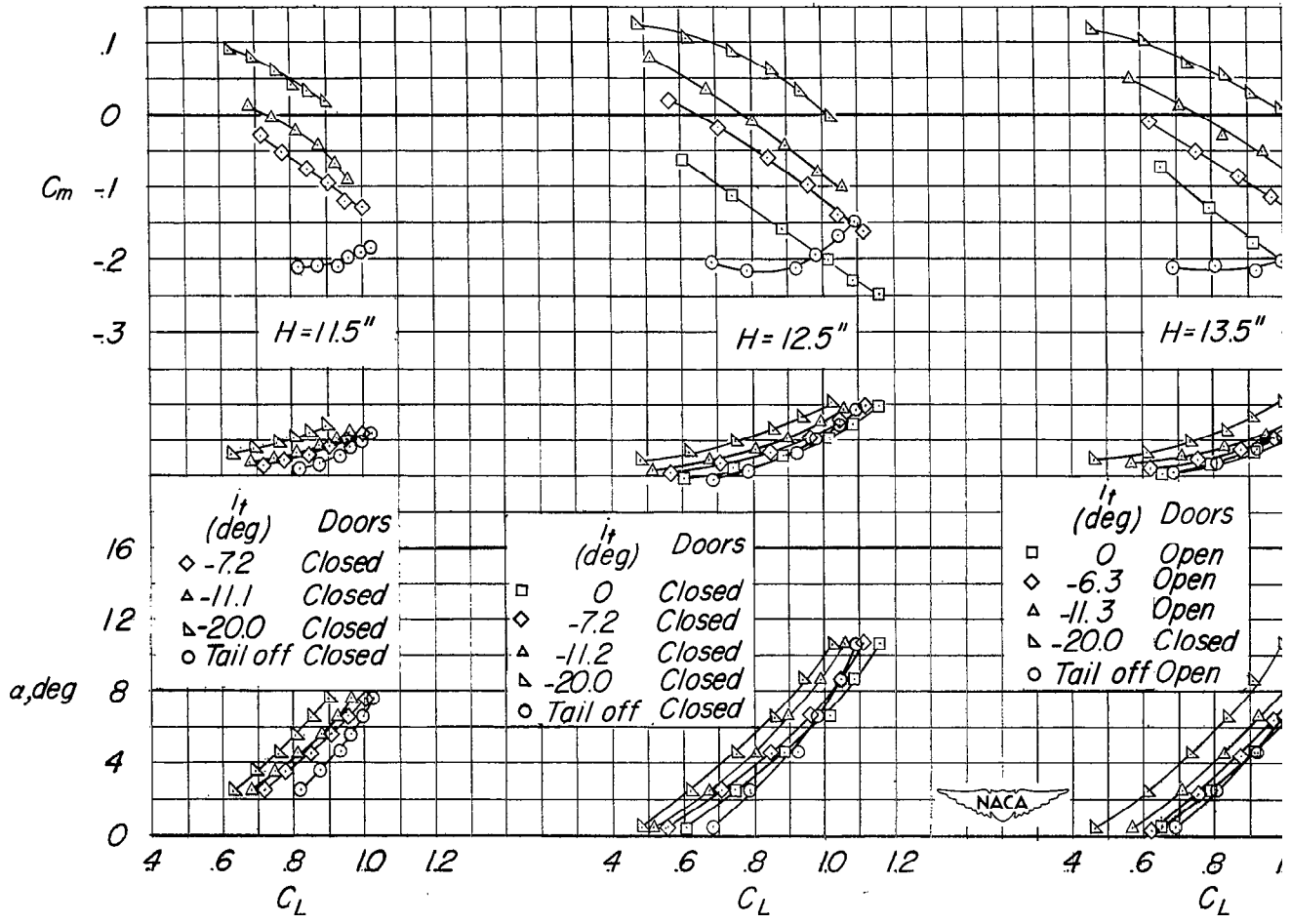

(a) Tanks off; brakes off.

Figure 45.- The effect of the tail on the aerodynamic characteristics in pitch in the presence of the ground board. $\delta_f = 57°$; wing position A; tail 2.

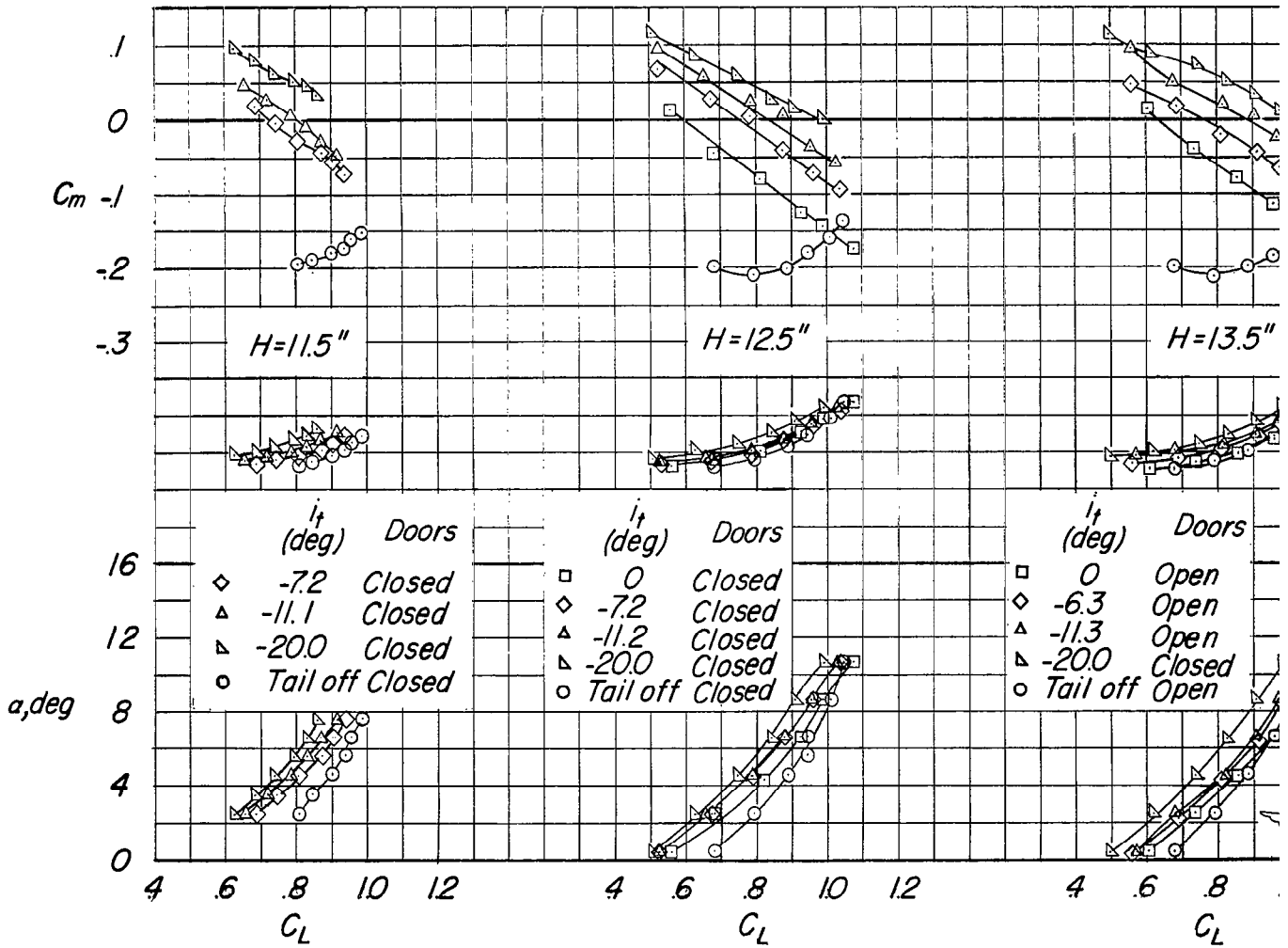

(b) Tanks on; brakes on.

Figure 45.- Continued.

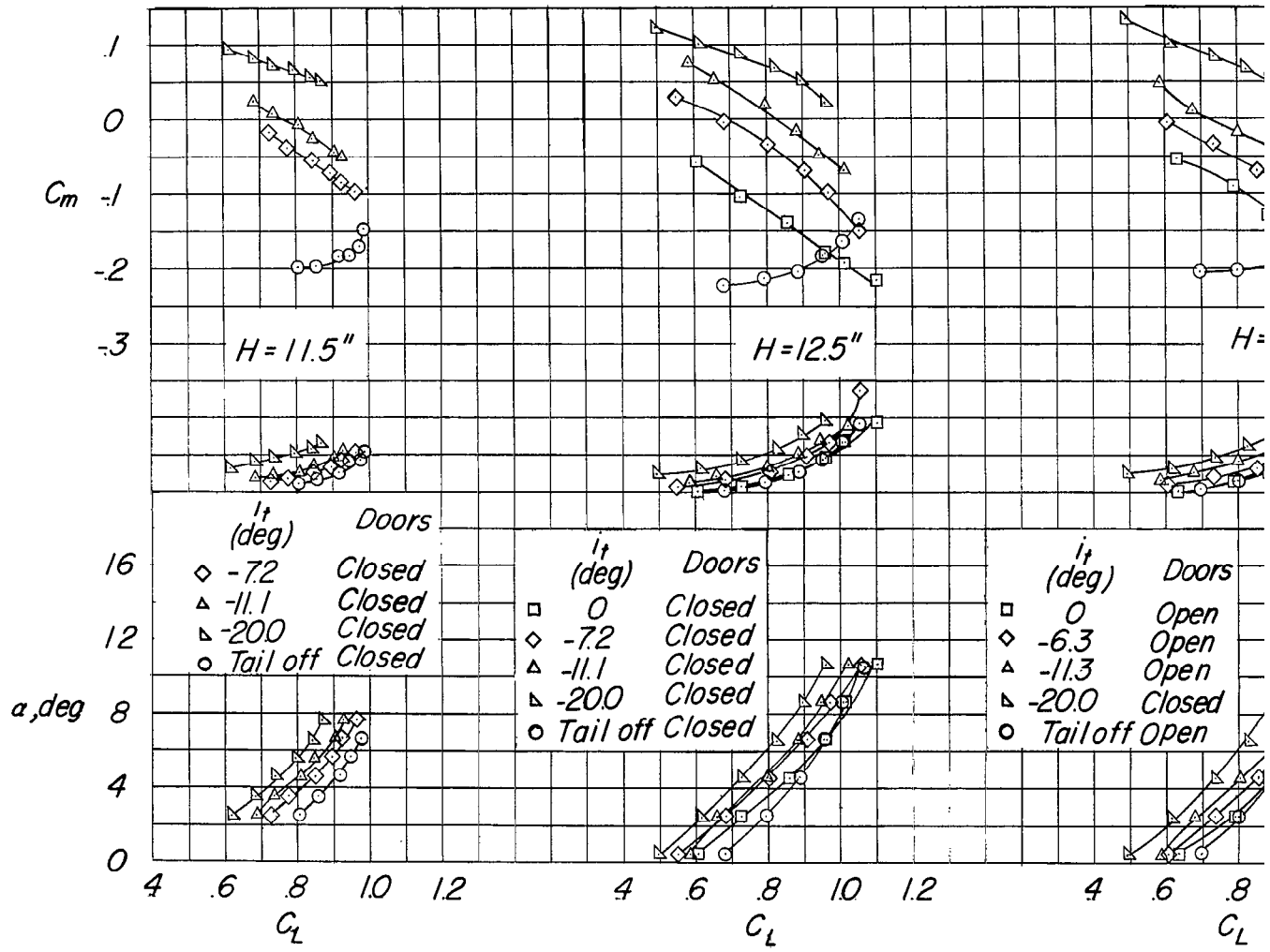

(c) Tanks on; brakes off.

Figure 45.- Continued.

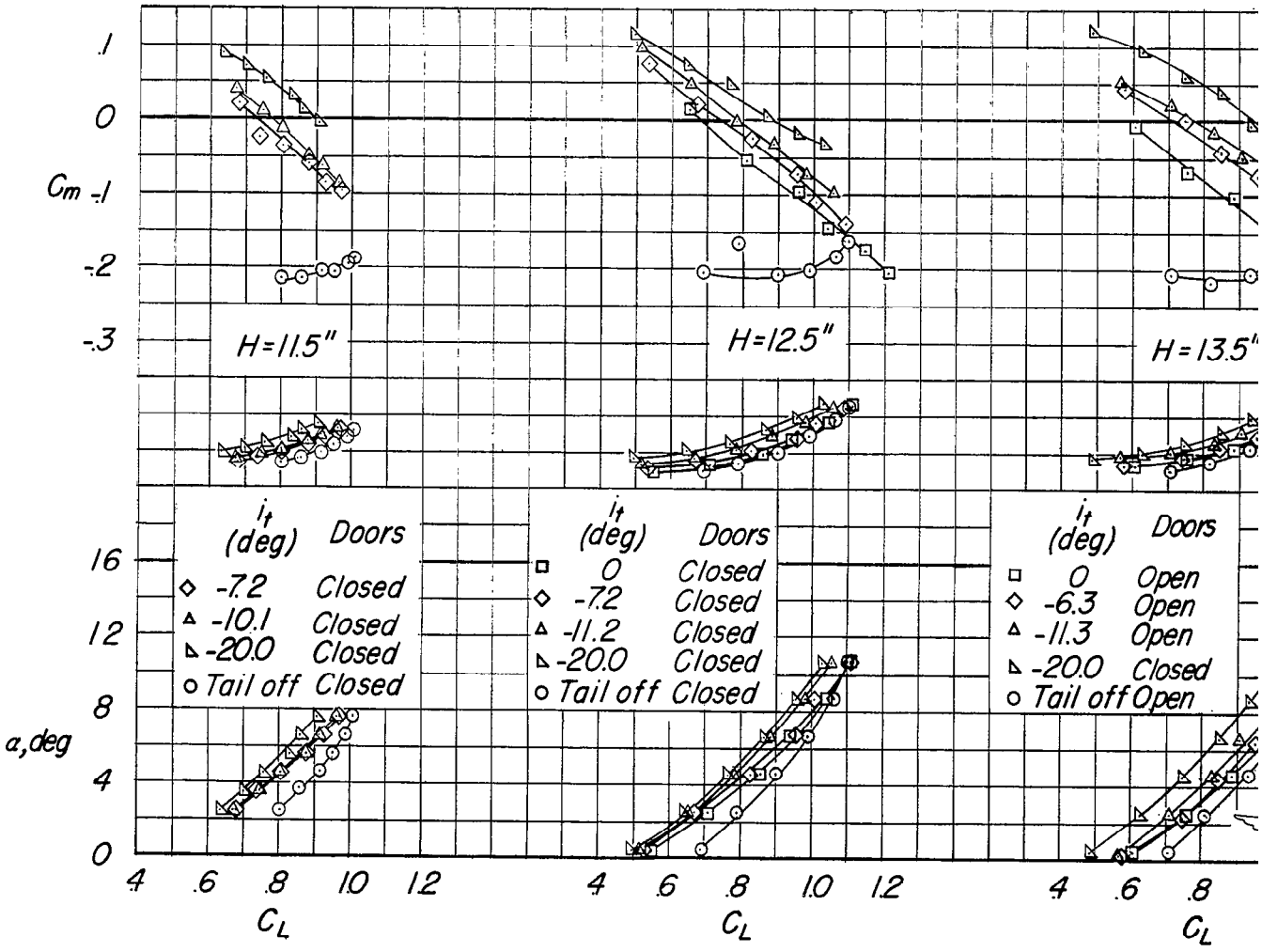

(d) Tanks off; brakes on.

Figure 45.- Concluded.

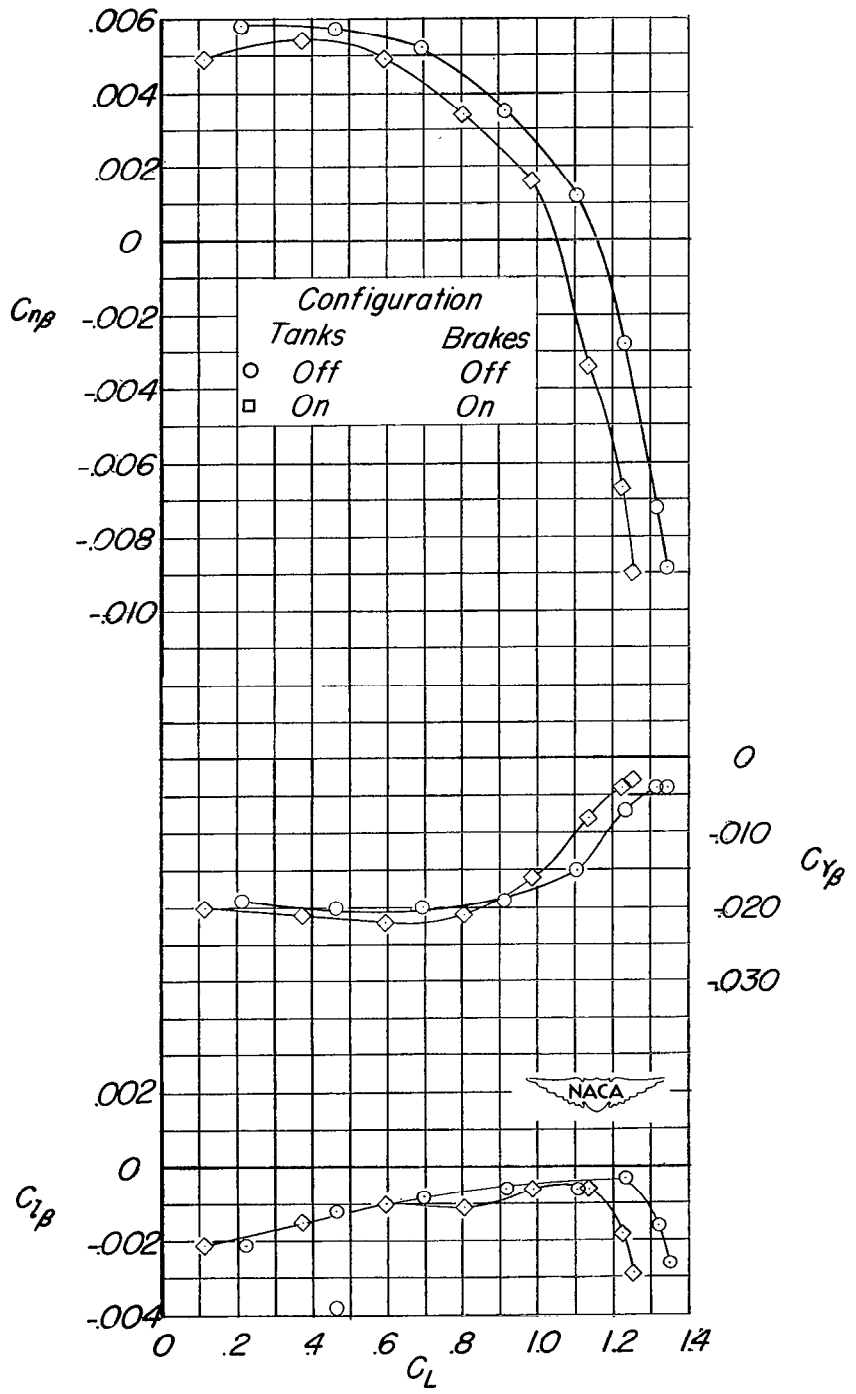

(a) $\delta_f = 0^\circ$; gear off.

Figure 46.- Effect of tanks and brakes on the variation of the lateral-stability parameter with lift coefficient. Wing position B; tail 2; $i_t = 0^\circ$.

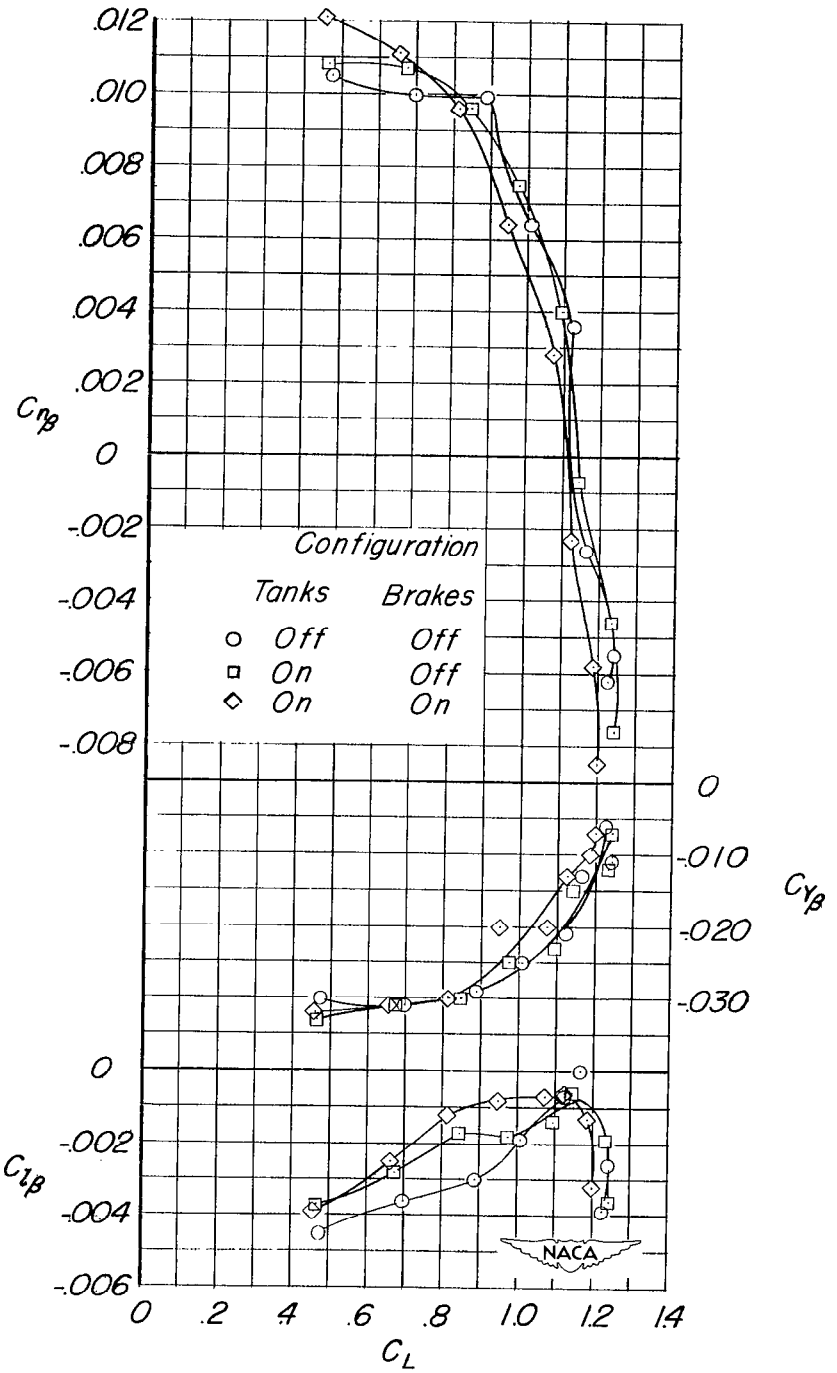

(b) $\delta_f = 57^\circ$; gear on; doors closed.

Figure 46.- Concluded.

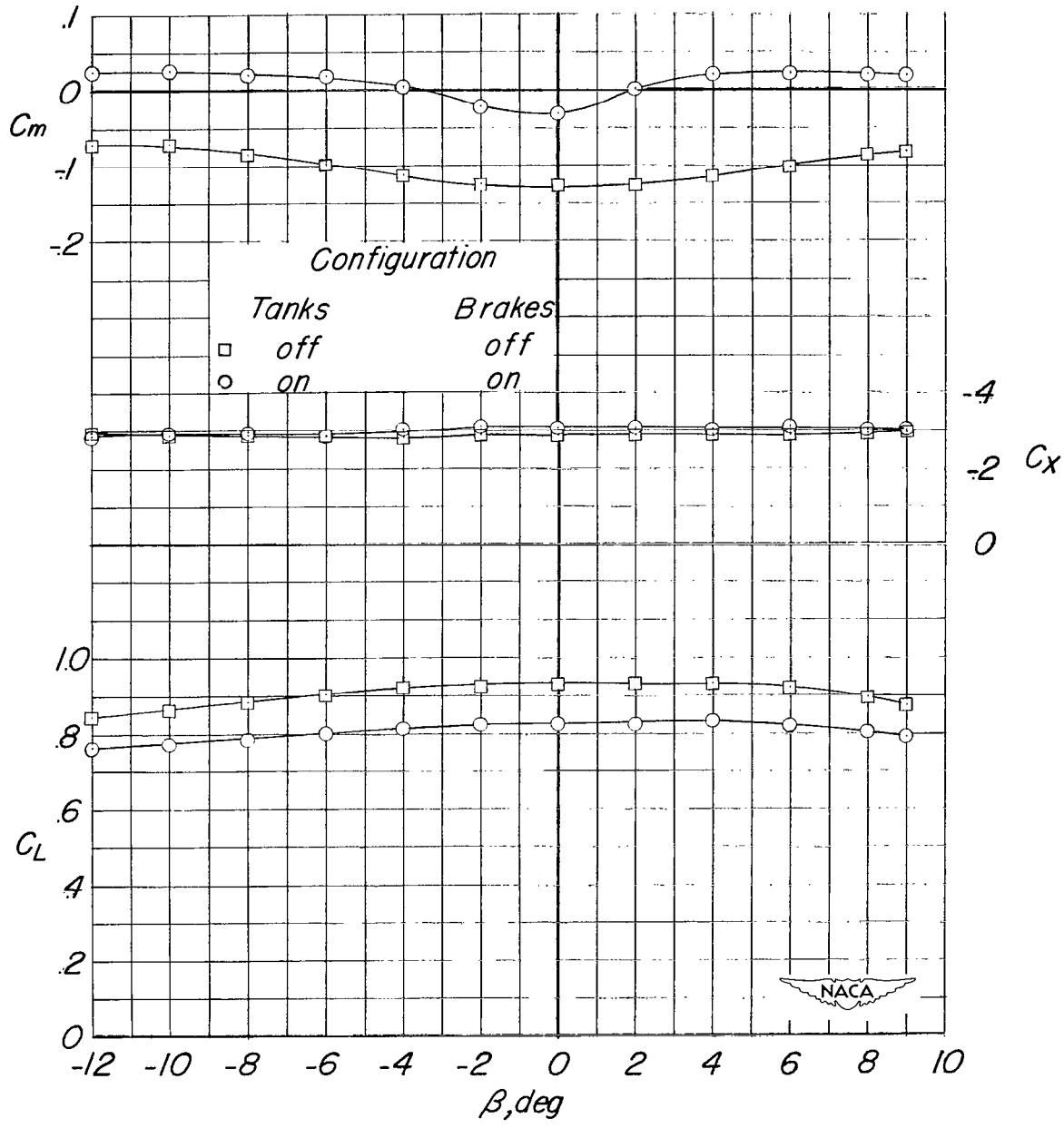

(a) $\delta_f = 0°$; $\alpha = 16.6°$; gear off; no ground board.

Figure 47.- Effect of tanks and brakes on the aerodynamic characteristics in sideslip. Wing position B; tail 2.

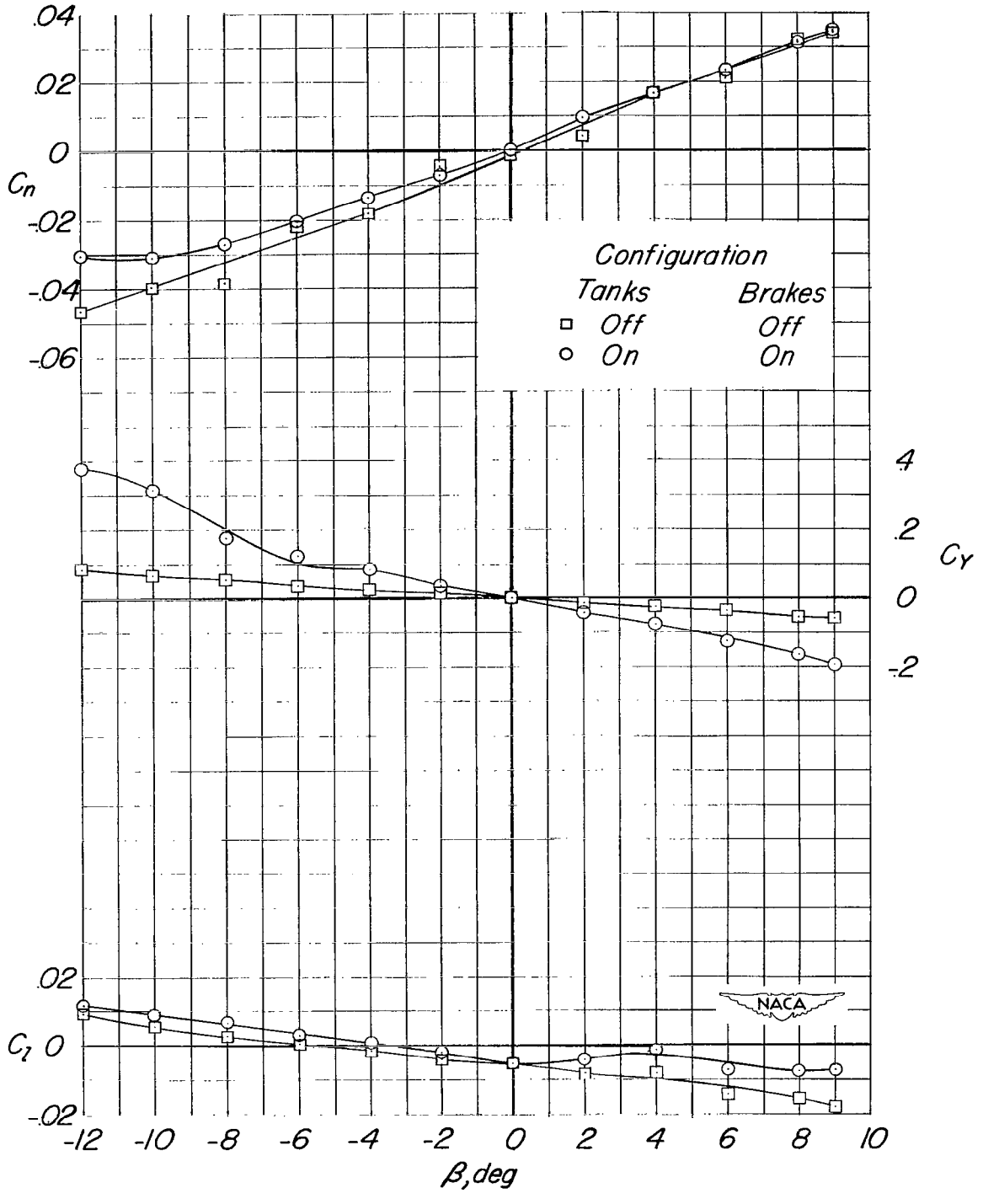

(a) Concluded.

Figure 47.- Continued.

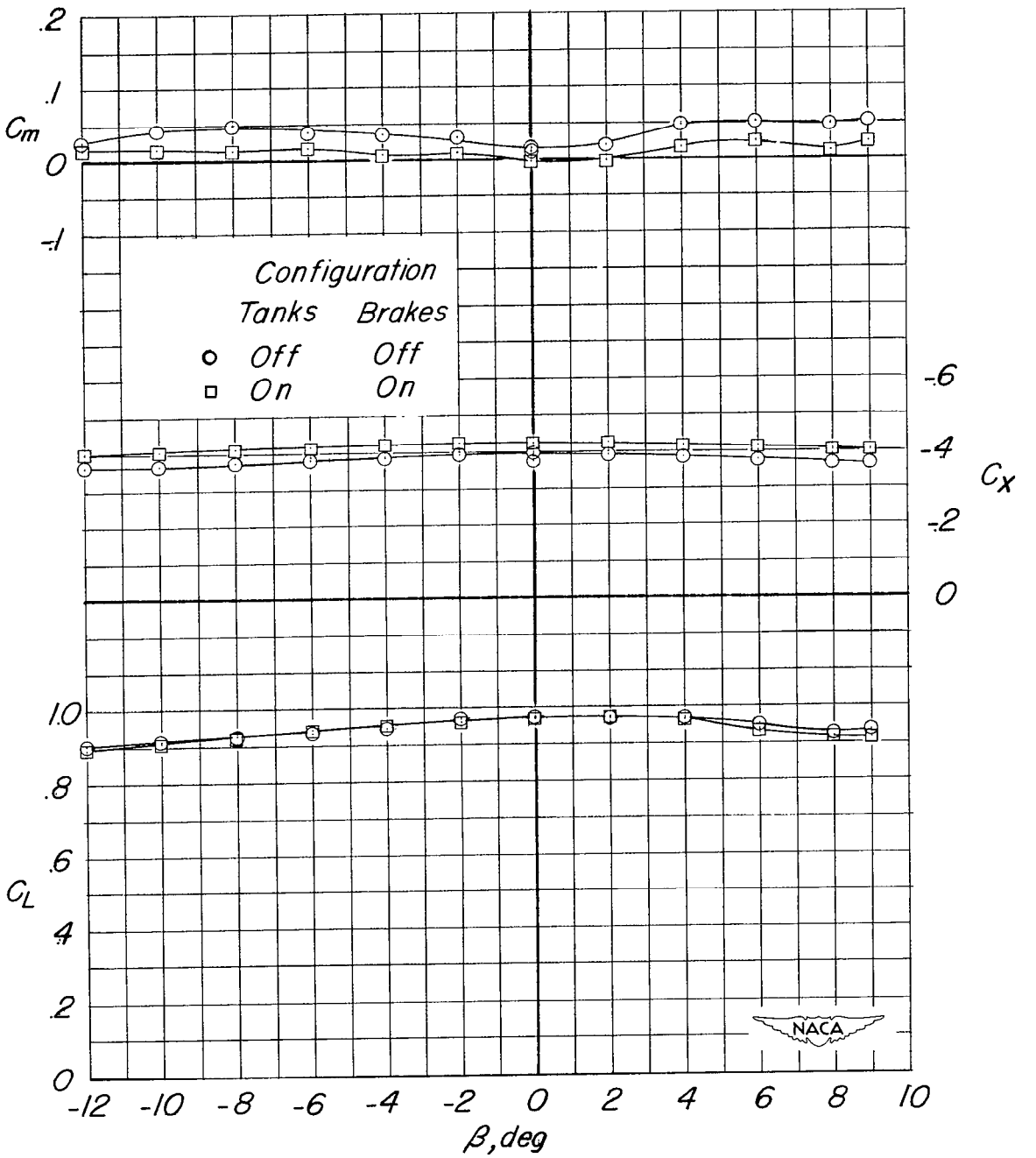

(b) $\delta_f = 57^\circ$; $\alpha = 10.6^\circ$; gear off; doors closed; H = 12.5 inches.

Figure 47.- Continued.

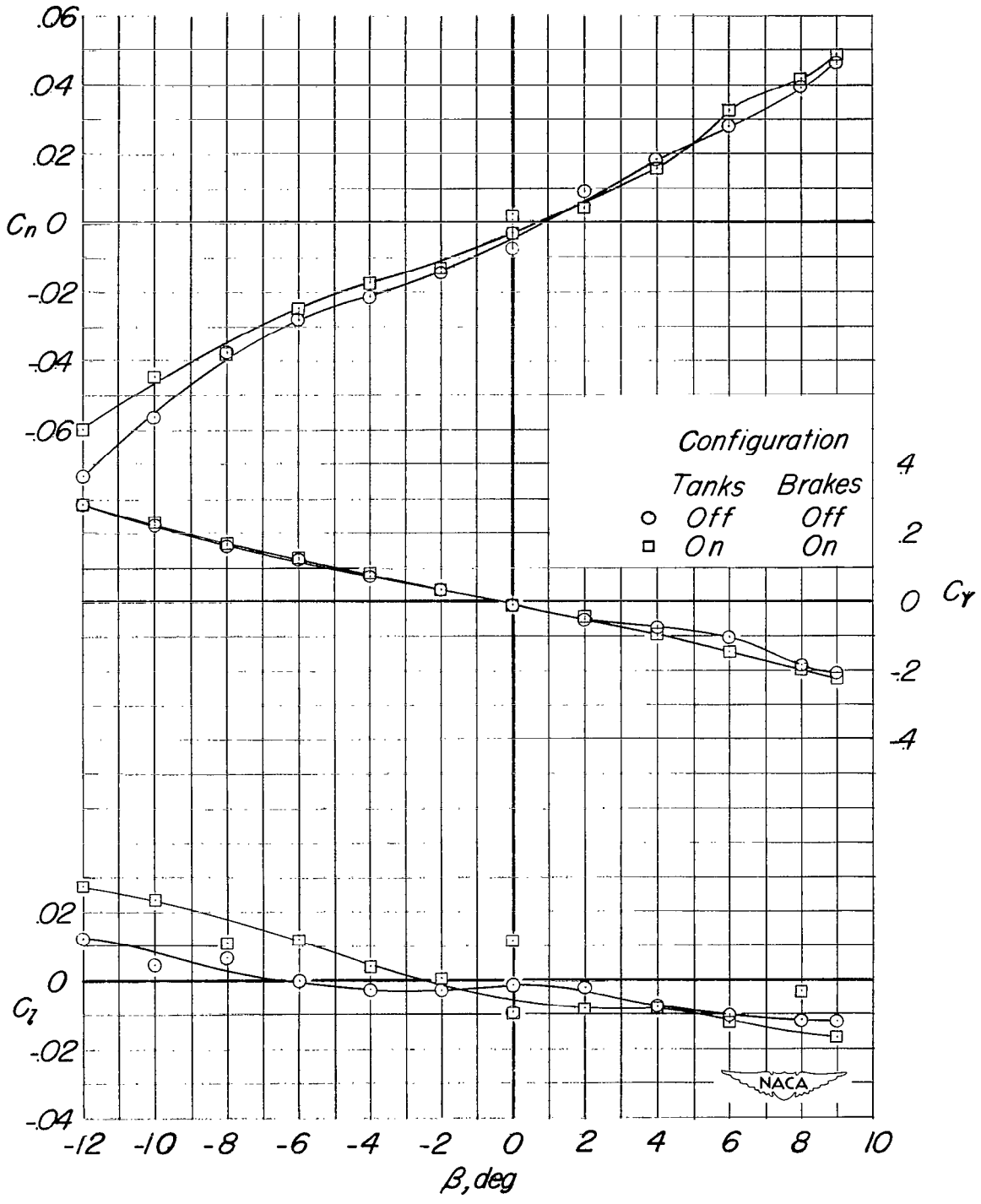

(b) Concluded.

Figure 47.- Concluded.

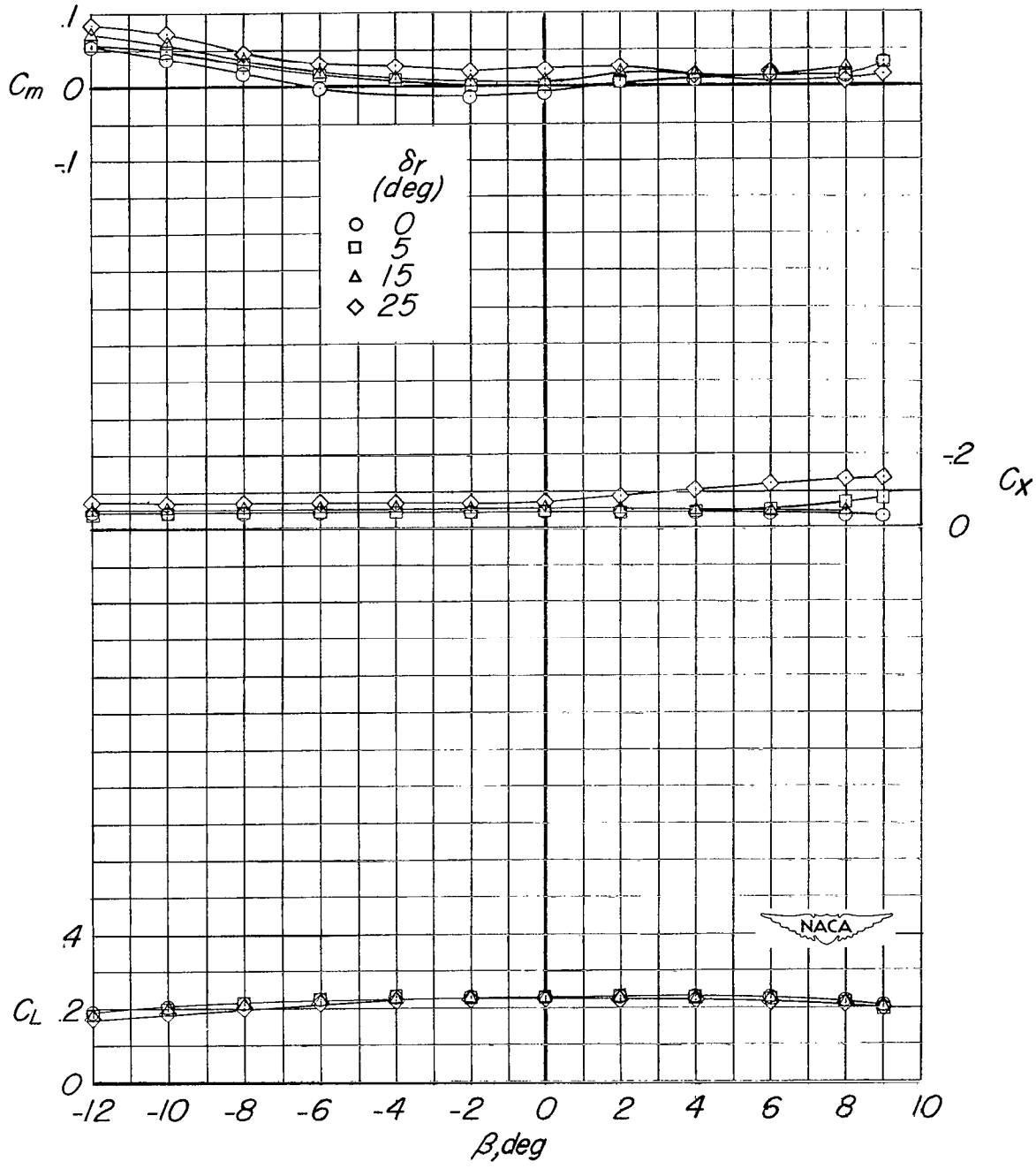

(a) $\delta_f = 0^\circ$; $\alpha = 4.3^\circ$; $i_t = 0^\circ$; gear off.

Figure 48.- Effect of rudder deflection on the aerodynamic characteristics in sideslip. Wing position B; tail 2.

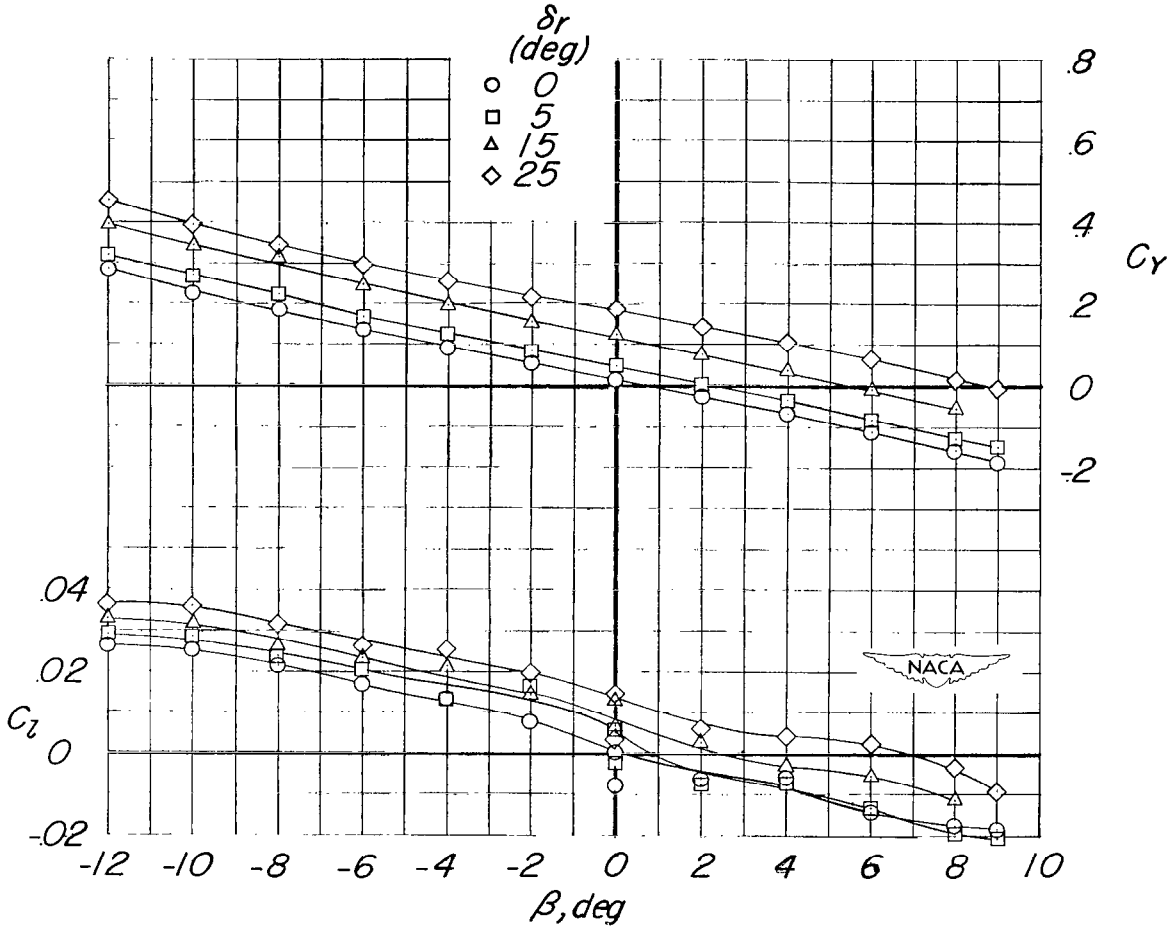

(a) Continued.

Figure 48.- Continued.

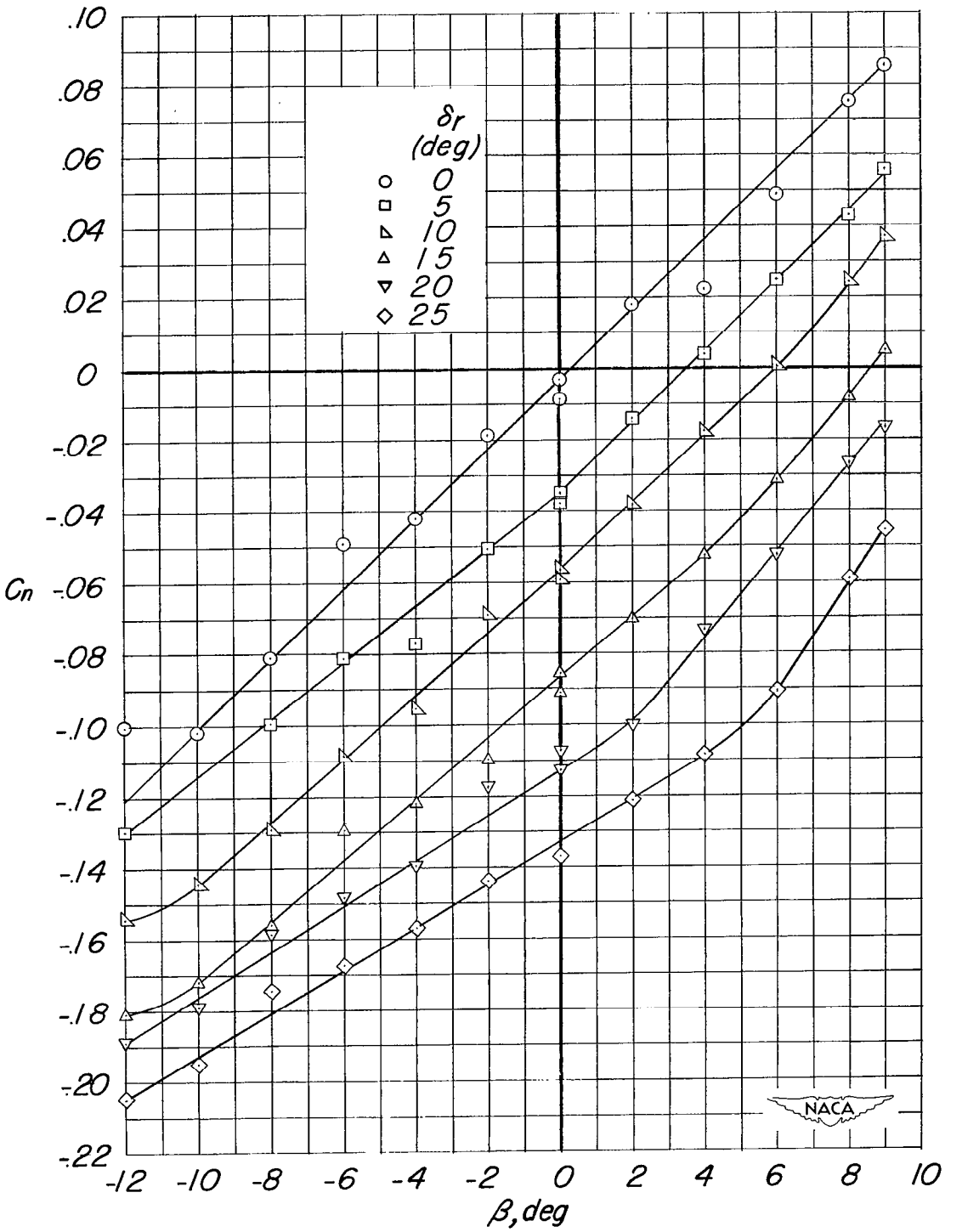

(a) Concluded.

Figure 48.- Continued.

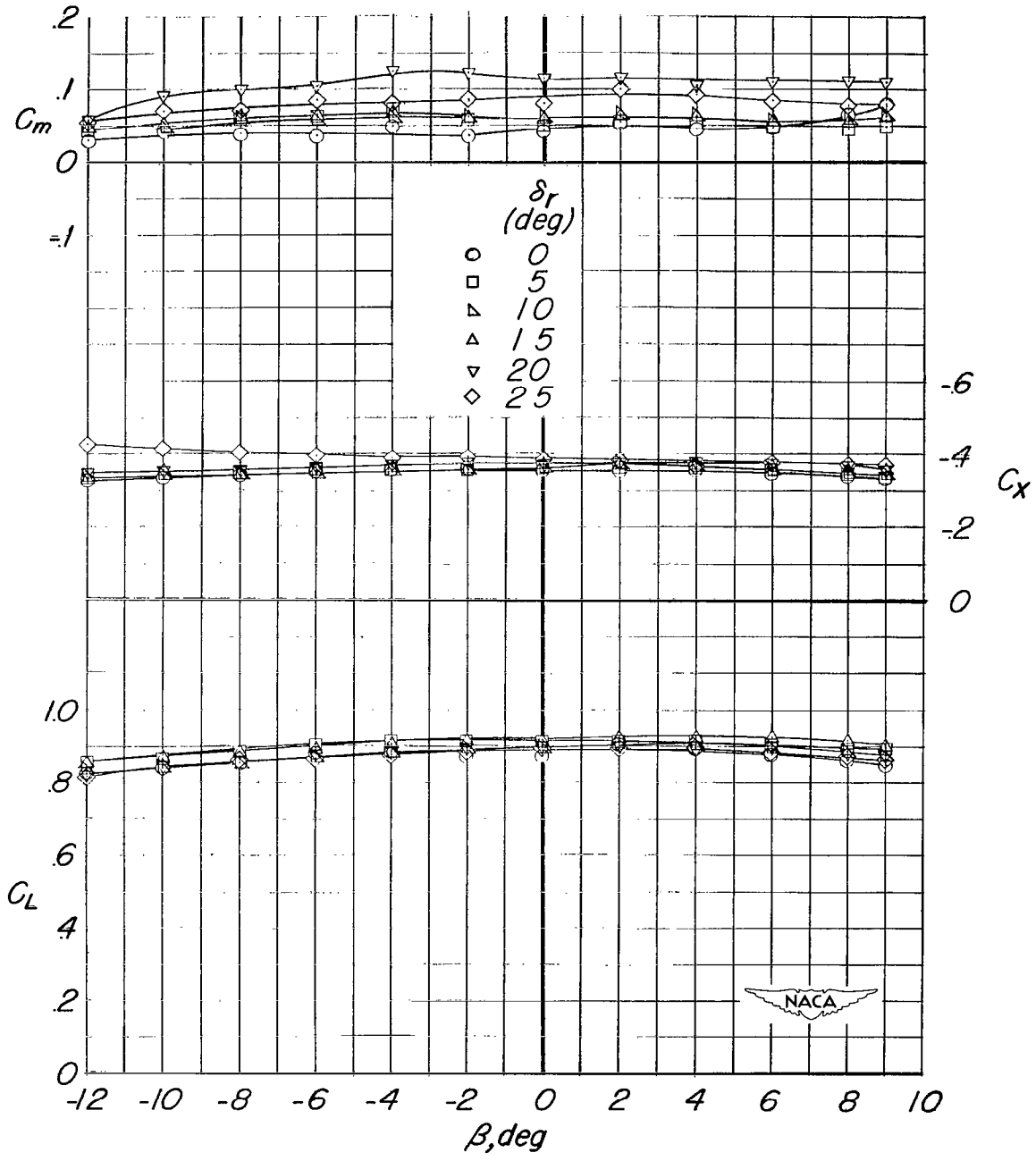

(b) $\delta_f = 57^\circ$; $\alpha = 8.6^\circ$; $i_t = -11.1^\circ$; gear on; doors closed.

Figure 48.- Continued.

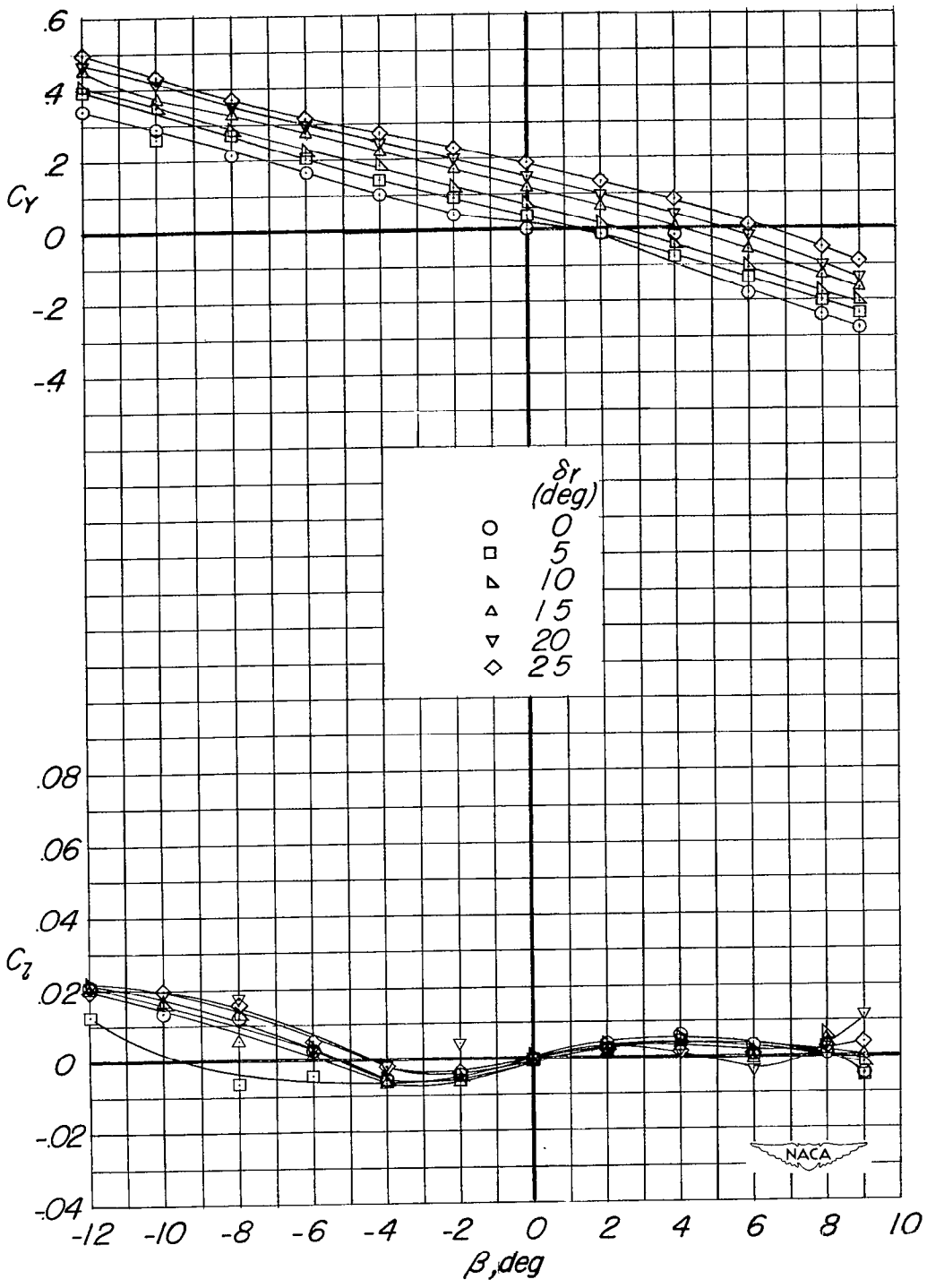

(b) Continued.

Figure 48.- Continued.

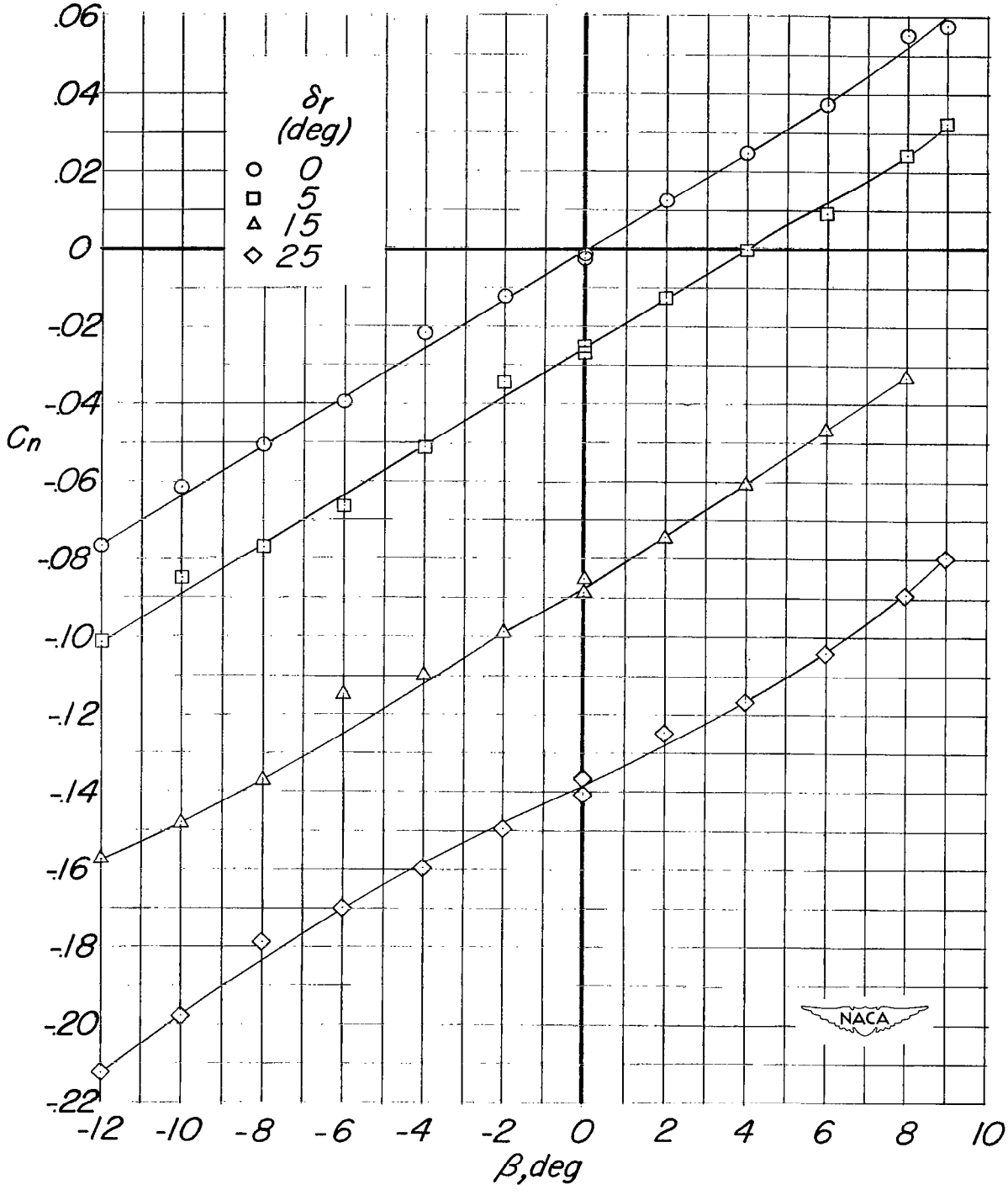

(b) Concluded.

Figure 48.- Concluded.

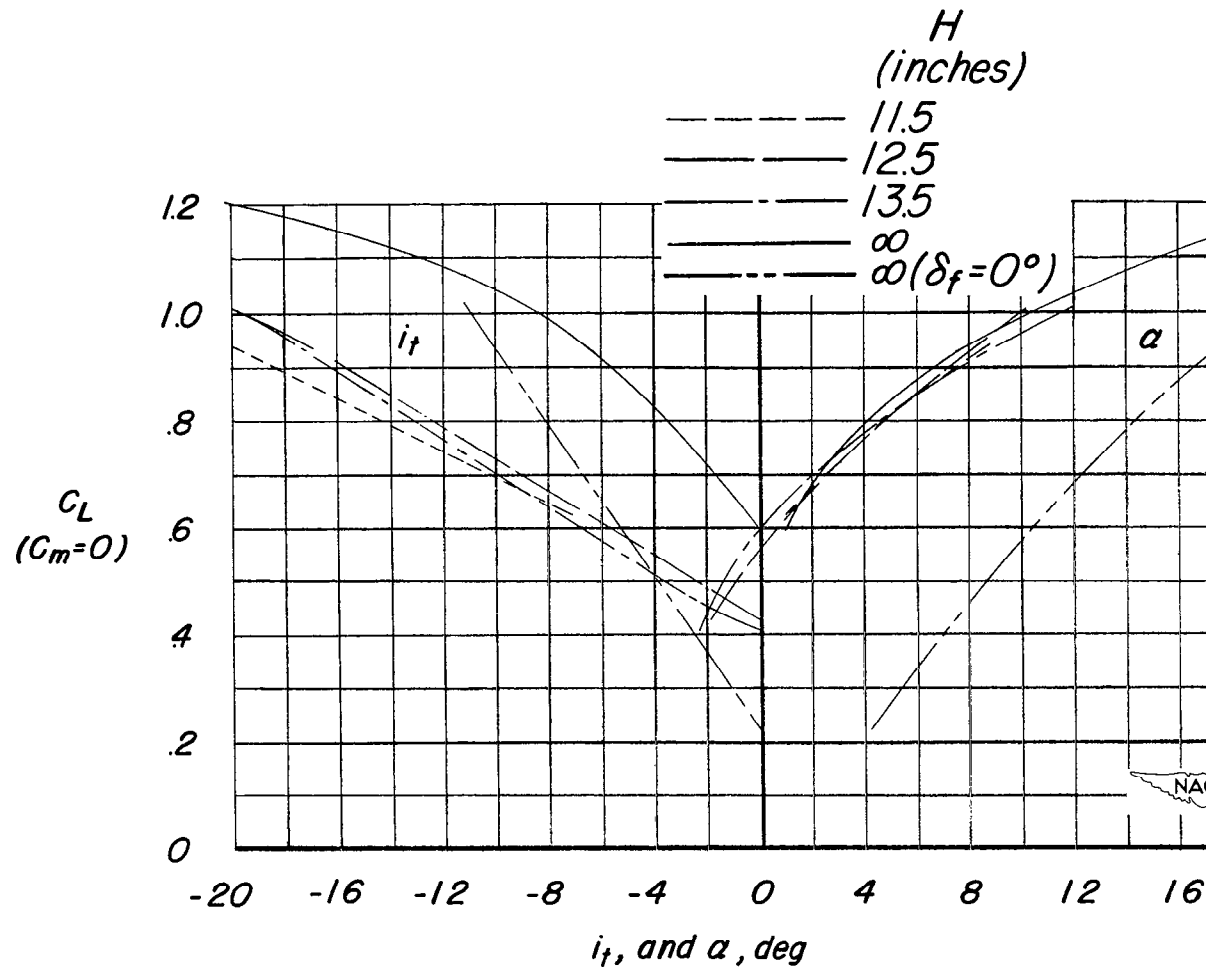

(a) Tanks off; brakes off.

Figure 49.- Trimmed lift variation with angle of attack and stabiliz setting. Wing position B; tail 2; $\delta_f = 57^\circ$.

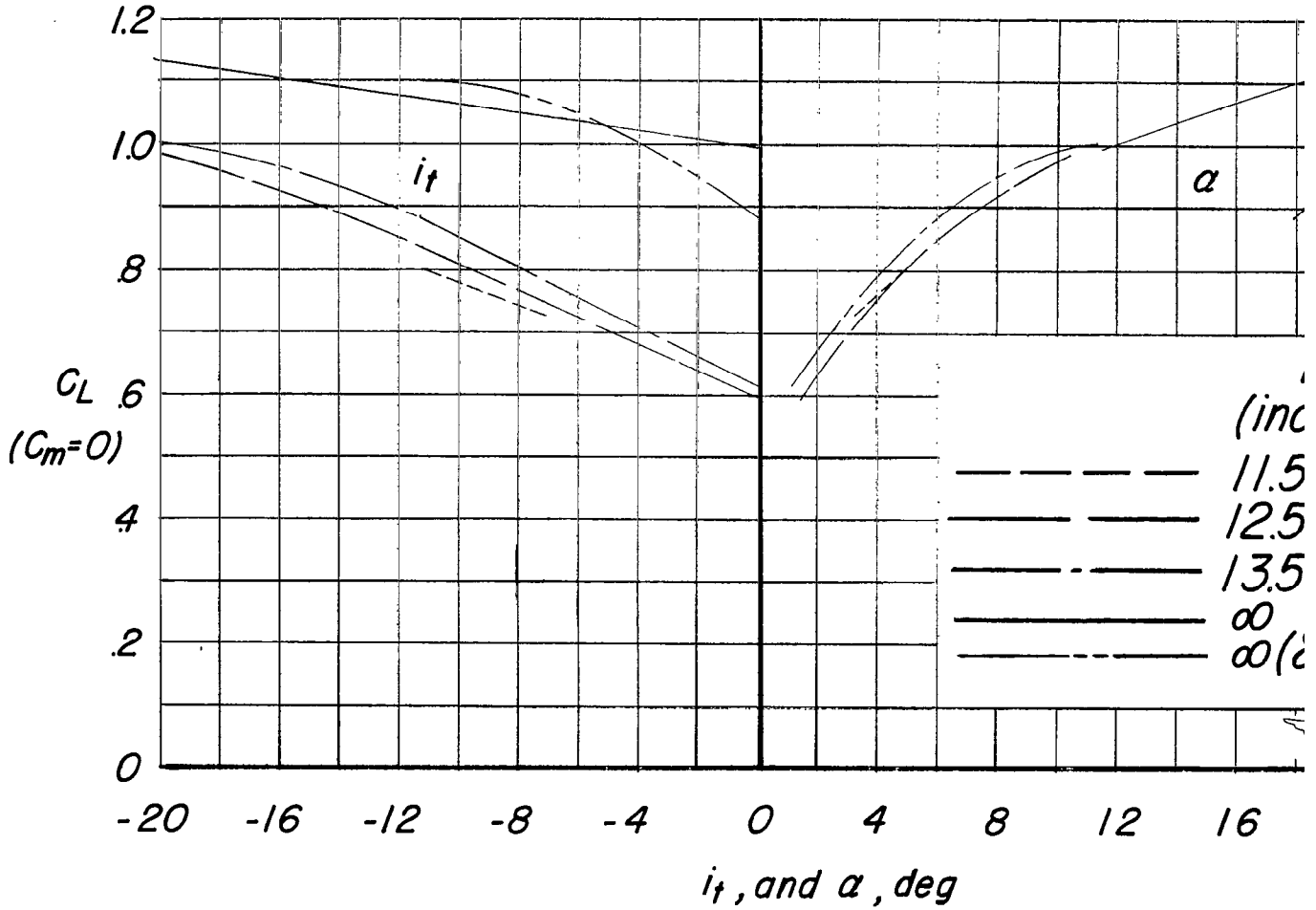

(b) Tanks on; brakes on.

Figure 49.- Continued.

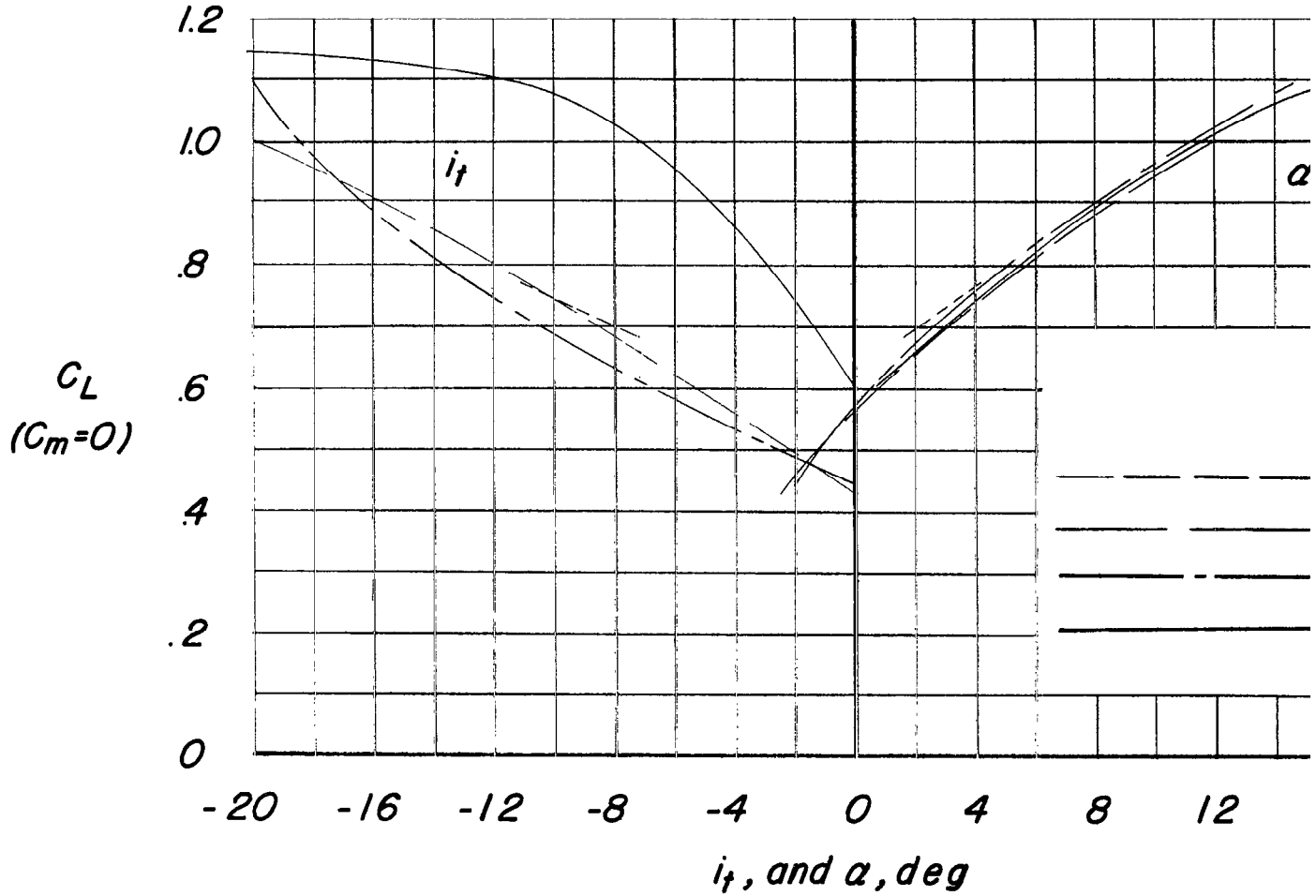

(c) Tanks on; brakes off.

Figure 49.- Continued.

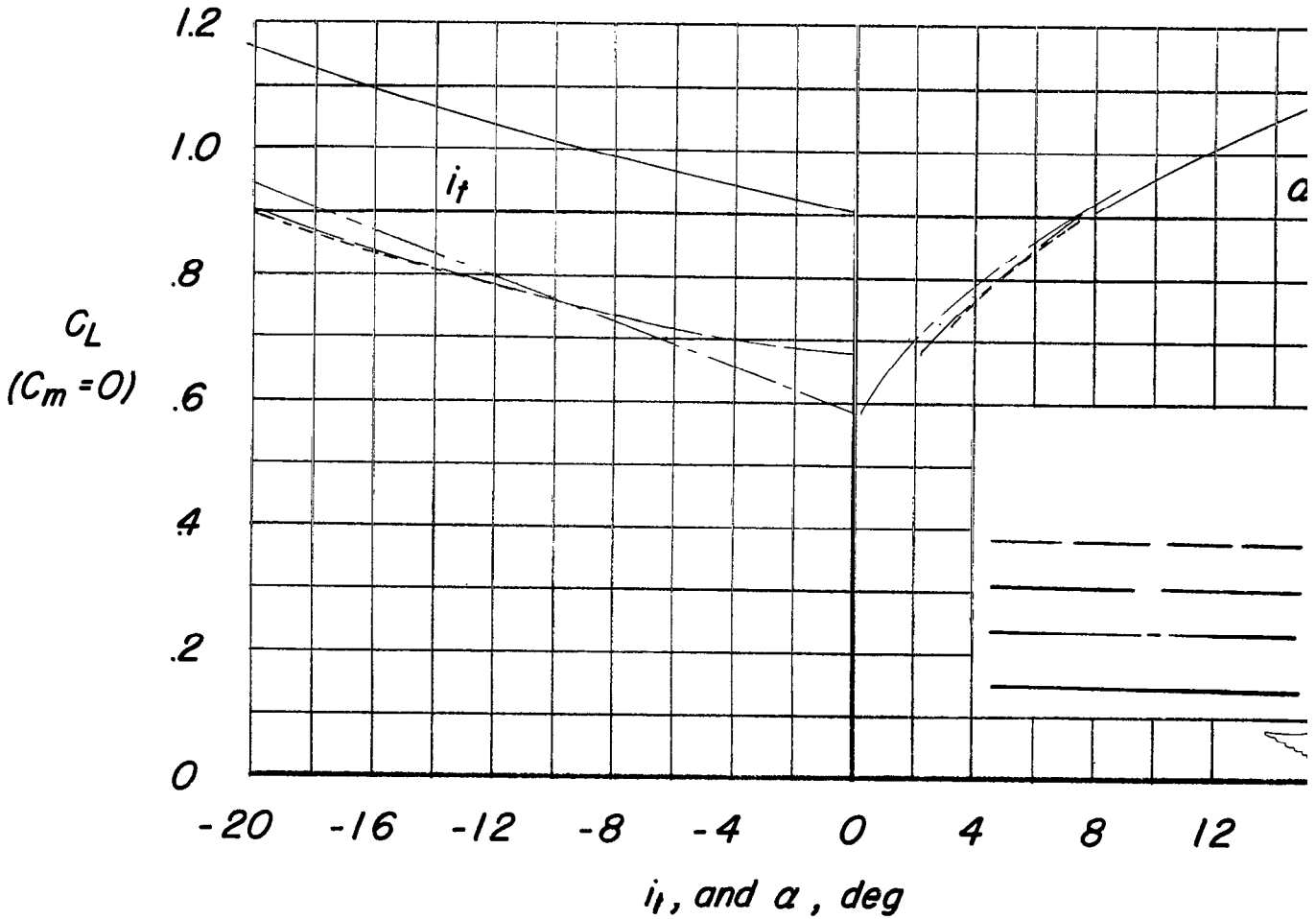

(d) Tanks off; brakes on.

Figure 49.- Concluded.

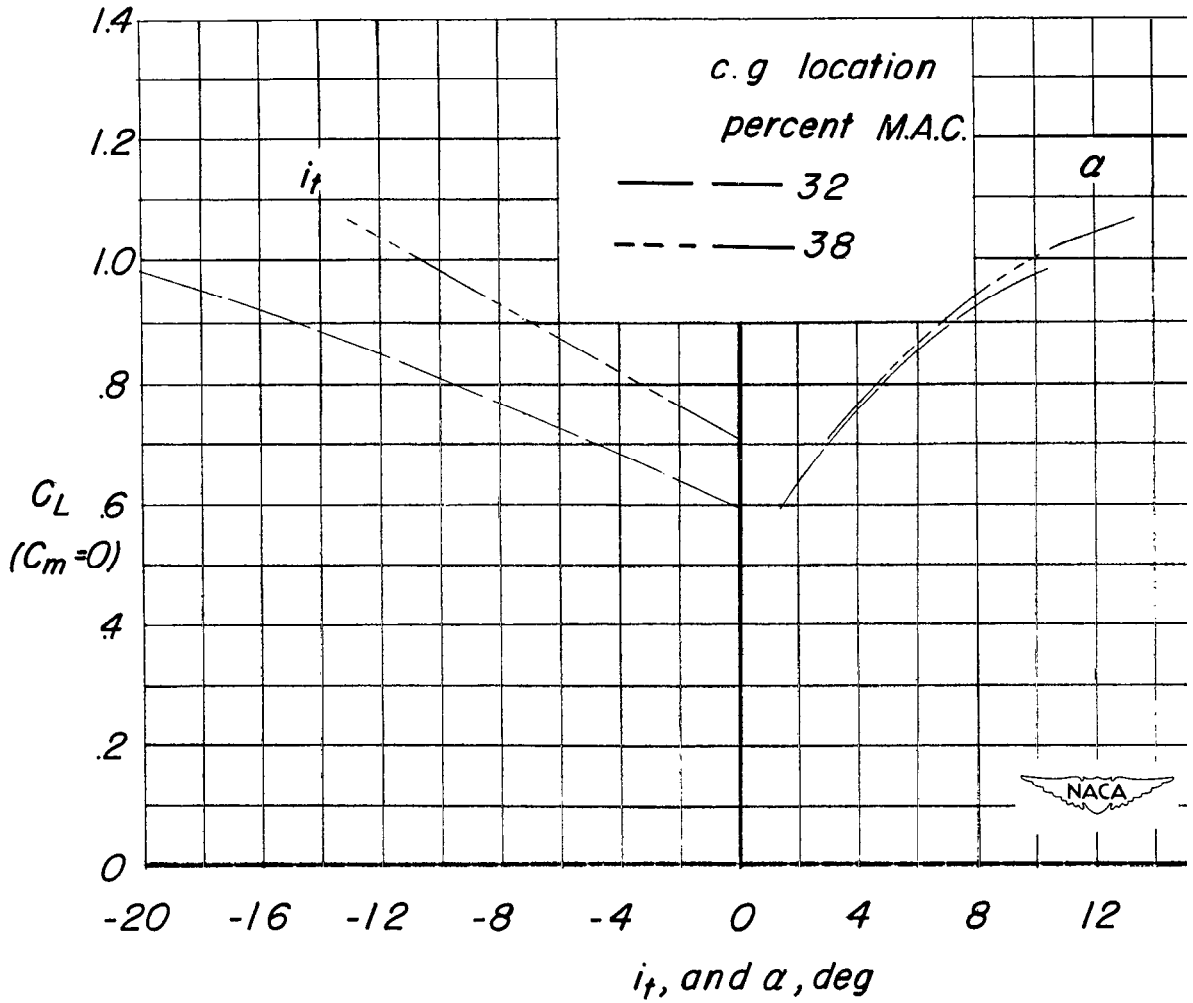

Figure 50.- The effect of center-of-gravity location on the angle of attack and stabilizer setting for trim. $\delta_f = 57^\circ$; tanks on; brakes on. H = 12.5 inches; wing position B; tail 2.

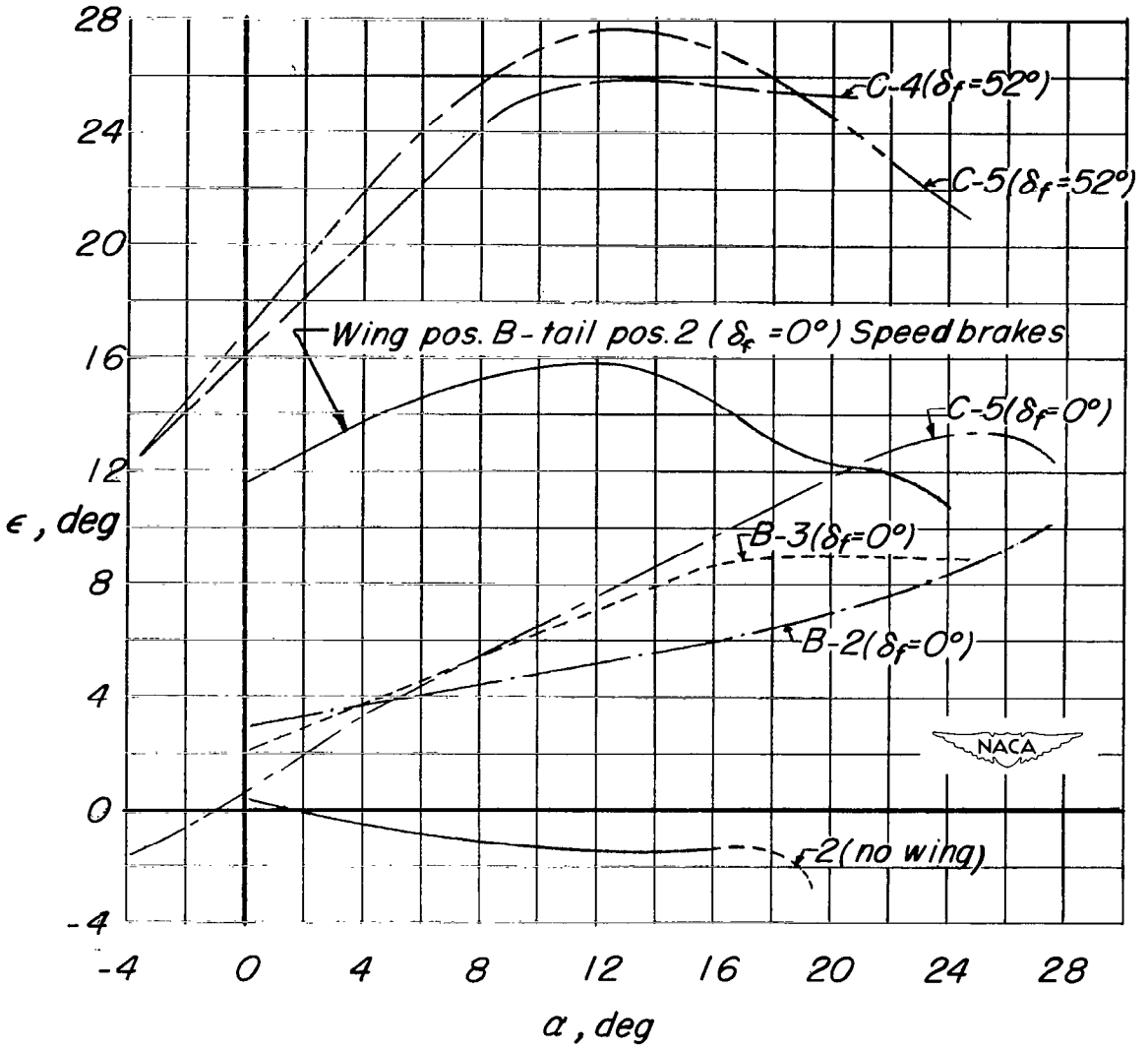

Figure 51.- Variation of effective downwash with angle of attack.

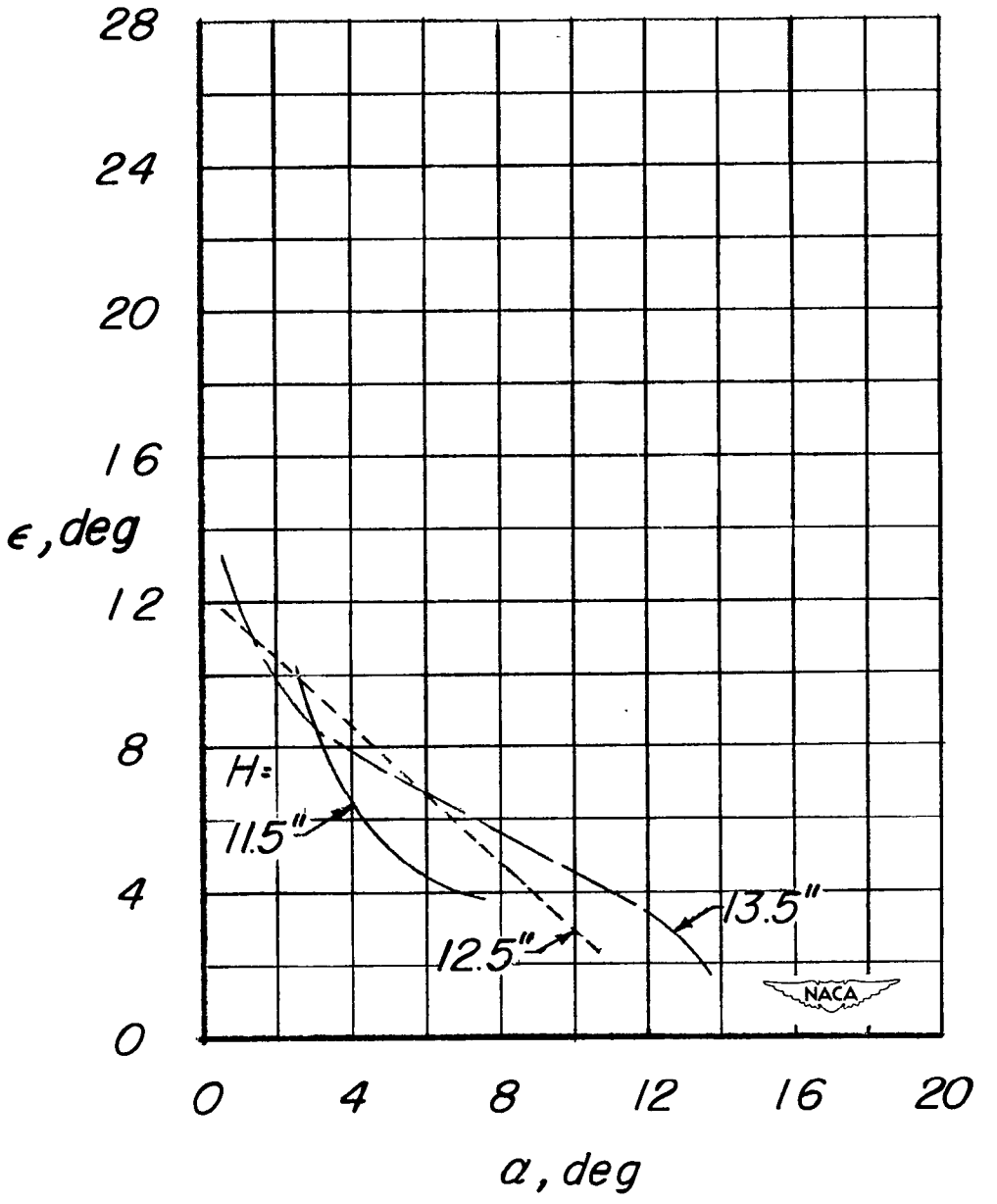

Figure 52.- Effect of ground-board height on the variation of effective downwash with angle of attack. Gear on; $\delta_f = 57^\circ$.